African Swine Fever Virus Multigene Family Interferon Inhibitory Proteins:

Functions and Applications to Vaccine Development

Rodrigo GONZÁLEZ GÓMEZ

Oriel College

University of Oxford

Supervisors:

Prof. Teresa LAMBE — *University of Oxford*

Dr. Ana Luisa REIS — *The Pirbright Institute*

Dr. Elisenda VIAPLANA — *Zoetis Inc.*

A thesis submitted for the degree of

Doctor of Philosophy, DPhil

Michaelmas 2024

Contents

Abstract **vii**

Acknowledgements **x**

List of Tables **xi**

List of Figures **xiii**

List of Abbreviations **xx**

1 Introduction **1**

1.1 African Swine Fever 2

1.1.1 ASF Aetiology and Virus Taxonomy 3

1.1.2 Epizootiology 5

1.1.3 Context and Relevance 7

1.2 ASFV Molecular Virology and Pathology 11

1.2.1 Virion Morphology and Virus Replication 11

1.2.2 Genome Structure and Organisation 14

1.2.3 Multigene Family (MGF) Proteins 16

1.2.4 Host Cell Tropism 16

1.2.5 Pathology 18

1.2.6 Pathophysiology 19

1.3 Host Innate Immunity 21

1.3.1 Overview of Innate Immune Sensing 21

1.3.2 Type I IFN Induction 22

1.3.3 Type I IFN Response 23

1.3.4 IRF7 24

1.3.5 Role of CRL Machinery in IFN Signalling 25

1.4 ASFV Immune Evasion: Type I IFNs 28

1.4.1 Inhibition of IFN Induction 28

1.4.2 Inhibition of IFN Response 33

1.4.3 Previous Unpublished Work 35

1.5 Vaccinology and Deletion Mutants 37

1.5.1 Subunit Vaccines . . . 37
1.5.2 Live Attenuated Vaccines . . . 38
1.5.3 Deletion Mutants . . . 39
1.6 Cell Culture Systems for ASFV Research . . . 41
1.7 Research Objectives . . . 43

2 Materials and Methods 45
2.1 Cell Culture . . . 46
2.1.1 Primary Porcine Bone Marrow Cells . . . 46
2.1.2 HEK293T and Vero Cells . . . 47
2.1.3 PLTA58s . . . 47
2.2 Virus Work . . . 48
2.2.1 Titrations . . . 48
2.2.2 Infections . . . 49
2.3 Inhibitors . . . 49
2.4 RT-qPCR . . . 49
2.5 ELISAs . . . 50
2.5.1 CXCL10 ELISA . . . 51
2.5.2 IFNα ELISA . . . 51
2.6 Cell Viability Assay . . . 52
2.7 Dual-Luciferase® Reporter . . . 52
2.8 Protein Analysis . . . 53
2.8.1 Sample Preparation . . . 53
2.8.2 Immunoprecipitation . . . 53
2.8.3 Immunoblotting . . . 53
2.9 Immunofluorescence . . . 54
2.10 Antibodies . . . 55
2.11 Plasmids . . . 56
2.12 Statistical Analysis . . . 57

3 Macrophage Responses to Infection with ASFV Deletion Mutants 59
3.1 Introduction . . . 59
3.2 Results . . . 61
3.2.1 Deletion of 12L strongly induces ISGs . . . 61
3.2.2 Induction of ISGs Occurs Early Following Infection with ASFV Δ12L . . . 62
3.2.3 Ruxo Reverses Δ12L Early Induction of ISGs . . . 64
3.2.4 Ruxo does not revert Δ12L growth defect . . . 66
3.2.5 Ultracentrifugation of Δ12L: Impact on IFN and ISGs . . . 69
3.2.6 Ultracentrifugation Does Not Revert Δ12L Growth Defect . . . 71
3.2.7 Cell Viability of PBMs Treated with Ruxo . . . 73
3.3 Discussion . . . 74

4 Host Interactions of MGFs **79**
4.1 Introduction . . . 79
4.2 IRF7 . . . 81
4.2.1 Impact of MGFs on *IFNA6* promoter activity . . . 81
4.2.2 12L Does Not Co-Immunoprecipitate With IRF7 . . . 85
4.2.3 Impact of 12L on IRF7 Protein Levels . . . 86
4.2.4 12L Inhibits IRF7 Nuclear Translocation . . . 88
4.3 IFN Response Pathway . . . 93
4.3.1 MGFs Inhibit Warthog ISG Promoter Activity . . . 93
4.3.2 MGFs Do Not Promote Degradation of STATs . . . 94
4.4 Discussion . . . 96

5 Potential of PLTA58s as a Replacement for Primary Macrophages 101
5.1 Introduction . . . 101
5.2 Results . . . 104
5.2.1 ISG profile in response to infection . . . 104
5.2.2 ASFV Growth in PLTA58s . . . 106
5.2.3 Cell Viability . . . 111
5.3 Discussion . . . 112

6 Discussion **115**
6.1 Research Aims . . . 115
6.2 Key Findings . . . 116
6.2.1 PBMs Infected with Deletion Mutants . . . 116
6.2.2 Host Interactions . . . 116
6.2.3 Validation of PLTA58 Cells for ASFV Research . . . 119
6.3 Future Work . . . 120
6.4 Conclusion . . . 121

References **123**

Abstract

African swine fever (ASF) poses a significant threat to global food security, with no commercially available vaccines against this viral disease. We investigated how African swine fever virus (ASFV) multigene family (MGF) proteins modulate host innate immunity, focusing on their role in type-I interferon (IFN) suppression. We characterised the impact of various MGF gene deletions on viral replication and immune responses in primary macrophages, corroborating previously published data that showed deletion of MGF360-12L (12L) significantly enhancing interferon-stimulated gene expression early in infection. Our assessment interferon alpha (IFN-α) levels in virus stocks revealed that an excess of interferon is carried over into subsequent experiments; we resolved this contingency by using ultracentrifuged virus in our experiments. Interestingly, we showed that the growth defect observed for the GeorgiaΔK145RΔMGF360-12L (Δ12L) deletion mutant does not seem to correlate with its inability to control the host IFN response. Through molecular *in vitro* assays, we demonstrated that 12L inhibits interferon regulatory factor 7 (IRF7)-dependent interferon alpha-6 (IFNα6)-promoter activity and promotes proteasomal degradation of IRF7 in a dose-dependent manner, through a mechanism dependent on its putative VHL-box motif. Additionally, 12L disrupts the nuclear translocation of this transcription factor. This represents a novel strategy for IFN induction inhibition by ASFV. Additionally, we evaluated the potential of a novel immortalized porcine macrophage cell line – porcine large tumour antigen 58 (PLTA58) – as an alternative to primary cells for ASFV research. Whilst PLTA58 cells supported enhanced viral replication, they failed to replicate key viral phenotypes observed during infection of primary macrophages, likely due to differences in cellular diversity and molecular phenotypes. Our findings advance understanding of ASFV immune evasion mechanisms and provide insights for rational vaccine design through targeted gene deletion, while also assessing new tools to reduce reliance on animal-derived cells in ASFV research.

Acknowledgements

Personal

First and foremost, I would like to express my deepest gratitude to my supervisors, who made this work possible. To Dr. Ana Reis, thank you for entrusting me with this project and for your expert guidance in working with ASFV in containment. Your mentorship, encouragement, support, and endless patience have been invaluable. To Professor Teresa Lambe, thank you for welcoming me into the Emergent Pathogens group and also for your firm mentorship and support. To Dr. Elisenda Viaplana, thank you for introducing me to pharmaceutical industry practices at Zoetis's manufacturing facilities in Olot and ensuring I gained exposure to all aspects of business, research, development, and manufacturing during my stay.

I am deeply grateful to all members of the ASFV Immune Evasion, ASFV, and ASFV Vaccinology groups at The Pirbright Institute (TPI) for their support and contributions throughout my research. Special thanks to Dr. Anusyah Rathakrishnan for providing the recombinant viruses essential to this work, and to the ASFV group members who contributed to their preparation. I am indebted to Dr. Chris Netherton and Lynnette Goatley for access to their IFNα ELISA assay, and to Dr. Kay Childs for the IFNα6-promoter Firefly reporter and IRF7 plasmids that were crucial to my experiments. I would also like to extend my gratitude to Dr. Raquel Portugal and Dr. Anusyah Rathakrishnan for maintaining the PLTA58 cultures, with particular thanks to Raquel for her thorough review and support of my work with this cell line.

I would like to thank my examiners, Dr. Kay Childs and Dr. Dominic Kelly, whose expertise and critical outside perspectives through my continuous examinations have significantly ameliorated this thesis. Your insights have been instrumental in shaping this work.

My sincere appreciation extends to all staff at Oriel College, the Doctoral Training Centre, and The University of Oxford for their support throughout this journey. These have been challenging years, and I am grateful to all my colleagues, professors, academic tutors, and non-academic advisors who have helped me navigate them successfully.

Last but not least, I would like to thank my family, partner and friends for their unwavering support and encouragement throughout this journey. Your presence has made all the difference.

Institutional

This project was funded by the BBSRC, through University of Oxford's Interdisciplinary Biosciences DTP, with studentship contributions from both The Pirbright Institute and Zoetis Inc.

This project has benefited from access to critical infrastructure at TPI, core funded by the Biotechnology and Biological Sciences Research Council (BBSRC), without which virus work at the required containment level would have not been possible. Thanks also for the support of the Biomaging and Sequencing teams at The Pirbright Institute.

Lastly, I would like to acknowledge Zoetis Inc. for supporting this project and my industrial training.

National Bioscience Research Infrastructures (NBRI) Funding: NBRI1 High containment – BBS/E/PI/23NB0004
Leica TCS SP8 laser scanning confocal microscope BBS/E/I/00007039

List of Tables

1.1 Asfarviridae Summary 4
1.2 ASFV MGF-Host Interactions Inhibiting IFN Induction 30
1.3 ASFV-Host Interactions Inhibiting IFN Induction 33
1.4 ASFV-Host Interactions Inhibiting IFN Signalling 35
1.5 MGF360-12L and MGF505-1R Functions 36

2.1 Primers used for qPCR 50
2.2 Antibodies Used in This Study 55
2.3 Plasmids Used in This Study 56
2.4 DNA Amounts Used for Cell Transfections 57

List of Figures

1.1 Phylogenetic Analysis 5
1.2 The Epizootiological Cycles of African Swine Fever 6
1.3 Global Distribution of ASFV Genotypes 8
1.4 ASF Disease Free Countries 9
1.5 ASFV Virion 12
1.6 ASFV Cell Entry Mechanisms 13
1.7 ASFV Replication Cycle 14
1.8 ASFV Genome Organigram 15
1.9 Type I IFN Induction and Response Signalling Pathways 23
1.10 CRL Complexes with Different Box Motifs 27
1.11 Antagonism of DNA Sensing Pathways by ASFV 29
1.12 Deletion of MGFs 40

2.1 Mutations of the Putative VHL/SOCS-Boxes of MGF360-12L and MGF505-1R 57

3.1 Impact of Deletion Mutants on CXCL10 Levels in Macrophages . . 62
3.2 ISG Expression Dynamics in Infected Cells 63
3.3 Inhibition of JAK/STAT Pathway Reverses ISG Induction 65
3.4 Impact of Ruxo on virus growth, S1 67
3.5 Impact of Ruxo on virus growth, S2 68
3.6 Ultracentrifugation: excess IFN-α and early *CXCL10* induction . . 70
3.7 Impact of Ruxo on ultracentrifuged virus growth, S1 71
3.8 Impact of Ruxo on ultracentrifuged virus growth, S2 72
3.9 Cell Viability of PBMs Treated with Ruxo 73

4.1 MGFs inhibit *IFNα6* promoter activity 82
4.2 Impact of 12L, 1R and Mutants on *IFNα6* Promoter Activity 84
4.3 12L Does Not Immunoprecipitate With IRF7 85
4.4 Impact of WT 12L and Mutants on IRF7 87
4.5 MG132 inhibits MGF360-12L dose-dependent IRF7 degradation . . 88
4.6 Immunofluorescence Imaging of MGF360-12L, WT and mutants, in Vero Cells 90

4.7 Immunofluorescence Imaging of IRF7-EGFP with MGF360-12L, WT and Mutants, in Vero Cells 92
4.8 MGFs inhibit warthog ISG reporter 94
4.9 MGFs Do Not Impact Endogenous STAT2 Levels 95
4.10 12L Does Not Have Dose-Dependent Impact on STAT1/2 96

5.1 CXCL10 ELISA in PLTA58s 104
5.2 Relative *CXCL10* mRNA in PLTA58s infected with deletion mutants 105
5.3 Impact of Ruxo on virus growth, PLTA58s 107
5.4 Impact of Ruxo on ultracentrifuged virus growth in PLTA58s -1 . . 108
5.5 Impact of Ruxo on ultracentrifuged virus growth in PLTA58s -2 . . 109
5.6 Reproducibility of data in PLTA58s 110
5.7 Impact of Ruxo on PLTA58 cell viability 111

List of Abbreviations

Δ12L GeorgiaΔK145RΔMGF360-12L .. vii, 39, 40, 61–66, 68–76, 104–106, 112, 113, 116, 119, 120

Δ1R GeorgiaΔK145RΔMGF505-1R 63, 65, 69, 70, 104–106

Δ1R12L GeorgiaΔK145RΔMGF505-1RΔMGF360-12L 39, 62, 77, 117

ΔK145R GeorgiaΔK145R 39

10L MGF360-10L 33, 34, 83

11L MGF360-11L 29, 30

12L MGF360-12L vii, 26, 29, 30, 34–36, 39, 40, 43, 59, 61–64, 69, 70, 74–78, 80, 81, 83–89, 91, 93–100, 113, 116–121

13L MGF360-13L 75

14L MGF360-14L 29, 30, 75

1R MGF505-1R ... 26, 35, 39, 43, 59, 75, 77, 80, 83–85, 93, 94, 97, 99, 100, 116

2R MGF505-2R 29, 30, 75, 83, 93, 97, 99

3R MGF505-3R 29, 30

3Rs Replacement, Reduction, and Refinement 102, 121

4R MGF505-4R 30, 83

aa amino acid 3

AAI pairwise average amino acid identity 3

AbALV abalone asfa-like virus 3

ANK ankyrin 35, 80, 115

APPBP1 amyloid precursor protein-binding protein 1 25

ASF African swine fever ..... vii, 2, 3, 5–10, 16, 18–21, 28, 44, 101

ASFV African swine fever virus ... vii, 2–8, 11–19, 21, 24–26, 28, 30, 31, 33–39, 41–44, 59–61, 74–84, 86, 87, 93, 95, 96, 100–105, 112–116, 118–121

BBSRC Biotechnology and Biological Sciences Research Council x, 10, 102, 103, 121

BSA bovine serum albumin 51, 52, 54

CBP CREB binding protein 22

cGAMP cyclic guanosine monophosphate–adenosine monophosphate 21, 31, 32

cGAS cyclic GMP-AMP synthase 21, 23, 28–30, 33

CME clathrin-mediated endocytosis 11, 13

CRL Cullin-RING E3 ubiquitin ligase 25, 26, 35, 80, 81, 97, 98, 116

CXCL10 C-X-C motif chemokine ligand 10 ... 23, 39, 50, 51, 60–64, 70, 74, 76, 104–106, 112, 116

DIVA differentiation of infected from vaccinated animals 38, 39

DLR™ Dual-Luciferase®-Reporter 52, 57, 82, 84, 93, 94, 97

DMEM Dulbecco's Modified Eagle Medium 47, 52

DMSO dimethyl sulfoxide 47, 49, 52, 65–68, 71–74, 87, 88, 107–109, 111

DNA deoxyribonucleic acid 3, 11, 15, 18, 21, 24, 25, 28, 29, 31, 52, 53, 60, 75, 79, 80

dpi days post-infection 18, 19, 68, 73, 106

dsDNA double-stranded DNA 3, 4, 14, 21

EBSS Earle's Balanced Salt Solution 46, 48

ELISA enzyme-linked immunosorbent assay 43, 49–51, 104, 112

ER endoplasmic reticulum 11–13, 21, 28

FBS Foetal Bovine Serum 46, 47

GAPDH glyceraldehyde 3-phosphate dehydrogenase 50, 61, 65, 70, 112

GST Glutathione *S*-transferase 36

HAD haemadsorption 11, 48

hpi hours post-infection 49, 50, 61–66, 69, 70, 74, 76, 104–106, 116

IFN type-I interferon vii, 17–19, 22–25, 28–31, 33, 35, 36, 40, 43, 52, 59–62, 64, 66, 69–78, 80, 81, 83, 85, 87, 88, 93, 94, 96, 98–100, 112, 113, 115–118, 121

IFN-α interferon alpha . vii, 19, 23, 24, 36, 39, 43, 51, 61, 69, 70, 75, 78, 80, 81, 96, 112, 117, 118, 120

IFN-β interferon beta 22–24, 29–32, 80, 81

IFNAR interferon-α/β receptor 24, 34

IFNα6 interferon alpha-6 ..... vii, 81–84, 86, 97, 116

IKK IκB kinase 22, 29, 32

IKKε inhibitor of nuclear factor kappa B kinase subunit epsilon . 22, 24, 33, 56, 82–84, 86, 88–90, 92, 97, 99, 116, 117

IL-10 interleukin-10 ..... 17, 113, 119

IL-12 interleukin-12 17

IL-1α interleukin-1 alpha 19

IL-1β interleukin-1 beta 17

IL-6 interleukin-6 19

IP immunoprecipitation 53, 85, 97, 117

IPKM immortalized porcine kidney macrophage 102, 103

IRF interferon regulatory factor 21, 22, 24, 25, 78

IRF3 interferon regulatory factor 3 .... 22–24, 28–33, 35, 36, 62, 80, 81, 99, 117

IRF7 interferon regulatory factor 7 ... vii, 22–25, 30, 36, 62, 80–91, 93, 97–100, 116–118, 120, 121

IRF9 interferon regulatory factor 9 ..... 24, 34, 35

ISG interferon stimulated gene . 23, 24, 33, 35, 39, 43, 60–66, 69, 70, 74–76, 81, 93, 94, 99, 100, 103, 104, 116, 117, 119

ISGF3 interferon-stimulated gene factor 3 ..... 24, 34, 35

ISRE interferon-stimulated response element 24, 34

JAK1 Janus kinase 1 ..... 24, 33–35

JAK2 Janus kinase 2 ..... 34, 35

kbp kilo base-pair 3

LAV live attenuated vaccine 18, 37, 38, 76–78, 100

LTA large tumour antigen 103, 113

LTA58 large tumour antigen 58 ..... 103, 113

m-MΦ monocytes-macrophages 16, 17, 21, 41, 60, 80, 96, 113, 118, 119

MAVS mitochondrial antiviral-signalling protein 21

MCT multiple comparison test 58, 82, 84, 88, 94

MDA5 melanoma differentiation-associated protein 5 21

MGF multigene family vii, 4, 14, 16, 28–31, 33–36, 38–40, 43, 53, 59–61, 66, 75, 77, 79–84, 86, 93–97, 99, 100, 113, 115–121

MOI multiplicity of infection 49, 62, 64, 66, 69, 74, 104, 113, 119

mRNA messenger RNA 4, 28, 74, 105, 106, 112

Mt million metric tonnes 10

MX2 interferon-induced GTP-binding protein 50, 62, 63, 93, 94, 99

NAE NEDD8-activating enzyme 25, 81, 98, 117

NC3Rs National Centre for the Replacement, Refinement and Reduction of Animals in Research 102, 121

NCLDV nucleocytoplasmic large DNA viruses 4

NEDD8 neural precursor cell expressed, developmentally down-regulated 8 25, 26

NEMO NF-κB essential modulator 22, 32

NF-κB nuclear factor kappa-light-chain-enhancer of activated B cells 21, 22, 29, 31, 32, 35, 36, 61, 80

ns non-significant 68, 85, 88, 105

OD optical density 51

ORF open reading frame 3, 14, 15

P/S Penicillin-Streptomycin 46, 47

PAM porcine alveolar macrophage 75, 113

PAMP pathogen-associated molecular pattern 21, 22, 60, 69

PBM porcine bone marrow 46–50, 60, 61, 64, 66, 68, 70, 73, 74, 76, 78, 104–106, 112, 119, 120

PBS Phosphate-Buffered Saline 46, 47, 51, 52, 54

PCR polymerase chain reaction 50

pDC plasmacytoid dendritic cell 17, 23, 78, 80, 118

PKR protein kinase RNA-activated 50, 62, 63

PLTA58 porcine large tumour antigen 58 ..... vii, 102–107, 111–114, 119–121

PRR pattern recognition receptor 21, 22

PRRSV porcine reproductive and respiratory syndrome virus 102, 103

PVDF polyvinylidene difluoride 53

qPCR quantitative PCR 50

RBC red blood cell 11, 46

RIG-I retinoic acid-inducible gene I 21, 31, 32

RLR RIG-I-like receptor 21

RNA ribonucleic acid 4, 21, 25, 31, 32, 49

RPMI 1640 Roswell Park Memorial Institute 1640 ..... 47, 49

RT-qPCR quantitative reverse transcription PCR 43, 49, 62, 63, 65, 70, 105, 112

Ruxo ruxolitinib 49, 64–69, 71–74, 76, 103, 107–109, 111, 113, 116

SOCS suppressor of cytokine signalling 26, 35, 36, 80, 83, 94, 97, 99

STAT signal transducer and activator of transcription ... 24, 33, 34, 64, 66, 69, 71–74, 76, 81, 93, 94, 96, 99, 100, 113, 118

STING stimulator of interferon genes 21, 28–33

SV40 simian virus 40 ..... 103, 113

T-175 tissue culture flasks of 175cm^2 ..... 47, 48

TAK1 Transforming growth factor-β-activated kinase 1 22

TBK1 TANK-binding kinase 1 ..... 21, 22, 28–33

TBS Tris-buffered saline 54

TGF-β transforming growth factor beta 17

TLR Toll-like receptor 21, 22, 31, 33

TNF-α tumor necrosis factor alpha 17, 19

TRAF3 TNF receptor-associated factor 3 ..... 22, 30, 36

TRAF6 TNF receptor-associated factor 6 ..... 22, 31, 36

TRIF TIR-domain-containing adapter-inducing interferon-β 22, 31, 33

TYK2 tyrosine kinase 2 ..... 24, 34

UBA3 ubiquitin-like modifier activating enzyme 3 .. 24, 25, 36, 81, 98, 117, 120

VC vehicle control 49, 52, 65–68, 71–74, 87, 106–109, 111

VHL von Hippel-Lindau 26, 35, 80, 83, 85–87, 90, 94, 97–99, 117, 120

VP30 viral protein 30 39

WAHIS World Animal Health Information System 9

WOAH World Organisation for Animal Health 8, 9

wt wild-type 39, 59, 62, 63, 65, 66, 68–70, 72, 74, 83–86, 89, 91, 94, 98, 99, 103–106, 120

β-actin beta-actin 87, 88, 95, 96

1 Introduction

Contents

1.1 African Swine Fever 2
1.1.1 ASF Aetiology and Virus Taxonomy 3
1.1.2 Epizootiology 5
1.1.3 Context and Relevance 7
1.2 ASFV Molecular Virology and Pathology 11
1.2.1 Virion Morphology and Virus Replication 11
1.2.2 Genome Structure and Organisation 14
1.2.3 Multigene Family (MGF) Proteins 16
1.2.4 Host Cell Tropism 16
1.2.5 Pathology 18
1.2.6 Pathophysiology 19
1.3 Host Innate Immunity 21
1.3.1 Overview of Innate Immune Sensing 21
1.3.2 Type I IFN Induction 22
1.3.3 Type I IFN Response 23
1.3.4 IRF7 24
1.3.5 Role of CRL Machinery in IFN Signalling 25
1.4 ASFV Immune Evasion: Type I IFNs 28
1.4.1 Inhibition of IFN Induction 28
1.4.2 Inhibition of IFN Response 33
1.4.3 Previous Unpublished Work 35
1.5 Vaccinology and Deletion Mutants 37
1.5.1 Subunit Vaccines 37
1.5.2 Live Attenuated Vaccines 38
1.5.3 Deletion Mutants 39
1.6 Cell Culture Systems for ASFV Research 41
1.7 Research Objectives 43

In general, our research aims to support the global efforts to contain and eventually eradicate African swine fever (ASF), which arguably represents the most serious threat to domestic pig livestock. African swine fever virus (ASFV), the emergent pathogen causing this disease, is a large and complex virus for which there are no commercially available vaccines, as its propagation imperils the pig meat industry's viability and, consequently, global food security and the livelihood of many farmers.

In particular, we sought to characterise mechanisms employed by the virus to evade host immunity, and, through this work of basic molecular virology, inform and accelerate efforts to develop safe and effective vaccines against this emergent pathogen of concern.

To achieve our goals, we assessed the dynamics of viral replication and molecular immunity in pig bone marrow cells infected with attenuated deletion mutants, and characterised how these differ from a virulent virus isolate. We also expressed cloned viral genes *in vitro*, and through various molecular assays qualified their impact on relevant host immune proteins and pathways. We also studied the reproducibility of our results in a novel porcine macrophage cell line.

This chapter seeks to contextualise our work and the scope of our research by providing an updated review of the field. This will cover all pertinent aspects of: the disease, molecular virology and pathology of the virus, host innate immunity and how the virus is known to evade it, and relevant vaccinology progress. This chapter also contains a review of cell culture systems used in our line of research, since we also tangentially supported efforts to replace the use of primary cells for the study of ASFV.

1.1 African Swine Fever

African swine fever (ASF) is a devastating haemorrhagic viral swine disease with a mortality rate of nearly 100% in domestic pigs and wild boar.[1, 2] The socioeconomic impact of ASF is very high because there are no widely available commercial

vaccines, and mass culling of animals is the main existing means available to control the spread of this disease.[2, 3] ASF is currently spreading through Africa and Eurasia, threatening food security and the viability of porcine agriculture around the globe.

1.1.1 ASF Aetiology and Virus Taxonomy

The causative agent of ASF is African swine fever virus (ASFV) (Table 1.1), a large deoxyribonucleic acid (DNA) virus. This vector-bourne pathogen has a host range limited to suids (Family *Suidae*) and *Ornithodoros* ticks.[1] ASFV is a member of the *Asfarviridae* family, and the single species of its genus, *Asfivirus*.[4, 5]

ASFV's extensive genome comprises a single molecule of linear double-stranded DNA (dsDNA), approximately 170–193 kilo base-pairs (kbp) long, which encodes between 150–200 open reading frames (ORFs) and whose terminal ends are covalently closed by hairpin-loops of imperfectly base-paired 2.1 kbp complementary sequence repeats.[6, 7] The viral genome is contained within complex multi-layered virions approximately 200 nm in diameter. ASFV replicates in the cytoplasm of cells, where it must strongly subvert innate immune barriers that seek to abort viral replication.[8]

This section contains a tabulated summary of relevant ASFV characteristics to contextualise the aetiology of ASF for reference purposes (Table 1.1). The molecular biology of ASFV will be explored in further detail within section 1.2.

As described above, ASFV is the only member of the *Asfivirus* genus and the only virus grouped within the *Asfarviridae* family. The recent characterisation of the abalone asfa-like virus (AbALV), a similarly large virus which infects molluscs and shares a 33.97% pairwise average amino acid identity (AAI, %) with ASFV Georgia 2007, led to discussions regarding its inclusion in the *Asfarviridae* family,[10], however this is not widely accepted. Until this recent discovery in 2023, the taxonomically closest viruses to ASFV were some unclassified *Faustoviridae* (Fig. 1.1), which infect amoebae and have a genome roughly $\sim 3\times$ larger than ASFV but with an AAI % of 29.71.[10, 11]

The most extensively studied family of viruses with any phylogenetic proximity to ASFV are *Poxviridae* (Fig. 1.1). Although their relation is not directly proximal,

Characteristic	Description
Typical member	African swine fever virus Georgia 2007/1 isolate (GenBank: FR682468.2),[9] species *African swine fever virus*, genus *Asfivirus*
Virion	Multiple layers of core, internal and external envelopes, and capsid. Polyprotein processing by a viral protease yields multiple subunit structural proteins
Genome	Linear dsDNA, 170–194 kbp with complementary terminal loops
Replication	Cytoplasmic with an early nuclear phase not fully characterised. Head-to-head concatemer replicative intermediates similar to poxviruses. Transcription and RNA processing uses virus-encoded enzymes
Translation	From mRNAs with 5′-caps and 3′-polyadenylation
Host range	Domestic pig, wild boar, warthog, bushpig, red river hog, and *Ornithodoros* ticks
Taxonomy	Single species in the genus *Asfivirus*

Table 1.1: African Swine Fever Virus Summary. Characteristics of Asfarviridae. Adapted and modified from Alonso et al. [5, ICTV Virus Taxonomy Profile: Asfarviridae].

their relatively close evolutionary relationship means that this extensively researched family of viruses still shares analogous molecular immune evasion strategies with ASFV, which continue to inform our field. For example, pox viruses also encode immediate early genes that inhibit interferon signalling along their genomic terminal ends and which have also arisen through duplication, highly resembling the subject of our study, the ASFV multigene family genes.[7, 12–14]

ASFV shares ancestry with and was grouped within the nucleocytoplasmic large DNA viruses (NCLDV) superfamily until the suggested reclassification of this grouping in 2012, which landed *Asfarviridae* within the Megavirales viral order.[15] This new taxonomy is proposed to better represent the evolutionary differences between distant members of the NCLDV superfamily.

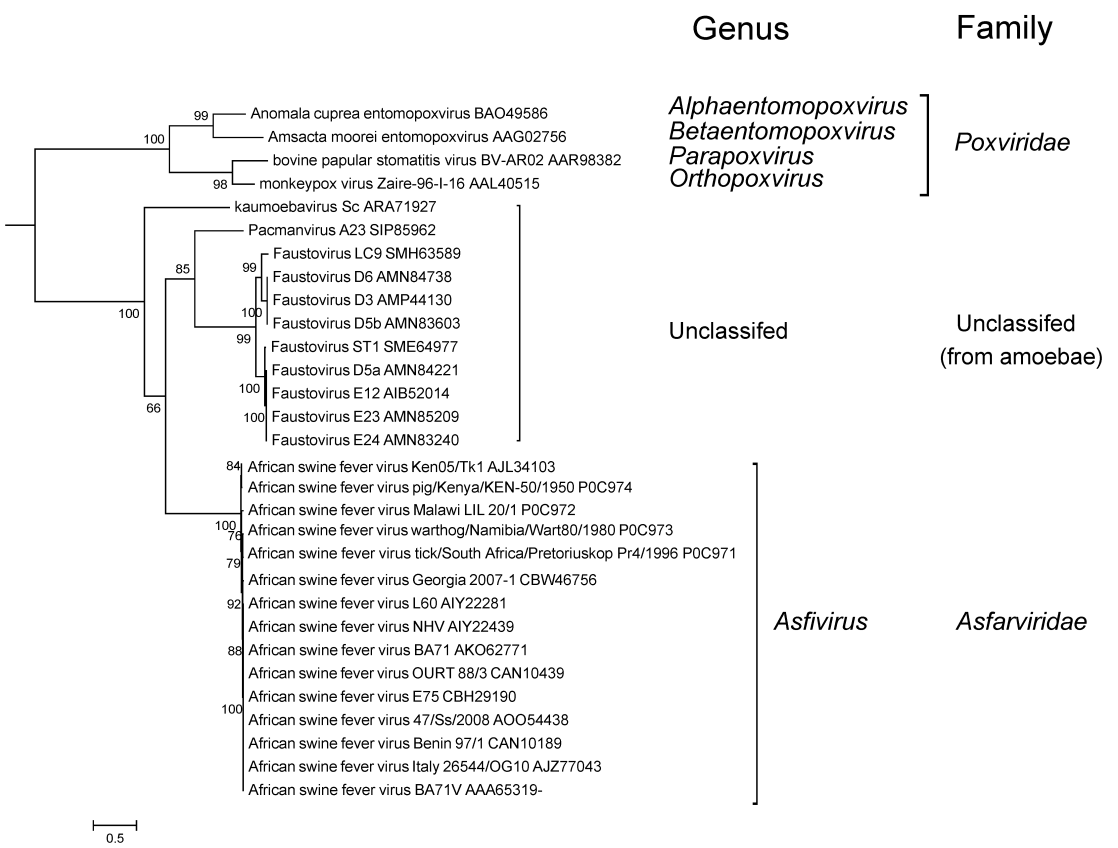

Figure 1.1: Phylogenetic analysis of African swine fever virus and related viruses, as of 2018. Maximum likelihood tree based on DNA polymerase B protein sequence alignment. Branch support values higher than 50% are indicated at nodes, showing the percentage of bootstrap replicates (out of 100) in which the grouping appeared. The scale bar represents the number of amino acid substitutions per site. Adapted from Alonso et al. [5].

1.1.2 Epizootiology of ASF

As an emergent pathogen of grave concern, the study of ASF's epizootiology, or how this disease interacts and spreads within animal populations, is key to achieve our goals of security, containment and eventual eradication. In this section, I sought to comprehensively summarise how ASF spreads between different animal populations, how we study this spread, differentiate between genotypes, as it relates to our research.

ASF persists through the continued replication of ASFV within its natural hosts and vectors in East and Southern Africa, where this disease is enzootic.[16] ASFV maintains diverse reservoirs within an ancient sylvatic cycle involving wild African

suids (such as: common warthogs, *Phacochoerus africanus*; and bushpigs or red river hogs, *Potamochoerus larvatus* or *P. porcus*), for which infection is largely asymptomatic, and the disease vector ticks, *Ornithodoros moubata*, whose geographic distribution and exclusive competency for ASFV vectored transmission limits ASF's sylvatic cycle to Eastern and Southern Africa. Other *Ornithodoros* species of concern, such as *O. erraticus* in the Iberian peninsula, have been shown to be permissive of ASFV replication, having enabled tick-pig transmission during earlier incursions into said territory.[17, 18] This highlights the potential of ticks as vectors during epizootic events, however their practical involvement in the epizootiology of ASF remains largely unclear.[17, 19, 20] Figure 1.2 depicts a graphical summary of the sylvatic and epizootic cycles of ASF epizootiology.

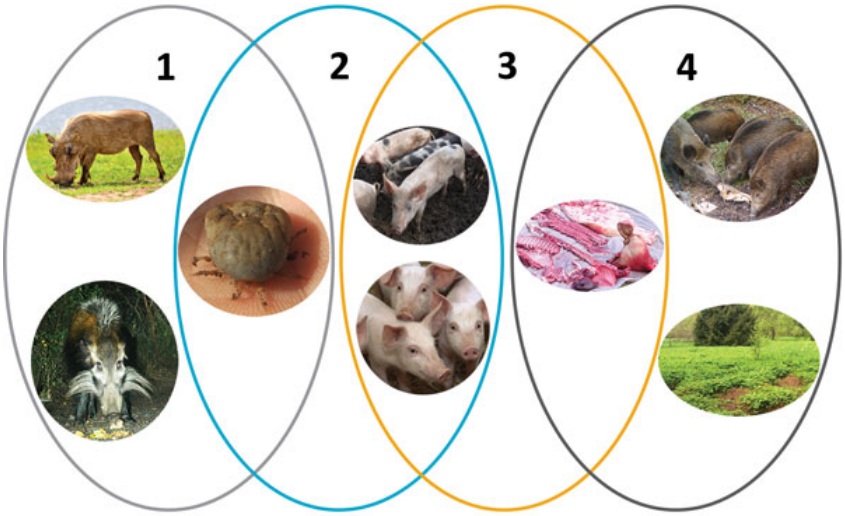

Figure 1.2: The Epizootiological Cycles of African Swine Fever comprise: **1)** the sylvatic cycle among warthogs, bushpigs, and soft ticks of Ornithodoros spp.; **2)** the tick-pig cycle between Ornithodoros vectors and domestic pigs; **3)** the epizootic cycle involving pigs and their derived products (meat, blood, tissues, and byproducts); and **4)** the wild boar-habitat cycle, which includes wild boar, their carcasses, contaminated products, and environmental persistence. Adapted from Chenais et al. [21].

ASF infection in domestic pig and wild boar (*Sus scrofa*) populations is nearly 100% lethal, due to their relative naiveté towards the virus in contrast to the natural immunity their African wild counterparts enjoy.[16] Countries where ASF is present face stringent export restrictions on their pork products, as they constitute a risk to biosecurity for importing countries as one the likeliest sources of international

spread.[22, 23] Uncontrolled wild boar can complicate efforts to contain ASF circulation, as the disease has been shown to persist in their populations, particularly well in colder climates.[24–27]

The serotyping of ASFV is a materially complex endevour which remains unstadarised, hence we characterise the diversity of ASFV isolates by genotype.[28] ASFV genotypes are based on the phylogeny arising from the sequence of the structural viral gene p72's C-terminal domain.[28, 29] The highest ASFV genotypic diversity understandably exists in countries where ASF is enzootic.[30] It should be noted that there has been some success with ongoing efforts to serotype ASFV, which is very important given that viral genotypes do not have a clear correlation to cross-protection, however these are yet rudimentary and not widely accessible.[31, 32] Only genotypes I and II have been detected outside of Africa, and, in so far, a total of 23 different genotypes have been described (labelled in Roman numerals I-XIV, no genotype XVIII, plus an additional I/II hybrid – recently found in China and quickly spreading through Asia) (See fig. 1.3).[16, 33] Hybridisation of genotypes in the field and the virus's high genotypic diversity complicate vaccine prospects, since attenuated vaccines are not necessarily protective across genotypes.[34]

1.1.3 Historical Context and Global Significance

In 1910, ASF was first reported in what is now the Republic of Kenya, then British East Africa, as an acute haemorrhagic fever that was causing the death of practically all infected domestic pigs, however it was not until 1921 that a scientific veterinary report of this pathology was published.[16, 36] Since then, the disease quickly spread and established itself through sub-Saharan Africa.[37] ASF first crossed continental borders in 1957 and 1960, when it was detected in Portugal, from where it crossed to other European countries and, eventually also, Brazil and the Caribbean.[2, 16] Through various efforts, eradication of this first epizootic event was achieved in the mid 1990s,[16] except in the Italian island of Sardinia, where the disease has remained endemic until now but authorities say they are working to achieve eradication in the

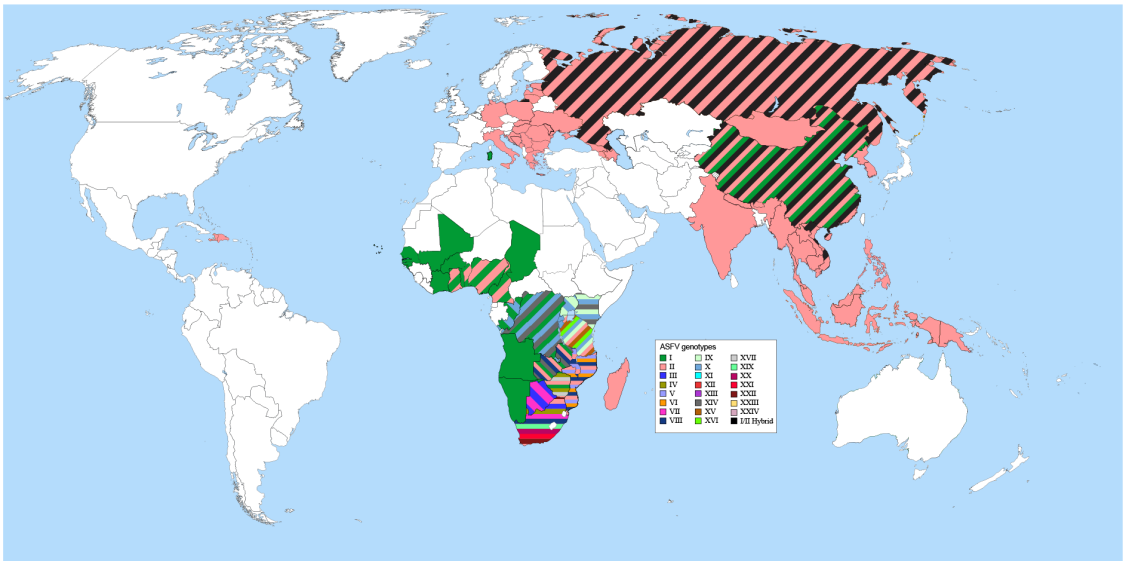

Figure 1.3: Distribution of ASFV Genotypes across the globe. Countries are colour-coded with the genotype that has been reported to the WOAH or in available literature. ASF disease-free countries are filled with white. Inclusion of the Republic of Mali is based on Minoungou et al. [35]. Designed using Adobe Illustrator™, data compiled by and used with permission from Dr. Christopher L. Netherton, The Pirbright Institute.

island.[38] Until 1969, African swine fever virus was not identified as the causative agent of ASF and as a pathogen arising from an ancient sylvatic cycle.[39]

In 2007 a genotype II variant of ASFV was introduced in Georgia, then it quickly spread onto the Russian Federation, Ukraine and Belarus, in 2014 it had crossed onto Poland and the Baltic countries.[16] ASFV was most likely introduced in Georgia in this instance via ship, containing contaminated pork meat products which were later fed to domestic pigs, however the available data is not conclusive in this regard.[40] This second epizootic event has only continued to worsen in gravity, as the disease disseminated through central and northern Europe, eventually reaching China in 2018, which holds the world's largest population of domestic pigs.[16, 41] The disease has continued to spread through Europe, the Caribbean, south and southeastern Asia, and Oceania, to the point where its spread could soon be considered to be panzootic (animal virus equivalent to pandemic). A reference map of ASF-Free countries is provided below to illustrate the dimensions of global ASF spread to date, whilst also noting those few countries which have recovered disease free status since 2017 (i.e.: Sweden, Belgium and Czechia) (Fig. 1.4). Although replication

of ASFV was detected in ticks found in the Iberian peninsula during the first epizootic event, the practical involvement of vectors in the current epizootiology of ASF remains largely unclear.[18]

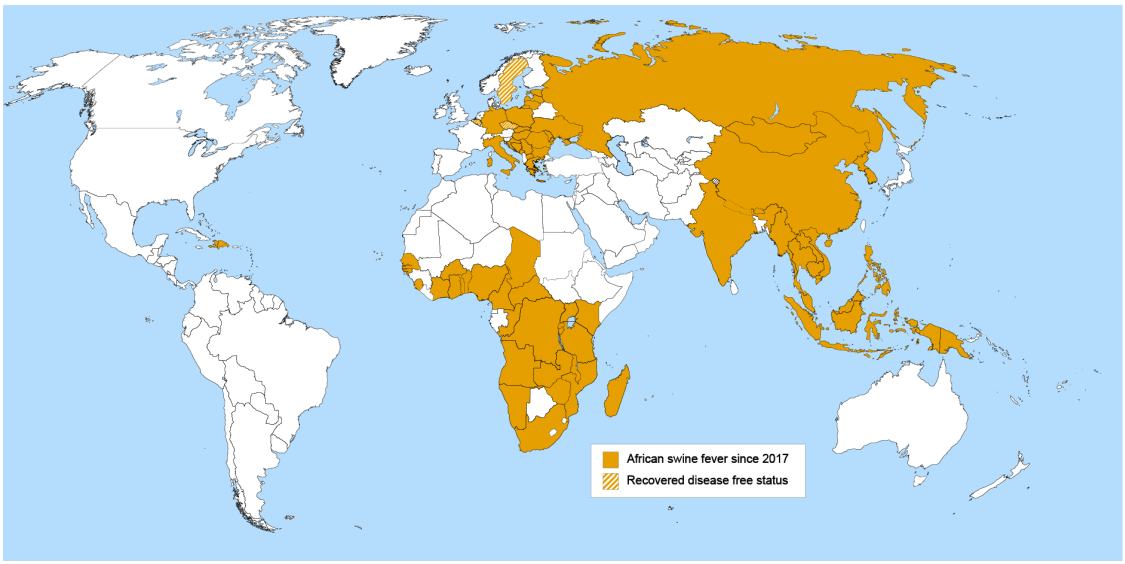

Figure 1.4: Updated Map of ASF Disease-Free Countries, filled in white. Highlighted orange are the nation-states that reported ASF directly to the WOAH (either immediate notification or 6-monthly reports) via WAHIS,[42] or where disease is suspected. Countries highlighted with orange and white stripes have recovered disease free status, after having confirmed a positive case since 2017. Designed on Adobe Illustrator™, data compiled by and used with permission from Dr. Christopher L. Netherton, The Pirbright Institute.

Disease Impact

African swine fever's impact on Global Health is multifaceted, as its spread threatens biodiversity, animal health and welfare, the livelihood of farmers, food security, and the pork livestock's viability.[3] The socioeconomic impact of ASF is particularly severe because there are no commercially available vaccines and the only existing control measure for the disease is culling.[43]

The impact that panzootic spread of ASF can have on the biodiversity of swine can be very significant. The conservation of local wild swine populations is threatened by the spread of ASF, against which they are relatively naive when compared to wild African suids. This is currently the case in South East Asia, where the survival of 11 endemic wild suid species is being threatened by ASF.[44]

Biodiversity within domestic pig populations is also vulnerable to ASF spread, which could severely limit the genetic pool of domestic pigs.

The pork industry, valued at over USD 250 billion annually,[45] represents one of the world's primary sources of animal protein, only second to poultry in total meat weight produced. To meet current food demand expectations, global food production is expected by 2030 to increase its yield by more than 44 million metric tonnes (Mt), to a total global production of over 373 Mt.[46] The consequences of ASF spread can reverberate throughout global markets. When ASF reached China in 2018, the subsequent control measures led to a dramatic decline in the country's pig population, decreasing by over 122 million pigs ($\approx 28\%$ decrease).[45] As China sought to compensate through increased pork imports, domestic pork prices more than doubled.[45] Such large fluctuations in food supply and retail prices can effectively exclude many consumers from accessing this important protein source, forcing them to seek alternatives when available. This volatility in pork prices affects both exporting and importing nations, as international traders face increasingly uncertain supply outlooks.[45]

The spread of this devastating emergent pathogen threatens the livelihood of farmers across different scales of production. Whilst larger farming operations may have the technical and financial resources to implement stringent biosecurity measures, their high-density livestock populations make them particularly vulnerable to rapid disease spread if containment fails.[47] Conversely, smaller-scale farmers, despite operating more sustainable extensive farming systems with naturally lower transmission rates, often lack the means to effectively control disease spread, making them more susceptible to devastating economic losses.[47]

The severity of these impacts highlights why promoting sustainable agriculture and food security through bioscience research is crucial, as emphasized by the BBSRC funding priorities. Understanding and controlling ASF is essential for maintaining stable global food systems and protecting the livelihoods of communities dependent on pork production.

1.2 ASFV Molecular Virology and Pathology

This section seeks to introduce the reader to relevant aspects of ASFV Molecular Virology and Pathology, as a means to contextualise the scope of our research.

1.2.1 Virion Morphology and Viral Replication

African swine fever virus forms a large, multilayered virion approximately 200 nm in diameter. The virion comprises a central nucleoid containing the genomic DNA, viral polymerases, transcription factors, and capping enzymes, surrounded by a core shell formed by processed polyproteins pp220 and pp62.[48, 49] An inner envelope derived from the host endoplasmic reticulum (ER) encloses the core shell, followed by the outer capsid composed primarily of the major capsid protein p72 (encoded by the B646L gene) and minor scaffolding proteins (Fig. 1.5). The virion's final layer, the outer envelope, contains host-derived lipids and the viral CD2v glycoprotein (EP402R), which is named for its homology with the human T-lymphocyte surface antigen CD2 (Fig. 1.5).[49, 50] CD2v mediates binding of virions and infected cells to red blood cells (RBCs) (haemadsorption), promoting the systemic spread of the virus.[51] The outer envelope is derived from the plasma membrane during the budding process, but it is not required for infectivity.[50, 52]

Cellular entry for ASFV can be achieved through a multitude of mechanisms (Fig. 1.6), contributing to the virus's tropism (See 1.2.4), infecting macrophages preferentially.[53] A significant path for viral entry is macropinocytosis, a mechanism of actin-mediated non-selective endocytosis, which other large DNA viruses such as poxviruses, herpesviruses and adenoviruses have also been shown to exploit and is constitutively active in macrophages.[54–56] ASFV can also enter cells through apoptotic mimicry, wherein host-derived phosphatidylserine displayed on the viral envelope is recognized by specific receptors on macrophages, notably AXL.[57] Direct cell-to-cell spread through the formation of apoptotic bodies, also contributes to ASFV infectivity.[58]

Clathrin-mediated endocytosis (CME) has also been shown to be an important mechanism for ASFV entry, and there is some evidence that the cellular receptor

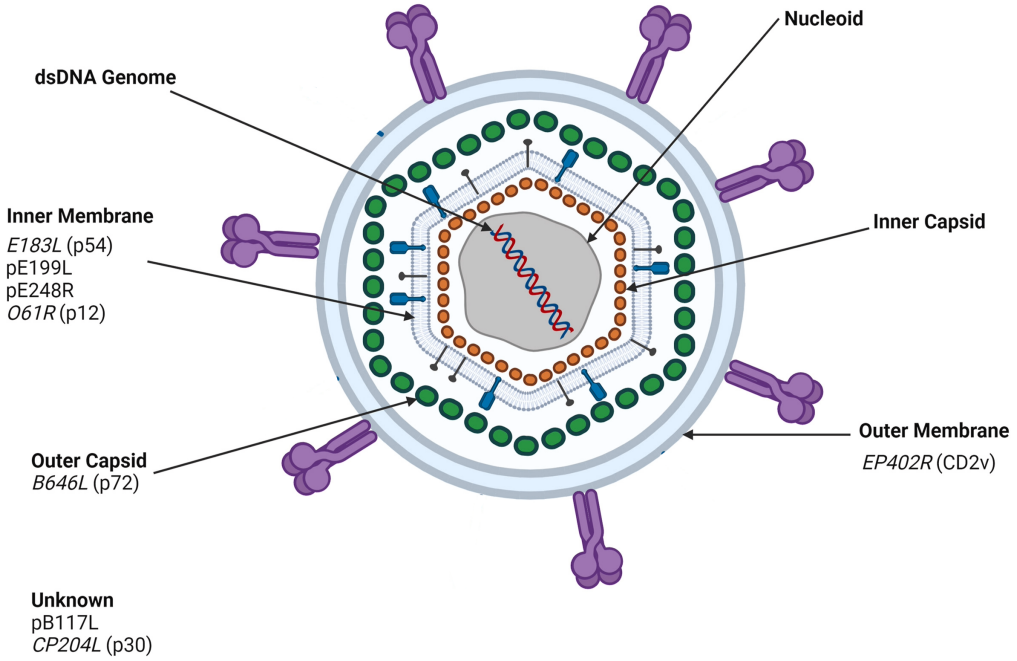

Figure 1.5: ASFV Virion. Virus layers are labelled, alongside the known localisation of viral proteins involved in cellular entry. Created with Biorender.com and adapted from Hooper et al. [53].

CD1d facilitates this mechanism of entry.[59, 60] Phagocytosis is likely to also play a role in cell entry, particularly after viraemia has been achieved *in vivo*.[53] Lastly, some yet unidentified cellular receptor may mediate cell entry specifically. CD163 is expressed on the surface of a certain subset of macrophages and its expression favours, but is not essential for, ASFV entry.[61]

Within cells, viruses in endosomes are transported along microtubules towards the nucleus; ASFV protein p54 (E183L) found in the inner membrane of the virion (Fig. 1.5) has been shown to interact with dynein to hijack the cytoskeletal motor protein.[62] Acidification within late endosomes triggers fusion of the inner membrane with the endosome, releasing the core into the cytoplasm.

Viral genome replication and virion assembly occur in perinuclear viral factories, specialized regions associated with the ER, which also facilitate inner membrane acquisition for virion morphogenesis (Fig. 1.7).[63] Structural proteins, synthesized as polyproteins, undergo processing by the viral protease S273R to form mature virion components.[64] Newly assembled virions acquire their inner envelope from collapsed

ER cisternae and are transported to the plasma membrane along microtubules exploiting kinesin-dependent transport.[52, 65, 66]

Virus egress occurs via several pathways: budding at the plasma membrane to produce extracellular enveloped virions, virological synapse employing apoptotic bodies, or through cell lysis, since non-enveloped ASFV virions are also infectious.[52, 58, 66, 67]

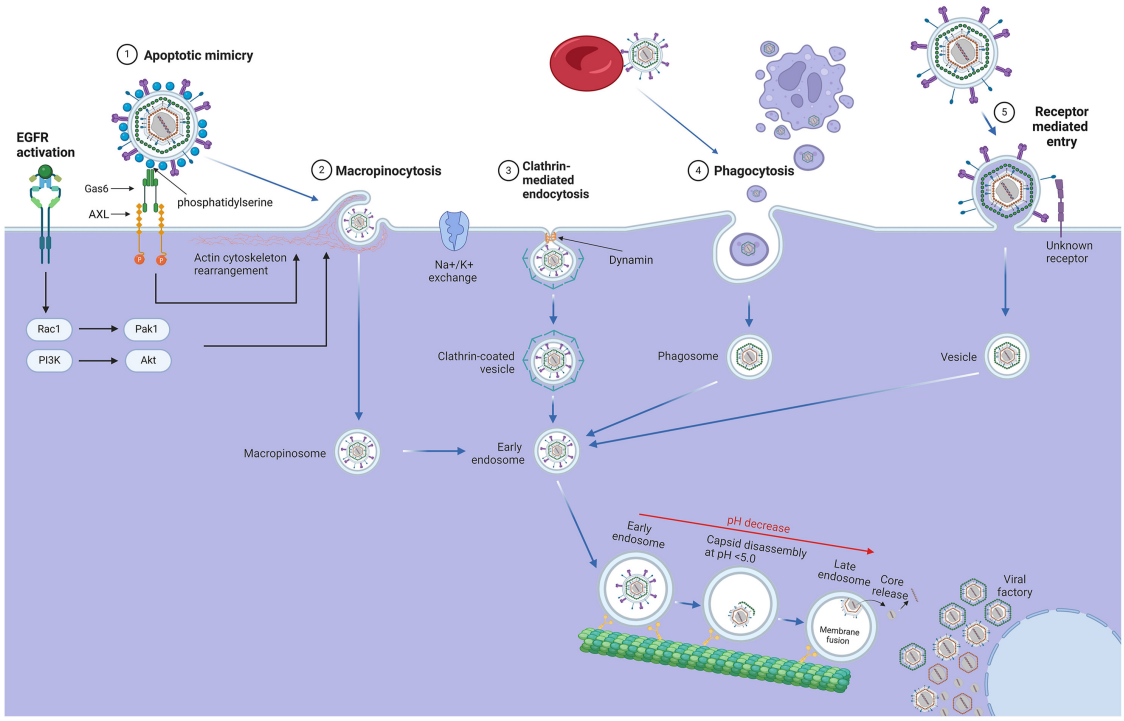

Figure 1.6: ASFV Cell Entry Mechanisms. Representation of all proposed mechanisms of cell entry for ASFV. The virus can enter cells using: apoptotic mimicry **(1)**, macropinocytosis **(2)**, clathrin-mediated endocytosis **(3)**, phagocytosis **(4)**, or a yet unidentified specific receptor mediated endocytosis **(5)**. Transport of endosomes along microtubules, and their acidification leading to perinuclear core release, represented at the bottom right. Created with Biorender.com and adapted from Hooper et al. [53].

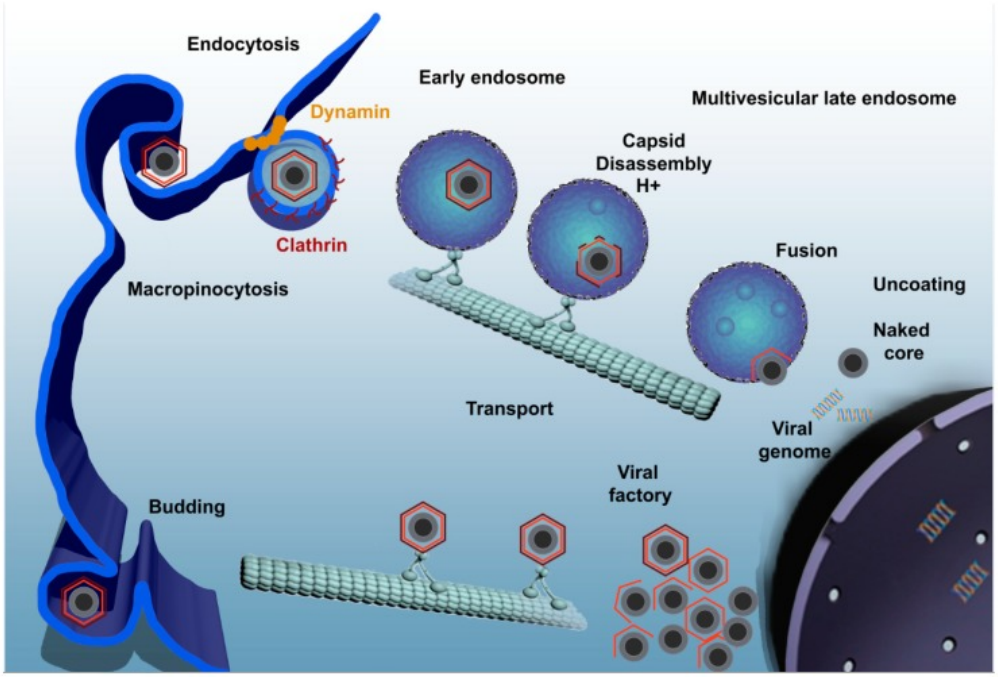

Figure 1.7: ASFV Replication Cycle. Simplified schematic of viral replication cycle within a host cell. The virus enters cells followed by viral decapsidation in mature endosomes. After cytoplasmic replication and assembly in viral factories, virions exit through exocytosis or apoptotic bodies. Adapted from Galindo et al. [67].

1.2.2 Genome Structure and Organisation

The ASFV genome comprises a linear double-stranded DNA molecule encoding between 150-200 ORFs that are closely spaced and read from both DNA strands (Fig. 1.8).[6, 7] These genes encode a diverse array of proteins including structural components, non-structural proteins involved in assembly, various enzymes for viral processes, and proteins that modulate host responses.[8] The variance observed amongst different isolates is mainly due to the gain or loss of multigene family (MGF) genes, adjacent to the terminal ends of the genome.[6, 16]

While many viral proteins are highly conserved between different ASFV isolates, a significant number remain of unknown function. The lack of structural homology with well-characterised proteins makes it challenging to infer their functions. The genome organisation reflects a strategic arrangement, with conserved central regions encoding essential viral functions, while the more variable terminal regions contain the MGFs that facilitate host adaptation.

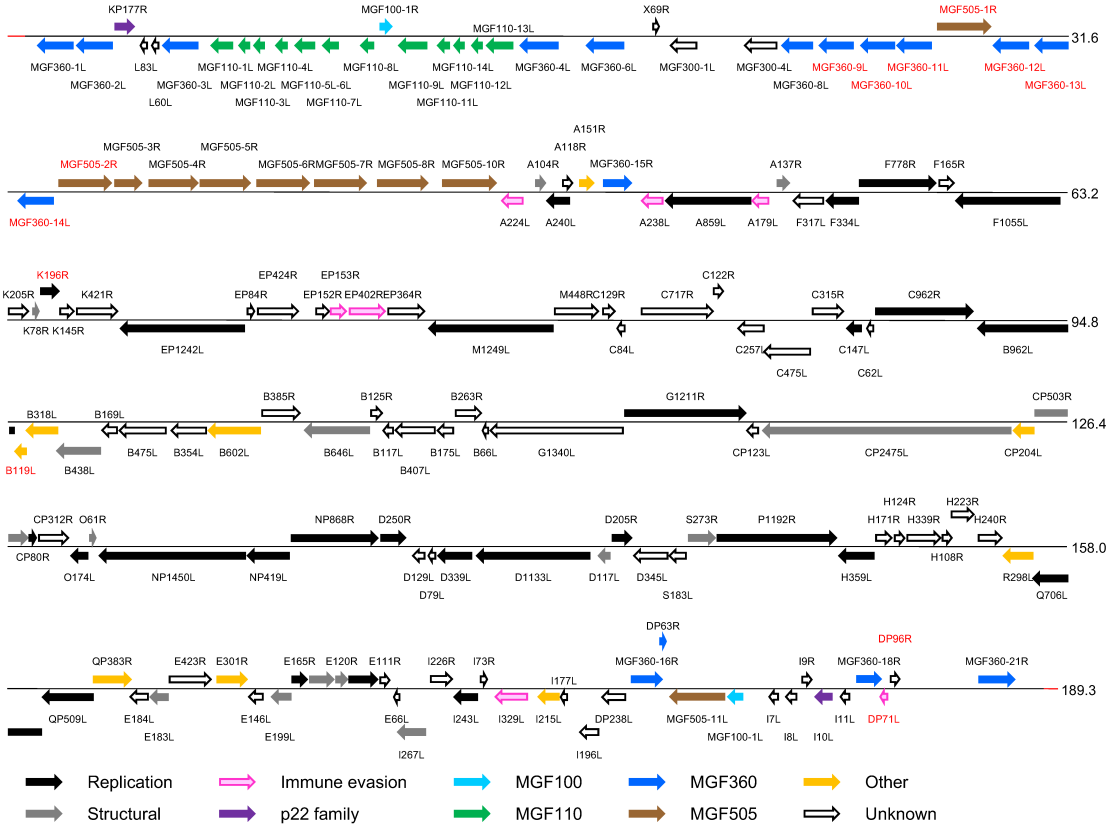

Figure 1.8: African Swine Fever Virus Genome Organigram. The organisation of ORFs on the genome of the virulent ASFV isolate Georgia 2007/1 is shown. ORFs are displayed as arrows to indicate their size and direction they are read. The colours correspond with ORFs known functions. Black indicates ORFs encoding enzymes and factors involved in genome replication, repair or transcription. Grey indicates ORFs encoding structural proteins. Pink indicates ORFs encoding proteins involved in evading the host defences. Turquoise, blue, green, brown and mauve indicate members of multigene families. ORFs encoding proteins with other predicted functions are shown in yellow. ORFs encoding proteins of unknown function are shown in white. Adapted from Dixon et al. [8].

As expected from a virus which replicates in the cytoplasm, segregated from the host's nucleus and its molecular machinery within, ASFV genes do not contain introns and transcripts are therefore not spliced.[8] This genomic organisation enables efficient viral replication independent of host nuclear functions, with the virus encoding its own transcriptional and DNA replication machinery. The virus also encodes DNA proofreading and repair mechanisms to counteract the effects of mutations, derived namely from oxidative damage during replication.[68]

1.2.3 Multigene Family (MGF) Proteins

Much of the genetic variation in ASFV happens within the MGF genes, which represents roughly 30% of its genome and are associated with virulence. MGFs are composed of 5 clusters of paralog genes (horizontally evolved) at the terminal ends of the ASFV genome.[8] The MGF family members are named after the average number of codons in each cluster, and, although the number of individual genes in each cluster varies by ASFV isolate, each cluster contains 2-19 single paralog genes.[69]

The terminal location of the MGFs is particularly significant as these regions are more susceptible to recombination and gene duplication events, facilitating rapid viral adaptation.[8] Their immediate early expression suggests a critical role in establishing infection and modulating early host responses.[7, 14] The localisation of these genes at the terminal ends of the genome as well as their function in immune evasion and immediate early expression, all parallel how poxviruses organise interferon inhibiting genes in their genomes.[12]

The study of how these genes modulate host immunity to enable viral replication will inform future efforts to develop ASFV vaccine candidates. Rather than relying exclusively on trial and error, researchers will benefit from better informed decisions regarding which genes to delete from virulent isolates to achieve sufficient attenuation to make a safe vaccine candidate, whilst eliciting a sufficient immunogenic response. This basic research into ASFV virology is fundamental and any specific knowledge gained regarding viral immune evasion mechanisms can inform vaccine development, even across different genotypes when homologous viral genes can be identified, ultimately accelerating efforts to contain ASF.

1.2.4 Host Cell Tropism

ASFV infection exhibits a permissive cellular tropism, preferentially targeting cells of myeloid lineage.[70] The virus primarily infects monocytes and macrophages (m-MΦ), with the latter becoming particularly susceptible after reaching their intermediate stage of differentiation.[71, 72] m-MΦs are immune cells, involved in antigen presentation, and, thus, central to T-cell-mediated immunity. When pigs

are infected with virulent strains of ASFV, their m-MΦs are overwhelmed by viral replication and depleted before the animal's adaptive immune system has a chance to achieve cellular immunity, a prerequisite to clear the infection.[73]

Macrophages exhibit remarkable phenotypic plasticity, modifying their protein expression and functional profiles in response to environmental signals. This plasticity enables specialised functions ranging from pro-inflammatory responses (M1 or classically activated macrophages) to tissue repair and anti-inflammatory homeostasis (M2 or alternatively activated macrophages).[74] M1 macrophages secrete pro-inflammatory cytokines like TNF-α (tumor necrosis factor alpha), IL-1β (interleukin-1 beta), and IL-12 (interleukin-12), promoting microbicidal activity, while M2 macrophages produce anti-inflammatory mediators such as IL-10 (interleukin-10) and TGF-β (transforming growth factor beta) that support tissue repair and homeostasis.[74] Virulent ASFV strains have been shown to infect both M1 and M2 populations, though viral replication occurs more rapidly and efficiently in monocyte-derived M2 macrophages compared to M1 populations, while attenuated isolate NH/P68 demonstrated a reduced ability to replicate in M1 macrophages.[71] This differential susceptibility suggests the virus may exploit macrophage plasticity to enhance its replication.

The virus is not reported to require a specific receptor for cell entry, some receptors associated with myeloid cells have been reported to facilitate viral entry in mononuclear cells, but they do not constitute a classical nor exclusive receptor-mediated mechanism for cellular entry and, if there is one, it remains uncharacterised (refer to section 1.2.1).[61] ASFV's permissive tropism means it can infect a wide range of cells (i.e. neutrophils, megakaryocytes, tonsillar epithelial cells, hepatocytes, kidney cells, granulocytes, plasmacytoid dendritic cell (pDC)), *in vivo* this happens at the later stages of disease, after viraemia is established.[75–77]

The preferential targeting of myeloid cells is significant as these cells are specialized in producing pro-inflammatory cytokines and IFNs, which are crucial for orchestrating immune responses.[74, 78] Virulent ASFV strains demonstrate enhanced replication efficiency in IFN-activated macrophages compared to attenuated strains

in vitro.[71, 79] Notably, while virulent isolates produce low levels of IFN in cultured macrophages, infection *in vivo* is characterized by cytokine storms and elevated IFN levels, suggesting systemic dysregulation of immune signalling contributes to pathogenesis.[80, 81] Understanding these interactions between ASFV and myeloid cells remains crucial for both basic research and the development of live attenuated vaccines (LAVs), as these cells serve as the primary platform for studying viral replication dynamics and immune responses to deletion mutants *in vitro*.[82]

1.2.5 Pathology

As obligate parasites, large DNA viruses, which, like ASFV, manage to achieve cytoplasmic replication, have had to evolve many effective countermeasures against the molecular barriers to infection that their natural hosts co-evolve. This evolutionary process over millions of years generally leads to a molecular equilibrium of infection where the virus successfully replicates without a high mortality in natural hosts.[83] However, when a virus jumps to another host, which is related enough to the natural host to be permissive towards viral replication but has not co-evolved its molecular defences with the virus, this can quickly overwhelm the new host's immunity, manifesting as a more severe pathological picture often with increased lethality. We find examples of this phenomenon with human immunodeficiency virus, influenza or coronaviruses, which in recent decades have threatened human and animal health through antigenic shift or zoonosis events.[83–85]

The clinical course of ASF varies greatly between acute, unapparent and chronic forms, depending on the host species and the ASFV isolate.[2, 3, 86] Highly virulent strains of ASFV cause acute signs 4-7 days post-infection (dpi) in domestic pigs, leading to high fever, loss of appetite, and lethargy; as the disease progresses, pigs present with haemorrhagic lesions in their mucosa and skin, respiratory distress, bloody vomit and diarrhoea, the animals usually die 7-10 dpi due to blood loss and systemic organ failure, with a mortality of nearly 100%.[87]

Sub-acute forms of the disease present with moderate to high fever and pronounced vascular changes, including haemorrhages and oedema, with mortality

ranging from 30-70% between 7-20 dpi.[87, 88] This presentation is typically associated with infection by moderately virulent or attenuated ASFV variants in domestic pigs.[87] Chronic forms of ASF are characterized by less severe clinical signs such as growth retardation and respiratory distress, but can persist for several months.[2, 87] Unlike acute or sub-acute forms, chronic ASF lacks vascular lesions but often presents with secondary bacterial infections leading to complications such as pneumonia.[87] Chronic disease is primarily caused by low-virulence isolates, such as the genotype I NH/P68 strain, which might have emerged from unsuccessful early vaccine trials in the Iberian Peninsula.[87]

1.2.6 Pathophysiology

The pathophysiology of ASF is characterised by severe disruption of immune homeostasis. Following initial infection of monocytes and macrophages in tonsils and lymph nodes draining the site of viral entry, ASFV rapidly disseminates to secondary lymphoid organs, particularly the spleen and lymph nodes.[89] During *in vivo* infection, an increase in pro-inflammatory cytokines coincides with the appearance of haemorrhagic fever signs.[90, 91] This dysregulation of cytokine production, particularly elevated levels of IL-1α (interleukin-1 alpha), IL-6 (interleukin-6), and TNF-α, contributes to vascular damage and the characteristic haemorrhagic manifestations of the disease.[90] High levels of interferon alpha (IFN-α) are also detected *in serum* as early as 3 dpi in pigs infected with virulent isolates,[92] making IFN an early correlate of infection and virulence.

A key feature of acute ASF pathogenesis is the massive apoptosis of lymphocytes in lymphoid tissues, particularly T and B cells, despite these cells not being directly infected by the virus.[89] This depletion of lymphocytes, driven by the pro-inflammatory cytokines released from infected macrophages, critically impairs the host's ability to mount an effective adaptive immune response.[89, 91] The destruction of infected mononuclear cells further releases cellular components that activate endothelial cells and impair coagulation, contributing to haemorrhagic signs.[81, 91] Once viraemia is established, ASFV infection extends beyond mononuclear cells

to endothelial cells, hepatocytes, and other cell types, leading to widespread tissue damage and organ dysfunction.[1, 87, 93] This systemic spread, combined with the immunological dysregulation and lymphoid depletion, ultimately results in the severe clinical manifestations characteristic of acute ASF.

1.3 Host Innate Immunity

In the context of viral infection, the host innate immune system consists of the molecular barriers to infection that viruses, as obligate parasites, must overcome to successfully replicate within a host cell.[94] ASFV preferentially infects monocytes-macrophages, which are specialised immune cells, yet virulent strains completely overwhelm *S. scrofa* hosts before they can ever clear this infection.[95] To make effective vaccines against ASF, we will require insight into the molecular mechanisms ASFV employs to subvert host innate immunity.

1.3.1 Overview of Innate Immune Sensing

Host cells employ multiple families of pattern recognition receptors (PRRs) to detect viral infection through recognition of conserved molecular signatures known as pathogen-associated molecular patterns (PAMPs). For dsDNA viruses like ASFV, the classical cytosolic sensor is cyclic GMP-AMP synthase (cGAS), which recognises cytoplasmic dsDNA and catalyses the synthesis of 2'3'-cGAMP (cyclic guanosine monophosphate–adenosine monophosphate). This cyclic dinucleotide binds to stimulator of interferon genes (STING), triggering its translocation from the ER to the Golgi Apparatus and the general perinuclear region, where it activates downstream signalling.[96–98]

Additional cytosolic sensors include: RNA polymerase III, which can transcribe viral DNA into RNA ligands for RIG-I-like receptors (RLRs) such as retinoic acid-inducible gene I (RIG-I); and melanoma differentiation-associated protein 5 (MDA5) which can sense cytosolic dsRNA.[99, 100] These RLRs signal through the mitochondrial antiviral-signalling protein, MAVS, to activate downstream immune responses. The endosomal compartment and the cytosolic membrane are monitored by Toll-like receptors (TLRs), which recognize various PAMPs, including: exogenous nucleic acids and their diverse motifs, glyco-/lipo-proteins.[101]

PRR-mediated signalling converges on two major cascades: the interferon regulatory factor (IRF) and nuclear factor kappa-light-chain-enhancer of activated B cells (NF-κB) pathways. The IRF pathway primarily involves TANK-binding

kinase 1 (TBK1)/inhibitor of nuclear factor kappa B kinase subunit epsilon (IKKε)-mediated phosphorylation of interferon regulatory factor 3 (IRF3) and interferon regulatory factor 7 (IRF7), while the NF-$\varkappa$B pathway requires activation of the I$\varkappa$B kinase (IKK) complex to release NF-$\varkappa$B from its inhibitor, I$\varkappa$B.[102] Both pathways ultimately lead to the production of type I IFNs and inflammatory cytokines.

1.3.2 Type I Interferon Induction

Phosphorylation of IRFs on specific serine residues results in their homo- or hetero-dimerization. Nuclear translocation of activated IRFs is facilitated by importin-α proteins, which recognize nuclear localization signals exposed by IRF dimerization.[103] For IFN-β induction, IRF3 homodimers, or IRF3/7 heterodimers, cooperate with NF-$\varkappa$B and additional transcriptional co-activators to form enhanceosomes that enable a strong activation of the promoter.

NF-$\varkappa$B signalling occurs in parallel to IRF activation, promoting the induction of IFN-β, pro-inflammatory chemokines and cytokines. Upon PAMP detection, the IKK complex [IKKα/β kinase subunits and scaffolding NF-$\varkappa$B essential modulator (NEMO) subunit] phosphorylates I$\varkappa$B proteins, triggering their degradation, thus releasing NF-$\varkappa$B dimers (p65/p50), exposing their nuclear localisation signal and enabling their translocation into the nucleus for enhanceosome assembly.[104]

The E3 ubiquitin ligases TNF receptor-associated factor 3 (TRAF3) and TRAF6 coordinate PRR signalling through distinct but complementary pathways. TRAF3 primarily facilitates TBK1/IKKε-mediated phosphorylation of IRF3/7, while TRAF6 activates the IKK complex through Transforming growth factor-β-activated kinase 1 (TAK1).[105] In TLR3-mediated responses, the adaptor protein TIR-domain-containing adapter-inducing interferon-β (TRIF) engages both pathways simultaneously, recruiting TBK1 through TRAF3 while activating NF-$\varkappa$B via TRAF6.[105, 106] This overlap of signalling cascades ensures robust antiviral responses.

In the nucleus, recruitment of CREB binding protein (CBP) and p300 is essential for enhanceosome assembly and subsequent IFN-β transcription.[107] The initial wave

of IFN-β production leads to the expression of various interferon stimulated genes (ISGs), including C-X-C motif chemokine ligand 10 (CXCL10) and IRF7.

The induction of IRF7 transcription enables cells to mount a second wave of type I IFN production (Fig. 1.9). Unlike IFN-β, IFN-α genes contain distinct promoter elements that can be activated by IRF7 homodimers or IRF3/IRF7 heterodimers.[108] This amplification loop through IRF7 is particularly important in cells that maintain low basal IRF7 levels.[109] However, specialized interferon-producing cells like pDCs and other myeloid cells constitutively express IRF7, enabling rapid production of both IFN-β and IFN-α upon infection.[110]

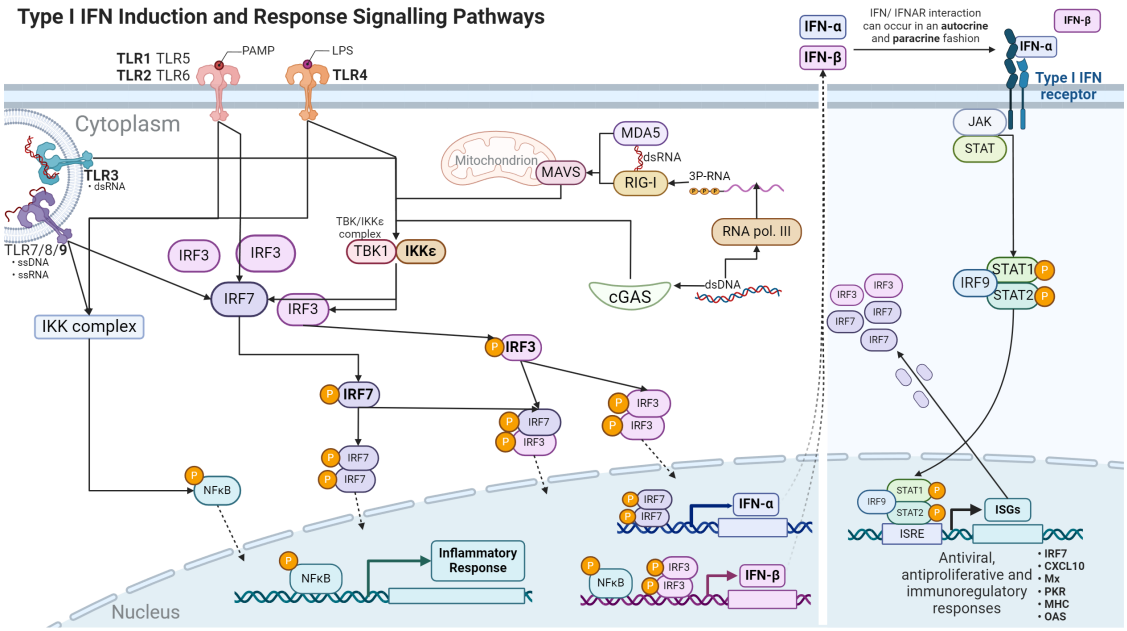

Figure 1.9: Type I IFN Induction and Response Signalling Pathways. Overview of the pathways involved in the induction and signalling of type I interferons (IFN-α and IFN-β). Key pathways include TLR, RLR, and cGAS-STING, which lead to the activation of IRF3 and IRF7, inducing type I IFN production. IFNs then activate the JAK-STAT pathway, resulting in the transcription of ISGs that mediate antiviral and inflammatory responses. Created with Biorender.com.

1.3.3 Type I IFN Response

Once activated, IFN acts as a signalling protein that stimulates an antiviral environment in the infected and nearby cells by inducing the expression of genes that inhibit viral replication, alter the cellular metabolism, and activate immune

responses. IFN binds to the interferon-α/β receptor (IFNAR)1/2 hetero-dimer inducing downstream pathways that act by altering the expression of over 300 genes aimed at limiting viral replication, known as ISGs[111, 112].

Each IFNAR monomer associates with intracellular proteins which facilitate signal transduction once the receptor becomes active upon ligand binding and posterior dimerization. IFNAR1 is associated with tyrosine kinase 2 (TYK2); IFNAR2 with Janus kinase 1 (JAK1) and signal transducer and activator of transcription (STAT)1/2. Activation through this pathway leads to the phosphorylation and dimerization of STAT1/2 and their consequent nuclear localisation, whereupon STAT1/2 forms a hetero-trimer with interferon regulatory factor 9 (IRF9), known as interferon-stimulated gene factor 3 (ISGF3).[111] ISGF3 binds to the interferon-stimulated response element (ISRE) of ISG promoters in the host genome leading to the induction of a large number of ISGs. These include cytokines, chemokines and IRFs which promote and enhance an antiviral state in the cell and its surroundings.[102, 113] To survive and thrive, viruses have evolved a myriad of molecular mechanisms to avoid, inhibit and subvert innate immunity (Fig. 1.9).

1.3.4 Interferon Regulatory Factor 7 (IRF7)

IRF7 plays a dual role in antiviral immunity as both a key transcription factor in IFN induction and an ISG.[109, 114] While most somatic cells maintain low basal IRF7 levels and primarily produce IFN-β through IRF3 homodimers binding to the IFN-β promoter, myeloid cells, which ASFV preferentially infects, express higher basal levels of IRF7.[110] This enables rapid production of both IFN-β and multiple IFN-α subtypes through IRF3/IRF7 heterodimers and IRF7 homodimers binding to distinct promoters.[108]

IRF7 activity is tightly regulated through multiple post-translational modifications, including phosphorylation by IKKε as described above, and neddylation mediated by ubiquitin-like modifier activating enzyme 3 (UBA3).[115, 116] These modifications control IRF7's stability, nuclear translocation, and DNA-binding activity. The essentiality of these modifications for IRF7 function makes their

regulatory machinery potential targets for viral interference, highlighting the complex interplay between viral evasion strategies and host immune regulation.

Myeloid neddylation is a crucial post-translational modification that involves the covalent conjugation of the ubiquitin-like modifier protein, neural precursor cell expressed, developmentally down-regulated 8 (NEDD8), to a substrate. UBA3 is the catalytic subunit of the only known NEDD8-activating enzyme (NAE) complex, a heterodimer with the scaffold amyloid precursor protein-binding protein 1 (APPBP1) that mediates IRF neddylation.[117] The importance of UBA3-mediated neddylation is highlighted by the fact that without this modification, nuclear translocation of IRF7 and the subsequent induction of type I IFN are prevented.[117–119] This modification promotes IRF7 interaction with the nuclear import machinery and increases binding to DNA promoter sequences, improving IRF7 stability, nuclear translocation, and transcriptional activity.[118, 119]

Because it has only been described relatively recently as a post-translational modification, the particulars of neddylation function in the context of ASFV infection remain uncharacterised. However our understanding of neddylation's function during infection has been informed through progress in other fields of research, such as: work with oncolytic virotherapy in humans has revealed that the inhibition of neddylation promotes viral infection in resistant cells,[120] and research with RNA viruses has shown how IRF7 neddylation promotes host innate immunity[119].

1.3.5 Role of Cullin-RING-Ligase Machinery in IFN Signalling

Cullin-RING E3 ubiquitin ligase (CRL) complexes represent a major cellular mechanism for targeted protein degradation in immune regulation. This E3 ubiquitin ligase machinery primarily facilitates K48-linked polyubiquitination, marking specific proteins for proteasomal degradation.[121] The molecular structure of CRLs enables precise substrate recognition and processing through distinct combinations of scaffold and adaptor proteins (Fig. 1.10).

Cullins represent the best-characterized targets of neddylation, a post-translational modification essential for CRL function. The covalent attachment of NEDD8 to cullins induces conformational changes that enhance the complexes' ubiquitin ligase activity, by regulating their stability.[122] This modification is crucial for CRL-mediated protein degradation; its inhibition disrupts homeostasis, increasing permissiveness to viral infection in various contexts.[120]

The recruitment of specific CRL machinery is determined by distinct box motifs in substrate receptor proteins. The suppressor of cytokine signalling (SOCS)-box motif recruits Elongin B/C adaptor proteins and Cullin5, directing the assembly of CRL5 complexes with the RING protein RBX2. In contrast, the von Hippel-Lindau (VHL)-box, while also containing a BC-box motif that binds Elongins B/C, specifically recruits Cullin2 through its distinct Cul2-box, forming CRL2 complexes with RBX1 (Fig. 1.10). This molecular selectivity enables different substrate receptors to assemble distinct CRL complexes for targeted protein degradation.

The central role of CRLs in immune regulation makes them attractive targets for viruses evolving to promote the degradation of host immune factors. Some ASFV proteins, such as MGF360-12L (12L) and MGF505-1R (1R), contain motifs that may allow them to interact with these cellular degradation pathways to target immune signalling components.[124] Other viral proteins (i.e I215L) share structural and functional homology with cellular ubiquitin ligases.[125] Understanding how viruses manipulate CRL machinery provides crucial insights into viral pathogenesis and potential therapeutic strategies.

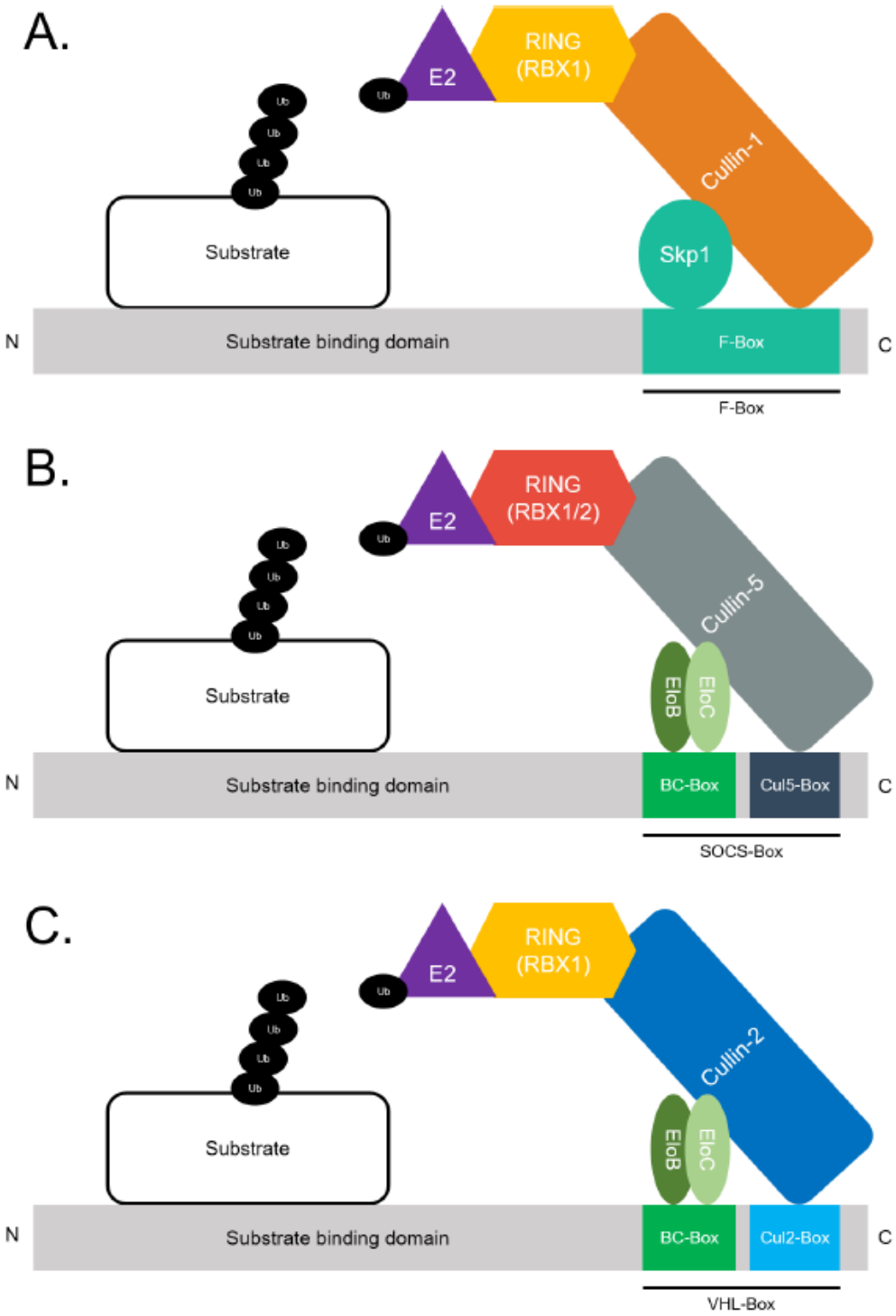

Figure 1.10: Molecular Architecture of Cullin-RING Ligase Complexes with Different Box-Motif Substrate Receptors. Highlights the difference between proteins containing the **(A)** F-Box, **(B)** SOCS-Box, and **(C)** VHL-Box motifs and the division of the VHL/SOCS-Box motif in to the two key components, the BC-Box, and the Cul-Box. Adapted from Petroski et al. [123].

1.4 ASFV Immune Evasion: Type I Interferons

Much like other large DNA viruses, ASFV targets most, if not all, aspects of the host innate immunity, modulating, amongst other things: overall protein synthesis, antiviral signalling and cellular apoptosis. The urgency brought about by the global spread of ASF has greatly expanded the breadth of available literature in the field of ASFV immune evasion. This inflow of knowledge is helping to advance the field and support our same efforts; however, in consideration for the reader and in the interest of clarity for the communication of our research, this section will limit its review of ASFV immune evasion to inhibition of the induction and response to type I IFN. We will also contextualise our research by summarising any previous work.

Given our research's focus on the MGF interferon inhibiting family, this section aims to explore the plethora of mechanisms employed by ASFV to inhibit type-I interferon induction and signalling, in particular. However, the means that ASFV employs to evade innate immune sensing and activation are complex and notably extend beyond IFN suppression. For example, the viral protein CD2v, which promotes virulence by enabling the systemic spread of the virus through haemadsorption, has also been shown to interact with host factor CSF2RA to regulate apoptosis via the JAK2/STAT3 pathway, inhibiting it during early infection and promoting it later.[126] Another important infectivity factor, EP152R, inhibits overall protein synthesis by inducing ER stress, triggering PERK/eIF2α pathway;[127] and the nuclear viral protein, I73R, also reduces protein expression by preventing the export of cellular mRNAs.[128] Some late viral genes can also promote the induction of type I IFNs, such as A238L, which favours the activation of TBK1/IRF3 signalling;[129] or MGF110-9L, which promotes IFN induction by weakening the autophagic degradation of TBK1.[130]

1.4.1 Inhibition of Type I Interferon Induction

The MGF proteins of ASFV have been reported to employ diverse strategies to inhibit type I IFN induction, with many studies focusing on their interactions with components of the cGAS-STING-mediated DNA sensing pathway (Fig. 1.11).

Several MGF proteins are reported to directly interact with and modulate STING function - MGF505-2R, -6R and -7R have been shown to target STING through mechanisms including preventing its dimerization and promoting its degradation.[131–133] Other MGF proteins are described to target downstream signalling components: MGF360-11L and MGF505-3R (3R) have been shown to interact with TBK1 to impair its kinase activity.[134, 135] The NF-$\varkappa$B arm of IFN induction is also targeted, with recent studies showing MGF300-2R and -4L promote the degradation of IKK complex components.[136, 137] Recent *in vitro* studies have also revealed that MGF360-12L (from the SY18 isolate) and MGF360-14L (14L) target multiple components of this pathway, with MGF360-12L reported to inhibit both TBK1 and IRF3 activity while competing with p65 for nuclear transport,[138, 139] and 14L has also been shown to promote IRF3 degradation.[140] Refer to Table 1.3 for a summary review of the available literature regarding inhibition of type I IFNs by MGFs.

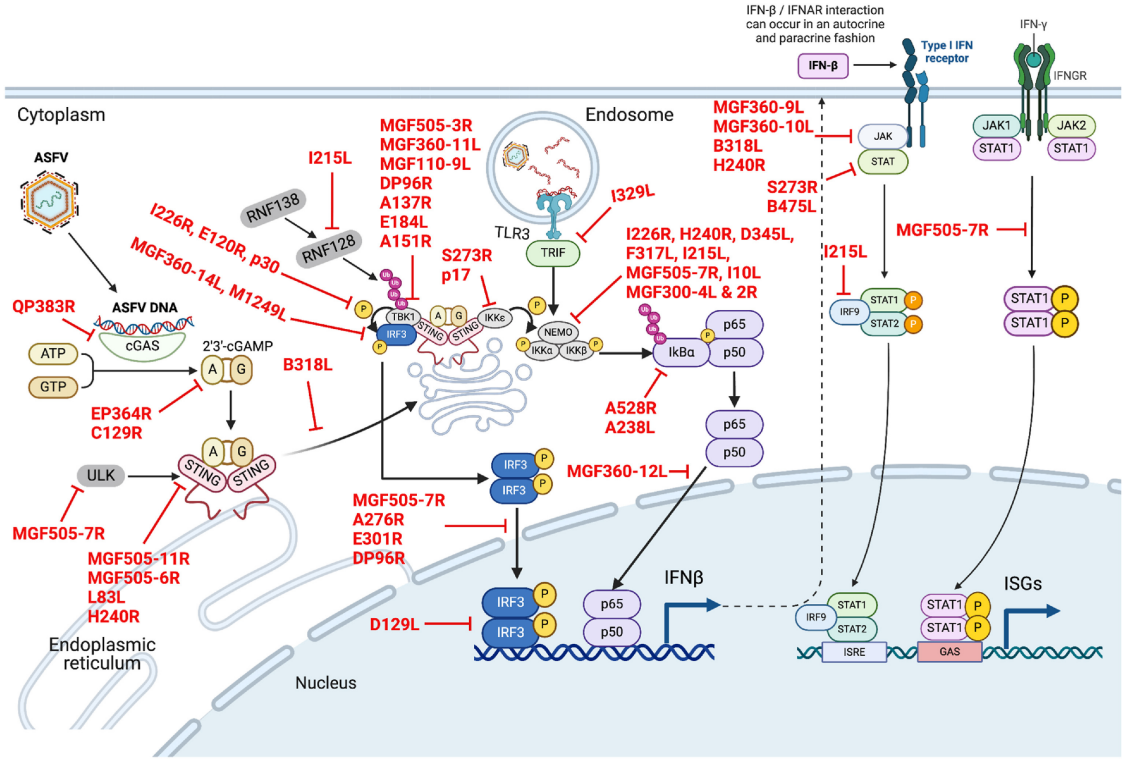

Figure 1.11: Antagonism of DNA Sensing Pathways by ASFV. Summary of where reviewed ASFV genes disrupt IFN-β induction signalling via the TRL3 and cGAS-STING pathways. Described genes are highlighted in red and point to the pathways and host proteins they are reported to disrupt. Created with Biorender.com and adapted from Chaudhari et al. [141].

ASFV Gene	Host Target(s)	Mechanism/Effect	References
MGF300-2R	IKKα IKKβ	Promotes degradation of targets via recruitment of TRIM21, resulting in poly-ubiquitination and Tollip mediated autophagy	Wang et al. [136] and Lu et al. [142]
MGF300-4L	IKKβ IκBα	Promotes proteasomal degradation of IKKβ and the stability of IκBα	Wang et al. [137]
MGF360-11L	TBK1 IRF7	Interacts with TBK1, decreases its phosphorylation; interacts with IRF7	Yang et al. [134]
MGF360-12L	Importin-α family TBK1 IRF3	Competes with p65 for nuclear transport Dose dependent inhibition of IFN-β induction by reducing overexpression of IRF3 and TBK1 *in vitro*	Zhuo et al. [138] and Chen et al. [139]
MGF360-14L	IRF3	Recruits TRIM21 to increase IRF3 K63-linked poly-ubiquitination, claiming to promote degradation	Wang et al. [140]
MGF505-2R	STING	Interacts with STING and its deletion promotes downstream signalling	Sunwoo et al. [131]
MGF505-3R	TBK1	Interacts with cGAS/TBK1/IRF3 to target TBK1 for degradation	Cheng et al. [135]
MGF505-4R	TRAF3	Interferes with the induction of type I IFNs	Dupré et al. [143]
MGF505-6R	STING	Prevents dimerisation and promotes its degradation through the autophagy-lysosomal pathway	Yao et al. [132]
MGF505-7R	TBK1 IRF7 STING p65 IKKα	Multiple targets: affects TBK1 phosphorylation, interacts with IRF7, promotes STING degradation, binds p65 Rel domain (inhibiting its phosphorylation and nuclear translocation), and interacts with IKKα	Li et al. [133], Yang et al. [144], Li et al. [145], and Liu et al. [146]

Table 1.2: ASFV MGF-Host Proteins Interactions Inhibiting IFN Induction. This table contains a summarised review of ASFV genes, their host targets, and how they inhibit type I IFN induction. This table is based on review of the available literature, incorporating sources collected in Netherton et al. [147] up to its publication in 2023, with additional updates from further review.

Beyond the MGFs, ASFV encodes numerous other proteins that have been shown to contribute to dampening IFN induction through complementary mechanisms targeting the pathway at multiple points (Tab. 1.3). Several viral proteins target the

pathway's initiation - B175L is reported to competitively inhibit cGAMP binding to STING, while B318L and L83L are shown to prevent STING trafficking and promote its degradation respectively.[148–150] Multiple viral proteins including DP96R, E120R, and E301R directly target the downstream effector IRF3 to prevent its activation and nuclear translocation.[151–153] The virus also employs proteins like A238L and I226R to inhibit NF-κB signalling through distinct mechanisms.[154, 155] Refer to Table 1.3 for a summary review of IFN induction inhibiting ASFV genes other than MGFs. While current literature has extensively characterized viral interference with DNA sensing pathways, this focus may reflect a research bias rather than the full scope of ASFV's immune evasion strategies, this bias may occlude other important viral mechanisms targeting host pathways that remain to be revealed. Indeed other immune sensing mechanisms are also targeted - I329L specifically inhibits TLR-mediated signalling by targeting TRIF,[156] while I267L blocks RNA polymerase III-RIG-I-mediated responses by disrupting Riplet-mediated activation of RIG-I.[157] These diverse strategies highlight the complex array of mechanisms that ASFV employs to evade host innate immunity.

ASFV Gene	**Host Target(s)**	**Mechanism/Effect**	**References**
A137R	TBK1	Directly interacts with TBK1 leading to its degradation through autophagy	Sun et al. [158]
A151R	TRAF6	Directly interacts with E3 ligase TRAF6, promoting its degradation, therefore preventing TBK1 K63-linked poly-ubiquitination and subsequent phosphorylation	Li et al. [159]
A238L	p65	Binds p65, inhibits κB element binding, impairs p65-p300 interaction	Revilla et al. [154] and Granja et al. [160–162]
A276R	IRF3	Downregulates IFN-β transcription	Correia et al. [163]
B175L	STING cGAMP	Binds to both targets, competitively inhibiting their interaction and downstream IFN-β induction	Ranathunga et al. [148]

Continued on next page...

ASFV Gene	Host Target(s)	Mechanism/Effect	References
B318L	STING	Prevents intracellular transport of STING	Liu et al. [149]
D129L	p300	Binds to this transcription co-activator to prevent its interaction with IRF3	Zhang et al. [164]
D345L	IKKα IKKβ	Interacts with both, inhibits IκBα phosphorylation and p65 translocation	Chen et al. [165]
DP96R	IRF3	Interacts with the transcription factor's KPNA binding site, disrupting its nuclear translocation	Dodantenna et al. [151]
E120R	IRF3	Interacts with IRF3, decreasing its interaction with TBK1 and phosphorylation	Liu et al. [152]
E184L	STING	Disrupts STING dimerization, STING-TBK1-IRF3 complex formation and downstream IFN induction	Zhu et al. [166]
E301R	IRF3	Inhibits phosphorylated IRF3 and its nuclear translocation	Liu et al. [153]
EP364R C129R	2′, 3′-cGAMP	Promote degradation of 2′, 3′-cGAMP	Dodantenna et al. [167]
F317L	IKKβ	Suppresses kinase activity	Yang et al. [168]
H240R	STING NEMO	Disrupts STING oligomerisation and promotes NEMO degradation	Zhou et al. [169], Ye et al. [170], and Huang et al. [171]
I10L	IKKβ	Reduces IKKβ phosphorylation and interacts with its N-terminal kinase domain, preventing downstream NF-$\varkappa$B signalling	Chen et al. [172]
I215L	TBK1 IKKβ	Reduces TBK1 activation by degrading RNF128 and suppresses NF-$\varkappa$B activation by interacting with IKKβ	Huang et al. [173]
I226R	NEMO	Increases NEMO ubiquitination leading to proteasomal degradation	Hong et al. [155]
I267L	Riplet	Interacts with this E3 ubiquitin ligase, preventing K63-polyubiquitination and activation of RIG-I. Impairs RNA polymerase III signalling leading to inhibition of IFN-β induction.	Ran et al. [157]

Continued on next page...

ASFV Gene	Host Target(s)	Mechanism/Effect	References
I329L	TLR3 TRIF	Inhibits downstream TLR signalling	Correia et al. [156]
L83L	cGAS STING	Promotes autophagy-lysosomal degradation of STING by recruiting Tollip	Cheng et al. [150]
M1249L	TBK1 IRF3	Inhibits TBK1 phosphorylation; interacts with IRF3 causing its degradation	Cui et al. [174]
p17	STING TBK1 IKKε	Inhibits recruitment of TBK1 and IKKε by STING Regulates the phosphorylation of IRF3 and TBK1; induces STING degradation	Zheng et al. [175] and Wang et al. [176]
QP383R	cGAS	Promotes cGAS palmitoylation to disrupt STING signalling	Hao et al. [177]
S273R	IKKε	Interacts with IKKε and inhibits its interaction with STING	Luo et al. [178] and Li et al. [179]

Table 1.3: ASFV-Host Proteins Interactions Inhibiting IFN Induction. This table contains a summarised review of ASFV genes (excluding MGFs), their host targets, and how they inhibit type I IFN induction. This table is based on review of the available literature, incorporating sources collected in Netherton et al. [147] up to its publication in 2023, with additional updates from further review.

1.4.2 Immune Evasion: Type I Interferon Response

Beyond preventing the initial induction of type I IFN, ASFV has evolved multiple mechanisms to inhibit downstream IFN signalling, targeting key components of the JAK-STAT pathway at various stages. These viral proteins interfere with IFN receptor complex formation, disrupt signal transduction through JAK kinases, and prevent the assembly and nuclear translocation of transcription factor complexes required for ISG expression (See Table 1.4).

The virus employs both MGF and non-MGF proteins to effectively suppress type-I interferon signalling. Among the MGFs, MGF360-9L and MGF360-10L (10L) have been shown to target early signalling events, with 10L reported to promote JAK1 degradation through recruitment of E3 ligase HERC5[180], while MGF360-9L induces degradation of both STAT1 and STAT2 through distinct pathways[181]. MGF505-7R has been reported to exhibit particularly broad activity, promoting

degradation of both JAK1 and JAK2 while also preventing ISGF3 complex formation through interaction with IRF9.[182, 183] Non-MGF viral proteins target similar pathway components through complementary mechanisms - B318L, H240R, and K205R are reported to disrupt IFNAR complex assembly and activation,[149, 184, 185] while others like I215L and S273R promote degradation of STAT2 and IRF9.[186, 187] This multilayered targeting of the JAK-STAT pathway reflects the strong evolutionary pressure on ASFV to suppress this critical antiviral defence.

ASFV Gene	**Host Target(s)**	**Mechanism/Effect**	**References**
A104R	STAT1/2	Interaction unclear but shown to decrease STAT1 phosphorylation and STAT2-dependent ISRE transcription	Chen et al. [188]
B318L	IFNARs	Reduced IFNAR1/TYK2 and IFNAR2/JAK1 interactions	Liu et al. [149]
B475L	STAT2	Interacts with STAT2 C-terminal domain, blocking heterodimerisation with STAT1	Huang et al. [189]
H240R	IFNARs	Interacts with IFNAR1/2 and inhibits interactions with TYK2 and JAK2 respectively Reduces phosphorylation of IFNAR1, TYK2, and JAK1	Ye et al. [184]
I215L	STAT2 IRF9	Causes STAT2 ubiquitination and degradation; targets IRF9 for degradation via autophagy-lysosome pathway	Li et al. [186] and Riera et al. [190]
F778R	STAT1	Impedes nuclear translocation	Chen et al. [191]
K205R	IFNAR1 IFNAR2	Inhibits interaction of IFNAR1/2 with JAK1 and TYK2	Huang et al. [185]
MGF360-9L	STAT1 STAT2	Causes STAT1 degradation via apoptosis and STAT2 via ubiquitin-proteasome pathway	Zhang et al. [181]
MGF360-10L	JAK1	Promotes its ubiquitination and degradation by recruiting E3 ligase HERC5	Li et al. [180]
MGF360-12L	IRF9	Dose dependent inhibition of ISRE-transcription by reducing total protein levels of IRF9 *in vitro*	Chen et al. [139]

Continued on next page...

ASFV Gene	Host Target(s)	Mechanism/Effect	References
MGF505-7R	JAK1 JAK2 IRF9	Interacts with both JAKs causing their degradation: recruits RNF125 for JAK1 and HES5 for JAK2 Inhibits ISGF3 heterotrimer formation through IRF9 interaction, preventing nuclear translocation of the ISG factor complex	Li et al. [182] and Huang et al. [183]
S273R	STAT2	Recruits E3 ubiquitin ligase DCST1 to mediate STAT2 K48 poly-ubiquitination and degradation	Li et al. [187]

Table 1.4: ASFV-Host Proteins Interactions Inhibiting IFN Signalling. This table contains a summarised review of ASFV genes, their host targets, and how they inhibit type-I interferon signalling. This table is based on review of the available literature, incorporating sources collected in Netherton et al. [147] up to its publication in 2023, with additional updates from further review.

1.4.3 Previous Unpublished Work

Several of the proteins encoded by MGF 360 and 505 genes are known to inhibit the IFN response, and the deletion of multiple copies of these genes has been shown to attenuate virulent ASFV[192, 193].

Previous work on MGF360 and 505 families immune evasion revealed significant insights into their structure and function.[124] Both families contain ankyrin (ANK) repeats, protein-protein interaction motifs which are widespread throughout eukaryotic signalling proteins;[124] ANK are rarely found in viruses, except for notable exception of within the *Poxviridae* family.[194] Structural analysis identified putative VHL/SOCS-Box motifs in the N-terminus of both MGF360-12L and MGF505-1R, which mediate the recruitment of CRL complexes. These motifs were validated through protein interaction studies, demonstrating that 12L contains a functional VHL-box enabling interactions with EloB, EloC, and Cul2, while 1R possesses a SOCS-box motif mediating interactions with EloB and Cul5. Both proteins demonstrated strong inhibition of NF-κB and IRF3-dependent transcription, though through distinct mechanisms. MGF505-1R was shown to reduce cellular levels of

the transcriptional co-activator p300 in a SOCS-box dependent manner, while MGF360-12L's mechanism remains to be fully characterized (Table 1.5).

In collaboration with our group, and as part of the ASFV-Int consortium, researchers in France identified UBA3 as a possible binding partner of MGF360-12L by Yeast-2-Hybrid library screening. They also confirmed this interaction by Glutathione *S*-transferase (GST) tagged pull-down (Dr. Grégory Caignard and Dr. Juliette Dupré, Unpublished) (Table 1.5).

The identification of UBA3 as a binding partner of 12L is particularly intriguing, as UBA3-mediated neddylation promotes IRF7 stability, nuclear translocation and transcriptional activity, suggesting a potential mechanism by which ASFV could interfere with IFN signalling. Despite these advances in understanding MGF mechanisms of action, their impact on IRF7-dependent transcription of IFN-α and its subsequent signalling remains largely uncharacterised, representing a crucial gap in our understanding of ASFV immune evasion strategies.

Protein	**Structural Motifs**	**Confirmed Host Interactions**	**Demonstrated Functions**
MGF360-12L	VHL-box TRAF6 binding motif	EloB, EloC, Cul2 TRAF3, TRAF6 UBA3	Inhibits NF-ϰB/IRF3-dependent transcription and IRF3 nuclear translocation
MGF505-1R	SOCS-box	EloB, Cul5	Reduces p300 levels SOCS-box dependent inhibition of NF-ϰB and IRF3 pathways

Table 1.5: Previously Identified Functions of MGF360-12L and MGF505-1R. Summary of structural motifs, experimentally confirmed protein interactions and functions in immune evasion pathways previously described in Connell [DPhil Thesis 2021, 124] and Dupré et al., Unpublished.

1.5 Vaccinology and ASFV Deletion Mutants

The development of a safe and effective vaccine against ASFV remains a critical challenge in animal health. Progress has been hampered by the virus's complexity, the requirement for high-containment facilities for research and vaccine trials, and historically limited funding.[195] Most efforts have focused on developing a LAV that can induce a long-lasting protective immune response with minimal side effects.[43, 196] However, the identification of antigens that can elicit vaccine-mediated protection is challenging, and immune correlates of protection against ASFV are insufficiently identified.[43]

1.5.1 Subunit Vaccines

The development of a subunit vaccine against ASFV remains a critical yet challenging endeavour, historically constrained by limited knowledge of protective antigens and difficulties in selecting optimal delivery systems.[197] Despite identification of immunogenic ASFV proteins, the absence of well-defined correlates of protection has confined progress to empirical approaches through systematic trial-and-error, which is both costly and time-consuming.

Early attempts delivering recombinant structural proteins p30, p54, p72, and p22 (encoded by CP204L, E183L, B646L, and KP177R genes respectively) demonstrated the ability to induce neutralizing antibodies but failed to protect animals against lethal disease.[198] However, work with an E183L-CP204L fusion protein showed enhanced efficacy, generating both neutralizing antibodies and partial protection against severe disease.[199] Similarly, recombinant CD2v (EP402R) showed promise by inducing antibodies that inhibited haemadsorption of infected macrophages and conferred protection in two thirds of pigs challenged.[200]

Significant progress in this approach came from recent work at The Pirbright Institute, where researchers evaluated a pool of 40 ASFV antigens using viral vectors. Through methodical screening, they identified eight antigens that, when delivered via modified vaccinia virus vectors, protected pigs against fatal disease following virulent virus challenge.[201] While this protection was not sterilising and may be

genotype-specific, this approach to antigen selection represents a substantial step forward in ASFV subunit vaccine development.

Despite ongoing challenges with incomplete protection and variable cross-genotype efficacy, subunit vaccines offer distinct advantages including defined composition, differentiation of infected from vaccinated animals (DIVA) capability, and enhanced safety profiles compared to live attenuated approaches. Current research focuses on optimizing antigen combinations and delivery systems to improve vaccine efficacy while maintaining these beneficial characteristics.

1.5.2 Live Attenuated Vaccines

The development of LAVs through targeted gene deletion remains one of the most promising approaches in ASFV vaccine development. This strategy relies on precise genetic modification of virulent ASFV isolates to attenuate their pathogenicity while maintaining immunogenicity.[82, 202] The effective selection of gene candidates for deletion requires a thorough understanding of both gene function and the effects of their deletion on viral pathogenesis. This understanding is crucial for making informed decisions about which genes to select, as deletions must achieve an optimal balance between attenuation and immunogenicity.[193, 202, 203]

Recent advances in genetic manipulation have demonstrated that deletion of interferon inhibitory proteins, particularly combinations of MGF360 and MGF505 genes, can generate promising vaccine candidates.[193, 204] The removal of these genes typically reduces viral replication in macrophages and virulence in pigs while preserving immunogenic potential.[205] This approach has gained significant validation through its recent implementation in Vietnam, where an emergency vaccine utilizing MGF deletions has been deployed, marking one of the first field applications of this strategy,[196] however the genotype I/II hybrid spreading through SE Asia is capable of escaping the genotype II LAV being used.[34]

Research efforts increasingly focus on developing deletion mutants with DIVA capability, allowing differentiation between vaccinated and naturally infected animals - a crucial feature for disease surveillance and control.[206, 207] This consideration

influences both the selection of target genes for deletion and the development of accompanying diagnostic tools.

The manipulation of immune evasion genes has proven particularly effective, with studies showing that deletion of specific interferon inhibitors can reduce pathogenicity, allowing the host to develop protection against virulent isolates. However, the development process faces several challenges, including the need to maintain sufficient immunogenicity for protection and ensure genetic stability to prevent reversion to virulence.[208]

1.5.3 Viral Deletion Mutants

For our research, we utilised a panel of genetically modified ASFV deletion mutants developed at The Pirbright Institute from the virulent genotype II Georgia 2007/1 wild-type (wt) ASFV isolate (Figure 1.12).[205] GeorgiaΔK145R (ΔK145R) was the parental virus for these MGF deletion mutants (Fig. 1.12B-G), because K145R was selected earlier as a candidate marker for DIVA.[205, 209] Different combinations of deletions in the MGFs were observed to reduce virus replication in macrophages and virulence in pigs. Notably, the deletion of two MGFs genes, 12L and 1R, in combination with K145R, from the wt virus (Δ1R12L) (Fig. 1.12E) was sufficient to drastically attenuate virus infection in pigs, although it only protected 2 of 5 pigs against challenge, and additional deletions of MGF360 genes were required to confer higher levels of protection. The deletion of 12L alone from the ΔK145R virus (Δ12L) (Fig. 1.12G) was enough to reduce viral replication in macrophages, underscoring the relevance of this gene for viral replication.[205]

Through recombination, the green fluorescent protein, mNeonGreen, preceded by a promoter of the early viral protein 30 (VP30), was incorporated into the genome of some mutants (Fig. 1.12C-G) to facilitate purification. The promoter for VP30 was selected because this viral protein is produced very early, before viral genomic replication, and is maintained through the viral lifecycle.[210–212]

The levels of IFN-α and the ISG CXCL10 protein detected in the supernatant of cells infected with Δ1R12L were elevated compared to the wt and other deletion

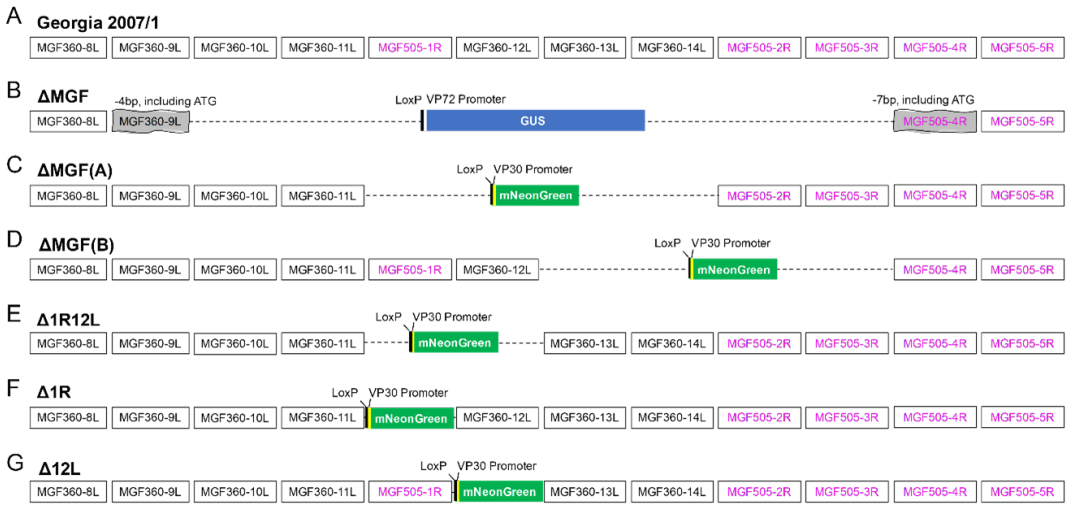

Figure 1.12: Diagram depicting the deletion of MGF genes in recombinant viruses from the Georgia2007/1 isolate. Adapted from Rathakrishnan et al. [205].

mutants, but they were even more greatly increased with GeorgiaΔK145RΔMGF360-12L (Δ12L) infection.[205] This indicates an important role of 12L in the control of IFN expression. Moreover, despite MGFs displaying similar effects in transfected cells, the effect of multiple deletions is not cumulative. This suggests a complex relationship between the different MGFs, perhaps competing for the same host factors or impacting differently on a positive feedback loop. We used these deletion mutants to investigate the importance of MGFs, particularly 12L, and thoroughly delineate the impact these genes have on viral replication and IFN signalling.

1.6 Cell Culture Systems for ASFV Research

The development of effective cell culture systems for ASFV represents a significant challenge in advancing both basic research and vaccine development. ASFV's preferential tropism for cells of myeloid lineage, particularly m-MΦ, has historically limited the available options for virus study and growth.[213] Researchers have necessitated the use of primary porcine macrophages, typically harvested from bone marrow or pig lungs (alveolar macrophages), making ASFV research heavily dependent on animal resources.[213]

Primary macrophages, whilst physiologically relevant, present several technical challenges for large-scale research and vaccine production. These cells exhibit significant biological variability between different pigs and even amongst macrophage subpopulations from the same animal.[61, 214] Furthermore, this variability can affect infection efficiency, potentially complicating the interpretation of experimental results and the standardization of vaccine production processes.[215]

Some success has been achieved in adapting certain ASFV strains to grow in established cell lines, such as Vero cells (African green monkey kidney cells), particularly the BA71V strain.[213] However, these adapted strains display attenuated virulence and do not likely represent field isolates accurately, limiting their usefulness for studying viral immune evasion or developing vaccines.[215] Moreover, most field isolates and virulent strains cannot be propagated in conventional cell lines, necessitating the continued use of primary macrophages.[216]

The development of sustainable cell culture systems is particularly crucial for vaccine production. Current methods relying on primary macrophages are not feasible for large-scale vaccine manufacturing, which require consistent, standardized, and cost-effective production systems.[217] Recent progress in developing immortalized porcine macrophage cell lines promise to help address these challenges.[217–219] Such advances can potentially provide more reliable and scalable platforms for both research and vaccine production, while also aligning with ethical considerations regarding the use of animals in research and our goal to reduce it.

Several groups have reported progress in establishing continuous cell lines permissive to ASFV infection. For example, researchers have developed derivatives of porcine alveolar macrophage cell lines that maintain key characteristics of primary cells while offering the advantages of immortalized lines.[218, 219] However, these systems still need extensive validation to ensure they accurately reflect the virus-host interactions observed in primary cells for them to be effectively used in innate immune evasion research. Their utility for these experiments must first be confirmed through replication studies of known results in primary cells.

The successful development of robust cell culture systems would significantly advance multiple aspects of ASFV research, from basic study of virus-host interactions to the development and production of vaccines. However, different cell lines may be required for distinct uses given that the requirements for vaccine production are to support efficient virus replication; while, for basic virology research, maintaining relevant cellular responses to infection, particularly innate immunity, is crucial for understanding viral pathogenesis and developing attenuated vaccine strains.

1.7 Research Objectives

Building upon the current understanding of ASFV immune evasion mechanisms and the critical need for effective vaccines, our research aimed to characterise how MGF proteins modulate host innate immunity, with particular focus on interferon signalling pathways. We focused our work mainly on the 12L and 1R MGFs due to the published growth defect observed in PBMs infected with deletion mutants lacking these genes and further unpublished data surrounding their hypothetical role in immune evasion as described in section 1.4.3.[205] We pursued three main objectives:

1. To characterise the *in vitro* impact of MGF gene deletions on viral replication dynamics, IFN-α induction and response in primary macrophages. This involved: evaluating viral growth kinetics in the context of different MGF deletions, quantifying the expression of IFN and ISGs using ELISAs and RT-qPCR, and the use of an interferon response inhibitor to distinguish between effects on type I IFN induction versus cellular responses to IFN.
2. To identify and characterise novel molecular mechanisms through which MGF proteins modulate host immunity. This was accomplished by: expressing individual MGF proteins exogenously using cloned constructs, including variants with mutations in previously identified regions of interest; investigating potential protein-protein interactions with host immune factors; assessing the impact of MGF protein expression on interferon pathway components through reporter assays, immunoblotting, and immunofluorescence; and examining their effects on relevant transcription factors and signalling proteins.
3. To evaluate the suitability of a novel immortalized porcine macrophage cell line as an alternative to primary cells for ASFV immune evasion research by: replicating key experiments from primary macrophages in the cell line, and comparing viral replication dynamics and immune responses between experimental systems to assess the reproducibility of results.

These objectives align with the broader goals of supporting ASFV vaccine development through improved understanding of viral immune evasion strategies. By characterising how specific viral proteins modulate host immunity, our findings can

inform rational approaches to viral attenuation for vaccine design. Additionally, our evaluation of alternative cell culture systems supports efforts to reduce dependence on primary cells and hence animal use, whilst also promoting the incorporation of new methods to the field, potentially accelerating both basic research and vaccine development processes.

Through this work, we aimed to contribute fundamental knowledge about ASFV-host interactions and immune evasion strategies, ultimately supporting global efforts to control ASF's significant threat to food security and animal health.

2

Materials and Methods

Contents

2.1 Cell Culture 46
2.1.1 Primary Porcine Bone Marrow Cells 46
2.1.2 HEK293T and Vero Cells 47
2.1.3 PLTA58s 47
2.2 Virus Work 48
2.2.1 Titrations 48
2.2.2 Infections 49
2.3 Inhibitors 49
2.4 RT-qPCR 49
2.5 ELISAs 50
2.5.1 CXCL10 ELISA 51
2.5.2 IFNα ELISA 51
2.6 Cell Viability Assay 52
2.7 Dual-Luciferase® Reporter 52
2.8 Protein Analysis 53
2.8.1 Sample Preparation 53
2.8.2 Immunoprecipitation 53
2.8.3 Immunoblotting 53
2.9 Immunofluorescence 54
2.10 Antibodies 55
2.11 Plasmids 56
2.12 Statistical Analysis 57

2.1 Cell Culture

2.1.1 Primary Porcine Bone Marrow Cells

Porcine bone marrow cells (PBMs) were extracted from the long bones of 4-week-old, outbred pigs. The bones were cleaned with a scalpel to remove all periosteum and cartilage, then the bone marrow was exposed by chopping the bones with a bone cutter into small fragments (around 1 cm at their longest point). Fragments were then transferred into conical flasks (up to 4 bones per flask), containing 500 mL of Phosphate-Buffered Saline (PBS) (Sigma-Aldrich) supplemented with 1% Foetal Bovine Serum (FBS) (Gibco) and 1% Penicillin-Streptomycin (P/S) (Gibco), and incubated in a shaking water bath at 37°C for 1.5 to 2 hours.

The bone suspension was then filtered using a sterile funnel with muslin cloth, transferred into 50 mL tubes (Falcon, USA) and centrifuged at 350 x g for 5 minutes. After discarding the supernatants, PBMs were resuspended in 10 mL of PBS, pooled together, centrifuged once more for 5 minutes at 350 x g, and their supernatant again discarded. All cells were then resuspended in Earle's Balanced Salt Solution (EBSS) (Merk, UK), completed with 10% Pig Serum (Gibco) and 1% P/S. Cells were diluted 1:10 in 3% acetic acid for cell counting. PBMs were then seeded at a cell density of 1.0-1.6 $\times 10^7$ cells/mL in complete EBSS.

Purification of PBMs

After isolating PBMs, as described above, the cells may be further purified. Purified PBMs consist mainly of macrophages and other monocytes, without red blood cells and other plasma derived impurities. If so, they were diluted in PBS and gently overlaid on Histopaque 1083 (Sigma-Aldrich) in 50 mL tubes. The tubes were centrifuged at 1000 x g for 30 minutes at room temperature, and the buffy coat of cells in the middle of the resulting gradients carefully collected into a clean 50mL tube. The tube was then topped up with PBS and centrifuged at 400 x g for 10 minutes, and the supernatant discarded. The cells were resuspended in 5mL of 1X RBC (red blood cell) Lysis Buffer (BioLegend) and incubated at room temperature for 5 minutes to lyse any remaining RBCs. The cells were then washed

with PBS and centrifuged at 400 x *g* for 10 minutes, repeating the wash step three times. The purified PBMs were then counted and seeded in complete Roswell Park Memorial Institute 1640 (RPMI 1640) medium (Gibco) with Porcine CSF1-Fc [100 ng/mL] (Roslin Tech) at a cell density of 2.0-5.0 $\times 10^6$ cells per mL, and always incubated for 2-5 days at 37°C (5% CO_2) before being used for any application. Alternatively, the cells were resuspended in freezing media (90% FBS, 10% dimethyl sulfoxide (DMSO)) and stored in freezing containers containing isopropanol, at -80°C for 1-2 days before storing at -80°C for later use.

2.1.2 HEK293T and Vero Cells

HEK293T and Vero cells (sourced from The Pirbright Institute's Cell Culture team) were maintained in sterile and filtered tissue culture flasks of 175cm^2 (T-175) (Greiner Bio-One) with complete (10% FBS and 1%P/S) Dulbecco's Modified Eagle Medium (DMEM) (Gibco) at 37°C with 5% CO_2. When approaching confluency, cells were delicately washed with 10 mL of PBS, and incubated with 4 mL of 1X Trypsin-EDTA (0.05%), phenol red Cell Culture Dissociation Reagent (Gibco) warmed to 37°C for approximately 4 minutes. The dissociated cells were gently resuspended in an additional 4-6 mL of complete DMEM media to inactivate the Trypsin. A cell aliquot was then diluted 1:10 in trypan blue (Gibco) and counted with a cytometer. Cells were diluted in complete DMEM at the desired cell density and seeded onto the required vessel or split onto a new T-175 flask and maintained in a final media volume of approximately 25mL.

2.1.3 PLTA58 cells

These cells (from Gyorgy Fejer, University of Plymouth) were cultured at 33°C (5% CO_2) in RPMI 1640 (5% FBS and 1% 1X antibiotic-antimycotic (Gibco)). The cells grew into suspension in the media and were harvested weekly (by Raquel Portugal and Anusyah Rathakrishnan, at The Pirbright Institute). Cell harvest implied pelleting and resuspending the cells in fresh media (with 1%P/S); cells

were counted using a cytometer, seeded at a concentration of approximately 1 $\times 10^6$ cells/mL and incubated during no less than 4 days at 37°C before their use.

2.2 Virus Handling

Virus stocks were grown by infecting non-purified PBMs in T-175 flasks with 1-2mL of virus stock (always with an MOI in excess of 1); incubating them at 37°C with 5% CO_2 for 5-7 days. The infected cells and media were then collected with the help of a pipette into 50mL tubes and centrifuged 1000 x g for 10 minutes at 4°C. The supernatant was then harvested and stored at -80°C. Before any further steps, sample pellets were freeze/thawed three times to maximise the number of infective particles present in the stocks, then mixed again with the stored supernatants. When ultracentrifuged, virus samples were transferred into centrifuge tubes (Red 361625, BECKMAN, Optiseal Bell) and centrifuged at 13500 rpm for 90mins at 4°C using an Optima™ L-100 XP Ultracentrifuge and a SW32Ti rotor (SERIAL 18U5467). Virus pellets were then resuspended in 2mL total volume of complete EBSS media, titrated directly when possible and/or stored directly at -80°C for later use.

2.2.1 Virus Titrations

Isolated PBMs were incubated in a 96-well microwell flat bottom plate (Fisher Scientific) at 37°C with 5% CO_2 for 1-2 days. Eight 10-fold serial dilutions of the virus stocks were prepared in 0.5 mL of complete EBSS media, and 100 µL of each dilution were added in four replicates to the PBMs. After incubation for at least 5 days, positive wells were identified by haemadsorption (HAD) and fluorescence; virus titres were calculated as Tissue Culture Infectious Dose units yielding a 50% of cumulative infection (TCDI50) per millilitre (TCDI50/mL) using the Spearman & Kärber algorithm as described in Hierholzer et al. [220]. We used TCDI50, as it is standard in the field, instead of HAD50 for its replicability, since not all ASFV isolates are haemoadsorpting.

2.2.2 Infections

Purified PBMs were seeded on either 24-well or 96-well plates (Fisher Scientific) at a density of 1.0×10^6 cells per mL in 500 (24-well) or 100 µL (96-well) of complete RPMI 1640 with Porcine CSF1-Fc [100ng/mL] and incubated for more than 24 hours before infection. If the experiment required a treatment, then the media was carefully aspirated from the wells and replaced with the same volume of complete RPMI 1640 media (including CSF1-Fc) and the corresponding treatment. The desired multiplicity of infection (MOI) was derived using the following formula: $MOI \cong \frac{TCID50}{number\ of\ cells} \times \ln 2$. After the desired number of hours post-infection (hpi) the supernatant was collected and stored at -80°C for ELISA experiments, the cells were harvested using 350 µL of lysis buffer (24-well plates) and either processed for RT-qPCR as described below or stored at -80°C for later processing.

2.3 Inhibitors

The following inhibitors were used in our study: Ruxolitinib (Ruxo) (Selleck UK, Cat. No. S1378) and MG-132 (Sigma-Aldrich, 474790). Inhibitor stocks were diluted to working concentrations in DMSO and stored at -20°C for short term storage, or -80°C for longer storage. Before experiments, they were diluted to the experimental concentration in cell-appropriate media. Same volume of DMSO was used as vehicle control (VC).

2.4 Quantitative Reverse-Transcription Polymerase Chain Reaction

After the media was removed, cells were lysed and RNA was extracted using RNeasy Kit (Qiagen) according to the manufacturer's instructions. 1 µg of RNA was reverse transcribed to cDNA using SuperScript III First-Strand Synthesis System for RT-PCR (Life Technologies, Cat# 18080051). 1 µL of cDNA was then loaded into an optical 96-well plate (Agilent Technologies) and gene amplification was measured in a Mx3005P qPCR System (Agilent Technologies) using the Brilliant

III Ultra-Fast SYBR Green qPCR(quantitative polymerase chain reaction) Master Mix (Agilent Technologies) and the primers described in Table 2.1. Thermal cycling conditions were as follows: UDG activation at 50°C for 2 minutes, initial denaturation at 95°C for 2 minutes, followed by 40 cycles of denaturation at 95°C for 15 seconds and annealing/extension at 60°C for 1 minute. Relative gene expression was calculated using the ΔΔCt method,[221] with *GAPDH* as the reference gene. Each sample was run in technical duplicates and the average threshold cycle (Ct) value was used for calculations using Microsoft® Excel®, for data display and statistical analysis refer to section 2.12.

Gene	Primer Sequence (Forward/Reverse)	Exon Position	Source/Reference
GAPDH *(NM_001206359.1)* *Gene ID: 397128*	F: 5′-TCAACGACCACTTTGTCAAGC-3′	1002-1022	In-house
	R: 5′-GGTGGTCCAGGGGCTCTTA-3′	1100-1118	
CXCL10 *(NM_001008691)* *Gene ID: 494019*	F: 5′-CCCACATGTTGAGATCATTGC-3′	239-259	Fishbourne et al. [222], 2013
	R: 5′-CATCCTTATCAGTAGTGCCG-3′	406-387	
MX2 *(AB258432.1)* *Gene ID: 396893*	F: 5′-GGAGGAGCTCTTCAACCC-3′	1767-1784	In-house
	R: 5′-GAGGTCCCCATGAAGTAC-3′	1901-1884	
PKR *(NC_010445.4)* *Gene ID: 397588*	F: 5′-GAGAAGGTAGAGCGTGAAG-3′	1119-1137	Loving et al. [223], 2006
	R: 5′-CCAGCAACCGTAGTAGAG-3′	1193-1176	

Table 2.1: Primers used for qPCR analysis, with corresponding references for their sequences. All forward (F) and reverse (R) primers were in different exons. Adapted from Connell [124].

2.5 Enzyme-Linked Immunosorbent Assays

Enzyme-linked immunosorbent assays (ELISAs) were performed using the undiluted supernatant of infected PBMs which were immediately stored at -80°C following their harvest at the appropriate time-points. When infected for ELISA experiments, fresh media was used to replace the inoculant after an hour incubation, establishing this point as 0 hpi.

Two ELISA assays were used for our research: a commercial one for porcine CXCL10 and one for IFN-α, developed in-house. Assays were first optimised to determine the appropriate range of standard curves, incubation and plate reading times. Each experiment was performed in duplicate, with sample duplicates and replicated once more anew in a biological duplicate. All incubations were performed at room temperature unless otherwise specified. Sample concentrations were calculated by interpolation from a four-parameter logarithmic standard curve using GraphPad Prism 10 (Statistics: 2.12).

2.5.1 CXCL10 ELISA

Swine CXCL10 Do-It-Yourself ELISA (Kingfisher, DIY0723S-003) was performed using flat-bottom 96-well plates coated with 100 µL of anti-pig CXCL10 capture antibody [2.5 µg/mL] in PBS overnight. After washing four times with wash buffer (0.05% Tween-20 (Thermo) in PBS), plates were blocked with 100 µL of 4% bovine serum albumin (BSA) in PBS for 1-3 hours. Following four washes, 100 µL of samples and standards (two-fold dilutions from 50 ng/mL to 0 ng/mL) were added in duplicate and incubated for 1 hour. After washing, 100 µL of biotinylated detection antibody [0.05 µg/mL] was added and incubated for 1 hour. Plates were washed and incubated with 100 µL of streptavidin-HRP (1:200) for 30 minutes, followed by 100 µL of TMB substrate in the dark for 30 minutes. The reaction was stopped with 100 µL of 2N H_2SO_4 and the optical density (OD) measured at 450 nm using a BioTek® micro-plate reader with Gen5 software (Promega).

2.5.2 Porcine IFNα ELISA

Maxisorp plates were coated with 100 µL of anti-pig IFN-α antibody (clone K9, 0.5 µg/mL) in coating buffer overnight. Plates were washed three times with 400 µL of wash buffer (0.05% Tween-20 in PBS) and blocked with 300 µL of 1% BSA in PBS for 2 hours. Following washing, 100 µL of samples and standards (two-fold dilutions of pig IFN-α, PBL 17105-1, from 2000 U/mL) were added and incubated for 2 hours. After washing, 100 µL of biotinylated anti-pig IFN-α antibody (in-house, clone F17,

1:5000) was added for 2 hours, followed by 100 µL of streptavidin-HRP (1:200) for 20 minutes. The reaction was developed using 100 µL of a 1:1 mixture of Color Reagent A (H_2O_2) and Color Reagent B (TMB) (R&D DY999) for 20 minutes in the dark and stopped with 50 µL of 2N H_2SO_4. Absorbance was measured at 450 nm and 540 nm.

2.6 Cell Viability Assay

Cell viability was assessed using the RealTime-Glo™ MT Cell Viability Assay (Promega, TM431).[224] Cells were seeded in white-walled, opaque 96-well plates and subjected to the same experimental conditions used in inhibitor studies. Following pretreatment with the indicated concentrations of inhibitors, vehicle control (DMSO), or left untreated, cells were cultured for 5 days, representing the longest experimental time-point. The viability assay reagents were then added according to the manufacturer's protocol. After 1 hour incubation at 37°C, luminescence measurements were performed to quantify cell viability.

2.7 Dual-Luciferase®-Reporter Assays

500µL of HEK293T cells [1 x $10^5/mL$] suspended in complete DMEM media were seeded into 24-well plates and grown to 40-80% confluency. 500ng of total plasmid DNA was transfected into each well in 50µL of OptiMEM serum-free media (Gibco) with TransIT-LT1 Transfection reagent (Mirus Bio LLC). Besides the viral genes of interest, cells were transfected with both a plasmid containing a firefly reporter gene linked to a promoter sequence and an empty renilla reporter plasmid, later used for data normalisation. For the assay including IFN treatment, media was replaced 5 hours before measuring activity with 500µL of complete DMEM media with either Universal Type I IFN (Alpha A/D (BgIII), 11200-2, PBL Assay Science, USA) (in 0.1% BSA DPBS) to the concentration displayed in results or the same amount of reagent diluent for VC. 24-72 hours post-transfection, luciferase activities were measured with Dual-Luciferase®-Reporter (DLR™) Assay System (Promega, Cat# E1910) in a Microplate Luminometer.

2.8 Protein Analysis

2.5mL of HEK293T cells [1 x $10^5/mL$] were seeded into 6-well plates and grown to 40-80% confluency. Cells were then transfected with 2.5µg of total plasmid DNA in 250µL of OptiMEM serum-free media with TransIT-LT1 Transfection reagent.

2.8.1 Sample Preparation

Cells were harvested 48-72 hours post-transfection and lysed in RIPA buffer (Thermo Scientific, Cat# 89900) supplemented with Halt™Protease Inhibitor Cocktail (100X) and 0.5M EDTA Solution (100X) (Thermo Scientific, Cat# 78430). Lysates were incubated on ice for 15 minutes with gentle mixing, then centrifuged at 14,000 × g for 15 minutes at 4°C to pellet cell debris. The resulting supernatant was collected for subsequent analysis. Proteins were stored at -80°C for later, or for immediate applications reduced using Lane Marker Reducing Sample Buffer (5X) (Thermo Scientific, Cat# 39000) at room temperature for 30 minutes, to prevent MGF protein agglutination that occurred under standard high-temperature reducing conditions.

2.8.2 Immunoprecipitation

Immunoprecipitation (IP) was performed using GFP-Trap® Magnetic Agarose (ChromoTek, gtma-20) according to the manufacturer's protocol with minor modifications. Briefly, 25 µL of bead slurry was equilibrated with dilution buffer, incubated with cleared cell lysate for 1 hour at 4°C with end-over-end rotation, and washed three times with wash buffer. Bound proteins were eluted by incubating the beads in 5X Lane Marker Sample Buffer at room temperature for 30 minutes.

2.8.3 Immunoblotting

Protein samples (10 µL) were resolved on 4-20% Mini-PROTEAN® TGX™ Precast Protein Gels (BioRad) alongside 5µL of the ladder Full Range Rainbow Recombinant Protein Molecular Weight Marker. Electrophoresis was performed at 200V for 30-35 minutes. Proteins were transferred onto methanol-activated PVDF (polyvinylidene difluoride) membranes using the Mini Trans-Blot® system (BioRad), for 90 minutes

100V, according to manufacturer's protocol. Electrophoresis and protein transfer were performed using the buffers recommended by gel manufacturer. Membranes were blocked in 5% non-fat milk in TBS-T (Tris-buffered saline + 0.1% Tween-20) and probed with primary antibodies for 1-2 hours at room temperature (or overnight at 4°C), washed three times with 10-15mL of TBS-T; lastly membranes were probed with secondary antibodies at room temperature for 2 hours before a final triple wash of the membranes prior to visualisation. Antibody concentrations used are described in table 2.2. Protein bands were visualized using a LI-COR® Odyssey CLx imaging system and quantified using Image Studio Lite software (Version 5.2).

2.9 Immunofluorescence

Vero cells (500µL)[1 x $10^5/mL$] were seeded onto glass coverslips in 24-well plates and grown to 40-80% confluency before transfection. After 48-72 hours post-transfection, cells were briefly washed with PBS and fixed with 4% formaldehyde for 20 minutes at room temperature. Following two PBS washes, cells were permeabilised with 0.2% Triton X-100 in PBS for 7 minutes and washed twice more with PBS. Cells were then blocked with 1% BSA in PBS for 30 minutes.

Primary antibody incubation was performed for 1 hour using mouse anti-V5 antibody diluted 1:200 in PBS containing 1% BSA (250 µL per well). After three further PBS washes, cells were incubated with Alexa Fluor 568-conjugated goat anti-mouse secondary antibody (1:500 in PBS + 1% BSA, 250 µL per well) for 1 hour in the dark. Following three final PBS washes, coverslips were mounted cell-side down onto glass slides using 7 µL VECTASHIELD Vibrance® Antifade Mounting Medium with DAPI (H-1800). Mounted slides were allowed to cure at room temperature for 2-24 hours before visualization or storage at 4°C.

Samples were visualised using a Leica TSC SP8 Confocal Laser Scanning Microscope. Images were captured using LAS-X (Version 3.5.7.23225, Leica™) software and processed with the same or with LAS AF Lite (Leica™) software. Later, they were arranged for display using Adobe™ Illustrator 2024.

2.10 Antibodies

Application	Species & Target	Source	Working Dilution
Primary Antibodies			
IF/IB	Mouse mAb Anti-V5-Tag IgG2a	BioRad (MCA1360)	1:200 (IF) 1:1000 (IB)
IB	Rabbit Anti-β-Actin	Cell Signaling (#4967)	1:1000
IB	Rabbit mAb Anti-STAT1 IgG	Cell Signaling (D1K9Y #14994)	1:1000
IB	Rabbit mAb Anti-STAT2 IgG	Cell Signaling (D9J7L #72604)	1:1000
IB	Rabbit Polyclonal Anti-GFP	Invitrogen (CAB4211)	1:1000
Secondary Antibodies			
IF	Goat Anti-Mouse Alexa Fluor 568	Life Technologies	1:500
IB	Goat Anti-Mouse IRDye800CW	LI-COR (925-32210)	1:10000
IB	Goat Anti-Rabbit IRDye680RD	LI-COR (925-68071)	1:10000

Table 2.2: Antibodies Used in This Study. List of primary and secondary antibodies used for immunofluorescence (IF) and immunoblotting (IB) experiments, with their corresponding working dilutions.

2.11 Plasmids

Plasmid	Vector	Description	Source
MGF Expression Constructs[*]			
MGF360-10L.V5 MGF360-11L.V5 MGF360-12L.V5 MGF360-13L.V5 MGF360-14L.V5 MGF505-1R.V5 MGF505-2R.V5 MGF505-3R.V5 MGF505-4R.V5	pcDNA3.1	ASFV MGF proteins	GeneArt Connell [124]
MGF Mutant Constructs[*]			
MGF360-12L.mVHL.V5 MGF360-12L.mBC.V5 MGF360-12L.mCUL.V5 MGF505-1R.mSOCS.V5 MGF505-1R.mBC.V5 MGF505-1R.mCUL.V5	pcDNA3.1	MGF mutants	GenScript Connell [124]
Reporter Constructs			
pGL3-Mx1 pGL3-whMx2 pGL3-basic-poMx1 pGL3-rrh-Mx1 pGL3-bp-Mx1	pGL3	Mx promoter Firefly luciferase reporters	In-house Dr. Chris Netherton, TPI
pGL3-Ifnα6	pGL3	Porcine Ifnα6 promoter Firefly luciferase reporter	Dr. Kay Childs, TPI
Other Plasmids			
pRL-null	pRL	Renilla luciferase control reporter	Promega
pIKKε-FLAG	pcDNA	Porcine IKKε with FLAG-tag	In house
pEGFP-C1-IRF7	pEGFP-C1	Human IRF7 with C-terminal eGFP tag	Dr. Julian Seago, TPI
Empty vector	pcDNA3.1	Empty expression vector control	Invitrogen

Table 2.3: Plasmids Used in This Study. List of expression constructs, reporter plasmids and control vectors used for transfection experiments. [*]MGF constructs were derived from ASFV Georgia 2007/1 isolate, codon-optimized for expression in mammalian cells, and include C-terminal V5 tags for detection. TPI: The Pirbright Institute.

Figure 2.1: Mutations of the Putative VHL/SOCS-Boxes of MGF360-12L and MGF505-1R. Schematic showing sequences of putative SOCS/VHL-Box-like in **A)** MGF360-12L and **B)** MGF505-1R, and corresponding mutations of said motif with the aim of impairing functionality. Residues highlighted in yellow correspond to MGF residues that are homologous with key residues of the BC-Box, highlighted green corresponds to Cul2-Box, and pink residues or residues highlighted in pink correspond to key Cul5-Box residues. Residues in bold are mutations. Adapted from Connell [2021, 124].

Plasmid	***IFNα6* DLR**	**Warthog *MX2* DLR**	**IF**	**IB**
Empty pcDNA3.1[1]	0–245	0–370	0–245	0–1250
pMGF[2]	245	370	245	1250
pIKKε	50	–	50	250
pIRF7	75	–	75	375
Firefly Reporter	100	100	–	–
pRL-null	30	30	–	–
Total DNA	0.5 µg	0.5 µg	0.5 µg	2.5 µg

Table 2.4: DNA Amounts Used for Cell Transfections. Quantities of plasmid DNA (in ng) used for different experimental conditions. DLR: Dual-Luciferase®-Reporter assay; IF: Immunofluorescence; IB: Immunoblotting. [1]Empty pcDNA3.1 vector was used to maintain consistent total DNA amounts across conditions. [2]For dose-dependent experiments, pMGF amounts were 250, 500, or 750 ng per transfection (multiplied by 5 for immunoblotting), with other plasmid quantities maintained.

2.12 Statistical Analysis

Data was organised and saved in Microsoft® Excel® (Version 2401 or earlier, Build 16.0.17231.20236) workbooks. For statistical analyses and figure display, organised

data was transposed onto Prism 10 for Windows 64-bit (GraphPad Software, LLC; Version 10.4.1 (627) or earlier) and the appropriate statistical tests (ANOVA, Tukey's or multiple comparison tests (MCTs)) were applied as described in results, according to the configuration of experimental data.

3

Macrophage Responses to Infection with ASFV Deletion Mutants

Contents

3.1 Introduction 59
3.2 Results 61
3.2.1 Deletion of 12L strongly induces ISGs 61
3.2.2 Induction of ISGs Occurs Early Following Infection with ASFV Δ12L 62
3.2.3 Ruxo Reverses Δ12L Early Induction of ISGs 64
3.2.4 Ruxo does not revert Δ12L growth defect 66
3.2.5 Ultracentrifugation of Δ12L: Impact on IFN and ISGs . 69
3.2.6 Ultracentrifugation Does Not Revert Δ12L Growth Defect 71
3.2.7 Cell Viability of PBMs Treated with Ruxo 73
3.3 Discussion 74

3.1 Introduction

ASFV MGF 360 and 505 genes, which include *1R* and *12L*, have been reported to play a role in virulence in pigs and in the suppression of the type I IFN response. The sensitivity of ASFV to type I IFN has also been previously linked to genes within the MGF family,[92] and the deletion of 1R and 12L genes from the Georgia2007/1 wt isolate has been reported to exacerbate the induction of type I IFN and downstream

ISGs, such as *CXCL10*, and reduce viral replication in macrophages.[205] The MGFs represent approximately 30% of the ASFV genome and account for most of the genetic variation observed between viral isolates.[8] These gene families, clustered at the terminal ends of the viral genome, are expressed very early during infection, paralleling strategies found in related large DNA viruses like poxviruses.[7, 14]

The type I IFN response represents a critical first line of defence against viral infections. Virulent ASFV strains have evolved sophisticated mechanisms to overcome these defences, enabling efficient viral replication even in IFN-activated macrophages.[71, 79] Virulent strains maintain remarkably low IFN levels in infected macrophages *in vitro* but trigger elevated IFN levels *in vivo*, whilst the opposite is true with MGF-deletion attenuated isolates, suggesting complex mechanisms of immune modulation.[79, 92] Understanding how viral proteins, particularly the MGFs, modulate this response is crucial for developing effective attenuation strategies. This is particularly relevant given its tropism for m-MΦs, which specialize in cytokine production and initiating adaptive cell immunity.[74, 78]

The study of ASFV-gene deletions presents significant technical challenges, particularly in distinguishing direct effects of deletions from secondary consequences of infection; specially given the large genome size of ASFV, which enables the virus to encode redundant immune inhibitory mechanisms. The use of primary macrophages, while physiologically relevant, introduces experimental variability that can complicate interpretation of results.[61, 214] ASFV's abundance of immune modulating genes can obfuscate the specific contributions of individual genes; clarifying this requires careful experimental design to minimise confounding effects, such as carry-over cytokines and PAMPs in virus preparations, the potential redundancy between viral proteins targeting similar host pathways, or the interaction with different cell types. To minimise these confounding effects we used purified PBMs and viral stocks, together with careful experimental design; however, the population of cells obtained by purifying primary PBMs is still heterogeneous.

Recent studies have revealed that MGFs target multiple components of both IFN induction and response pathways (See 1.4). These viral proteins have been shown to

interact with and affect cellular levels of key IFN signalling factors (Tables 1.2& 1.4). However, the mechanisms by which individual MGF proteins, particularly 12L, contribute to immune evasion remain incompletely understood.

This understanding is particularly relevant for vaccine development, as recent advances have shown that deletion of interferon inhibitory proteins can generate promising vaccine candidates.[193, 204] However, the optimal combination of gene deletions required for effective attenuation while maintaining immunogenicity remains to be determined.[193, 202]

To confirm the reported function of these genes in the suppression of type I IFN response[92], we infected primary PBM cells with our panel of deletion mutants to characterise the effects these deletions have on porcine innate immunity, particularly the IFN response.

3.2 Results

3.2.1 Deletion of MGF360-12L Strongly Induces ISGs

Previously published data suggested that the deletion of 12L from Georgia2007/1 ASFV isolate had the highest impact, of all other tested MGF gene deletions, on the levels of IFN-α and interferon-stimulated cytokine, CXCL10 in the supernatants of infected PBMs.[92] We confirmed these results, demonstrating that 12L and other MGFs strongly suppress type-I interferon. CXCL10 was selected for its strong induction as an ISG in response to infection, however it is important to note that its transcription is also activated in an interferon independent way, via NF-κB.

Purified PBMs of two different swine were infected with our panel of virus deletion mutants, and 16 hpi we assessed the levels of gene and protein expressions of the *CXCL10* ISG (Fig. 3.1). Cells infected with the Δ12L mutant exhibited a 26-fold increase in *CXCL10* mRNA levels compared to the virulent isolate, normalised to *GAPDH* (***: p=0.0.0004) (Fig. 3.1A).

The level of CXCL10 protein was also measured in the supernatant of infected cells. The levels of CXCL10 detected in the supernatant at 16 hpi were, approximately, ten times higher after infection with Δ12L than with the virulent

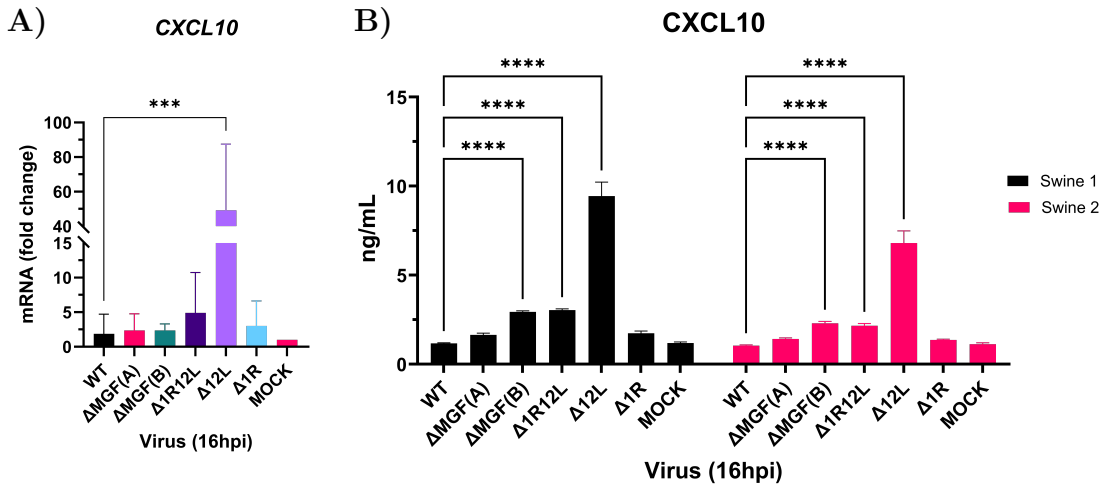

Figure 3.1: Impact of Deletion Mutants on CXCL10 Levels in PBMs.CXCL10 **A)** mRNA and **B)** protein levels detected at 16 hours post-infection in porcine macrophages infected with wild-type ASFV and virus deletion mutants with ∼0.7 MOI. Ordinary two-way ANOVA. Šidák's multiple comparisons test, with a single pooled variance. Two biological replicates with two further technical replicates each.

wt isolate (****: p<0.0001) (Fig. 3.1B). The Δ1R12L and ΔMGF(B) deletion mutants also produced CXCL10 protein levels significantly higher than the wt (****: p<0.0001), however the detected ISG concentration in both was less than half that of Δ12L (Fig. 3.1B).

We therefore confirmed the reproducibility of previously reported data.

3.2.2 Induction of ISGs Occurs at Early Time Points Following Infection with ASFV Δ12L

It is unclear if the observed high levels of the ISG, *CXCL10*, result from deficient viral evasion of the IFN induction (e.g. at the level of *IRF3/IRF7*) or inability to control the response to IFN (JAK/STAT pathway) following infection with Δ12L.[205]

To investigate the timing and mechanism of the antiviral response stimulated by the deletion of MGF360-12L, we infected approximately 5×10^5 PBMs with our panel of deletion mutants at a MOI of ∼0.4 (as close to 0.5 as possible, on account of Δ12L growth-limiting defect) and measured the relative expression levels of ISGs *CXCL10*, *PKR*, and *MX2* by RT-qPCR at different time points (2, 5, and 16 hpi). All viral mutants with the 12L deletion showed higher relative expression

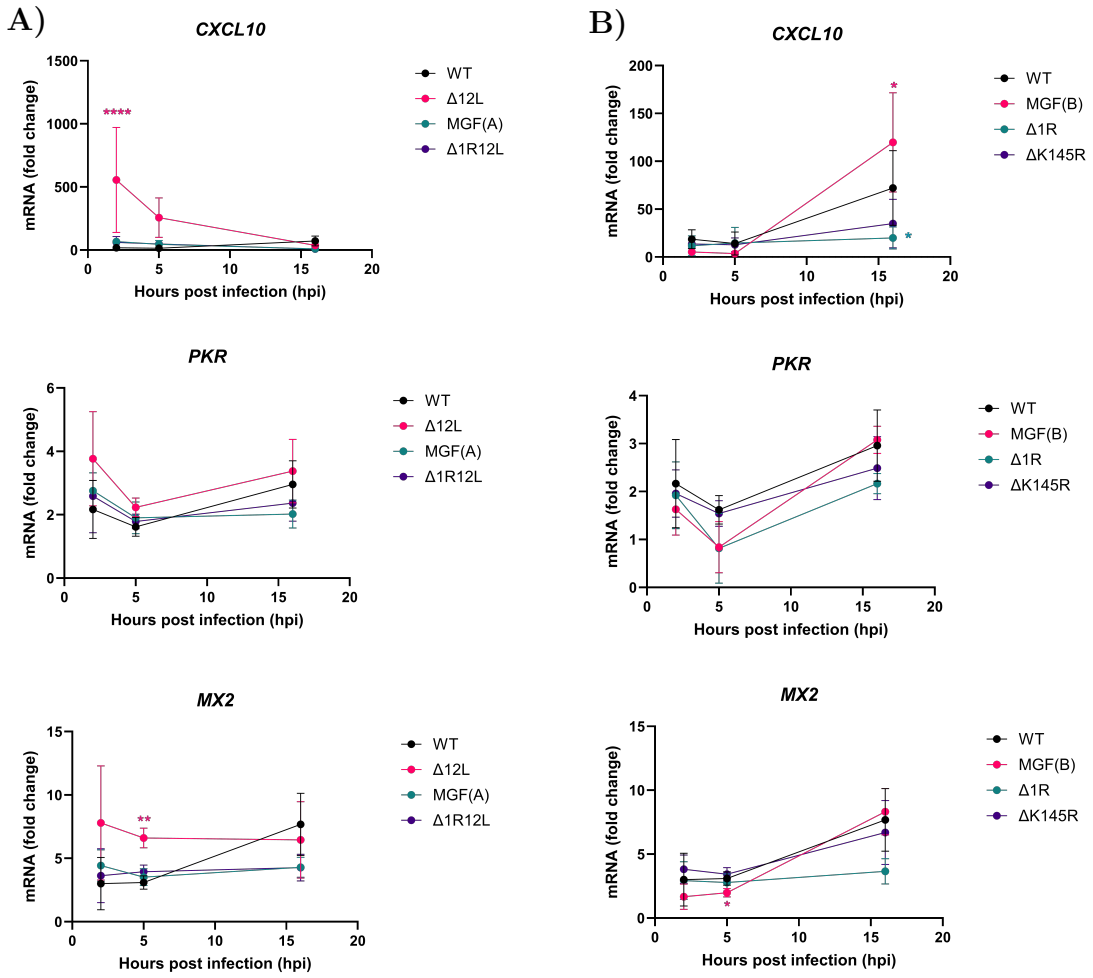

Figure 3.2: Expression dynamics of interferon-stimulated genes in infected cells over time. The relative levels of *CXCL10*, *PKR*, and *MX2* mRNA were measured by RT-qPCR at 2, 5, and 16 hpi in porcine macrophages infected with Δ12L, Δ1R, and wt ASFV. Data was normalised to GAPDH mRNA measurements of each sample and corrected using the normalised mRNA levels of each gene in cells mock infected in parallel. **A)** Viral mutants with the 12L deletion exhibited higher relative expression levels of all surveyed ISGs at 2 hpi, which decreased over time. **B)** The wild-type isolate and deletion mutants without the 12L deletion showed lower levels of ISG expression at 2 hpi that increased over time.

levels of all ISGs surveyed at 2hpi (Fig.3.2A), which decreased over time, while the wild-type isolate and deletion mutants without the 12L deletion showed lower levels of ISG expression at 2hpi that increased over time (Fig. 3.2B). The results at 16hpi likely vary in relation to 3.1A, in part, on account to the differences in MOI between the experiments, 0.7 versus 0.4; however, given that this difference in MOIs is not great, this variation is likely best explained by phenotypic differences in cells from separate biological replicates. These findings suggest that the deletion of 12L stimulates the type I IFN response and the expression of ISGs as early as 2hpi (Fig. 3.2). This rapid induction of a type I IFN response may underpin the inability to easily generate bulk amounts of the Δ12L deletion mutant due to the rapid induction of an anti-viral state in infected cells.

3.2.3 Inhibition of the Type I IFN Response Reverses Δ12L Early Induction of ISGs

The early induction of the CXCL10 ISG in PBMs infected with Δ12L reported in section 3.2.2 raised concerns about potential indirect effects of the gene deletion. Specifically, we hypothesized that Δ12L might cause infected cells to produce excess IFN when being cultured and harvested, which could be carried over into the virus preparations. This could confound the interpretation of experimental results, as excess IFN could cause the observed growth defect, rather than a direct impact of the deletion on replication.

To address this question, we decided to employ Ruxo: an inhibitor of the response to type I IFN that prevents the phosphorylation of STAT1/2 by JAK immediately after binding of IFN to its receptor at the host cell surface (Fig. 1.9).[225]

We first tested the inhibitory effect of Ruxo on ISG expression in porcine macrophages by pre-treating cells with increasing concentrations of Ruxo prior to stimulation with IFN. The results showed that the relative expression of *CXCL10* and other ISGs was reduced in all conditions tested (not shown), with the greatest inhibition in cells treated with 10μM Ruxo overnight. These conditions were used in subsequent experiments.

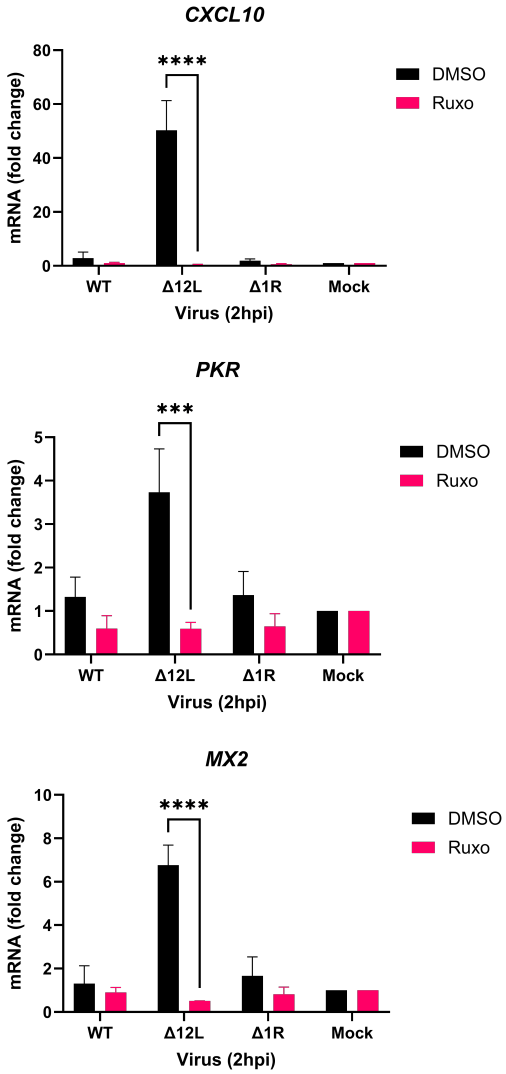

Figure 3.3: Inhibition of JAK/STAT pathway reverses early induction of ISGs: Expression of ISGs 2hpi was quantified relative to *GAPDH* by RT-qPCR. Cells pre-treated overnight with Ruxo [10 μM] or DMSO VC [1 μL/mL], then mock-infected or infected at an MOI of 0.5 with wt, Δ12L or Δ1R. Ordinary two-way ANOVA. Šidák's multiple comparisons test, with a single pooled variance. Two biological replicates with two further technical replicates each.

The ISG expression levels in Ruxo pretreated cells infected with Δ12L were similar, at 2 hpi and in all instances, to those observed after infection with the virulent wt isolate under the same conditions, and significantly different from the corresponding vehicle control (Fig. 3.3) (****: $p<0.0001$; ***: $p=0.0005$). Because Ruxo inhibits JAK/STAT signalling, the observed early stimulation of ISGs in the Δ12L samples may be due to high levels of IFN already present in the virus stock. The timing of this experiment further corroborates this point since at 2hpi there is not enough time for the cells to produce new interferon in response to the infection. This needs to be further confirmed by using purified virus stocks in this type of experiment.

3.2.4 Ruxolitinib Does Not Revert Δ12L Growth Defect

Δ12L has been reported to display a growth deffect when grown *in vitro*.[205] To assess whether JAK/STAT inhibition is enough to revert the *in vitro* growth defect of the Δ12L deletion mutant, we investigated the impact of inhibiting the type I IFN response. Previous findings demonstrated the early induction of ISGs upon infection with Δ12L (Fig. 3.2) and its reversal under JAK/STAT inhibition (Fig. 3.3). Here, we aimed to determine if such inhibition could counteract the *in vitro* growth defect of Δ12L. Understanding the deleterious impact of Δ12L on virus growth compared to other MGF family gene deletions could provide insights into its role in immune evasion.

Given that the type I IFN response prevents cell-to-cell infection by activating an antiviral gene expression profile,[226] we conducted growth curve experiments using a low MOI of 0.01. This allowed us to investigate the ability of deletion mutant viruses to infect subsequent cells compared to the wt isolate. Cells were pretreated overnight with Ruxo or DMSO and infected at an MOI of 0.01 over a five-day period. Virus growth at each time point was titrated in technical duplicates, and each experiment was replicated in a biological duplicate, using a second set of purified PBMs from a different pig.

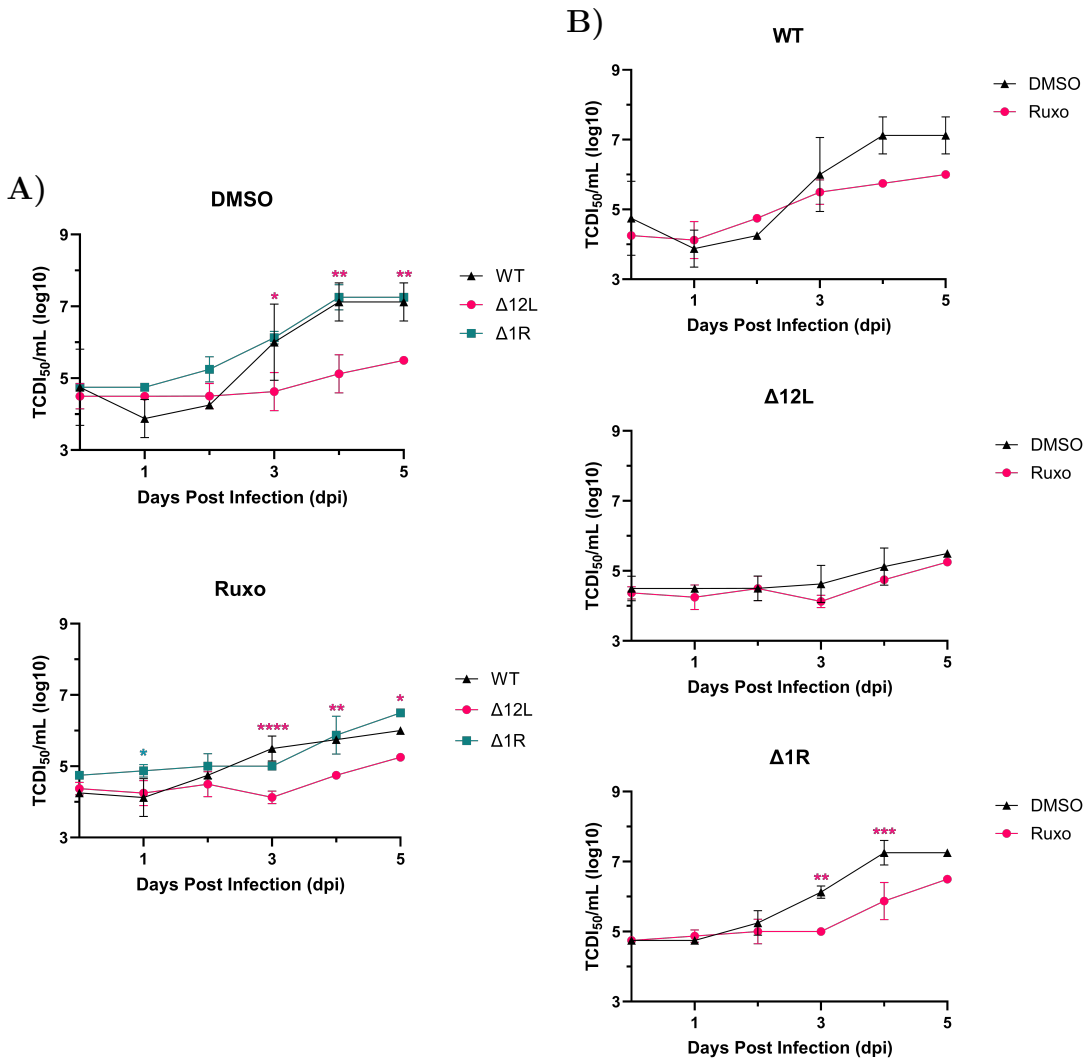

Figure 3.4: Impact of ruxolitinib on WT and recombinant virus growth *in vitro* in cells from *Swine 1*. Multistep growth curves of the mutant gene-deleted viruses were performed over 5 days in cells pre-treated overnight with Ruxo [10 μM] or DMSO VC [1 μL/mL]. Grouped by **A)** treatment or **B)** by viral inoculant. Cells were infected in technical duplicates with an MOI of 0.01, titrations of each time-point were performed simultaneously in non-purified PBMs from a single swine. Statistical analysis was performed by RM two-way ANOVA, with matched valued stacked into a subcolumn, **A)** Dunnett's or **B)** Šidák's multiple comparisons tests, with a single pooled variance.

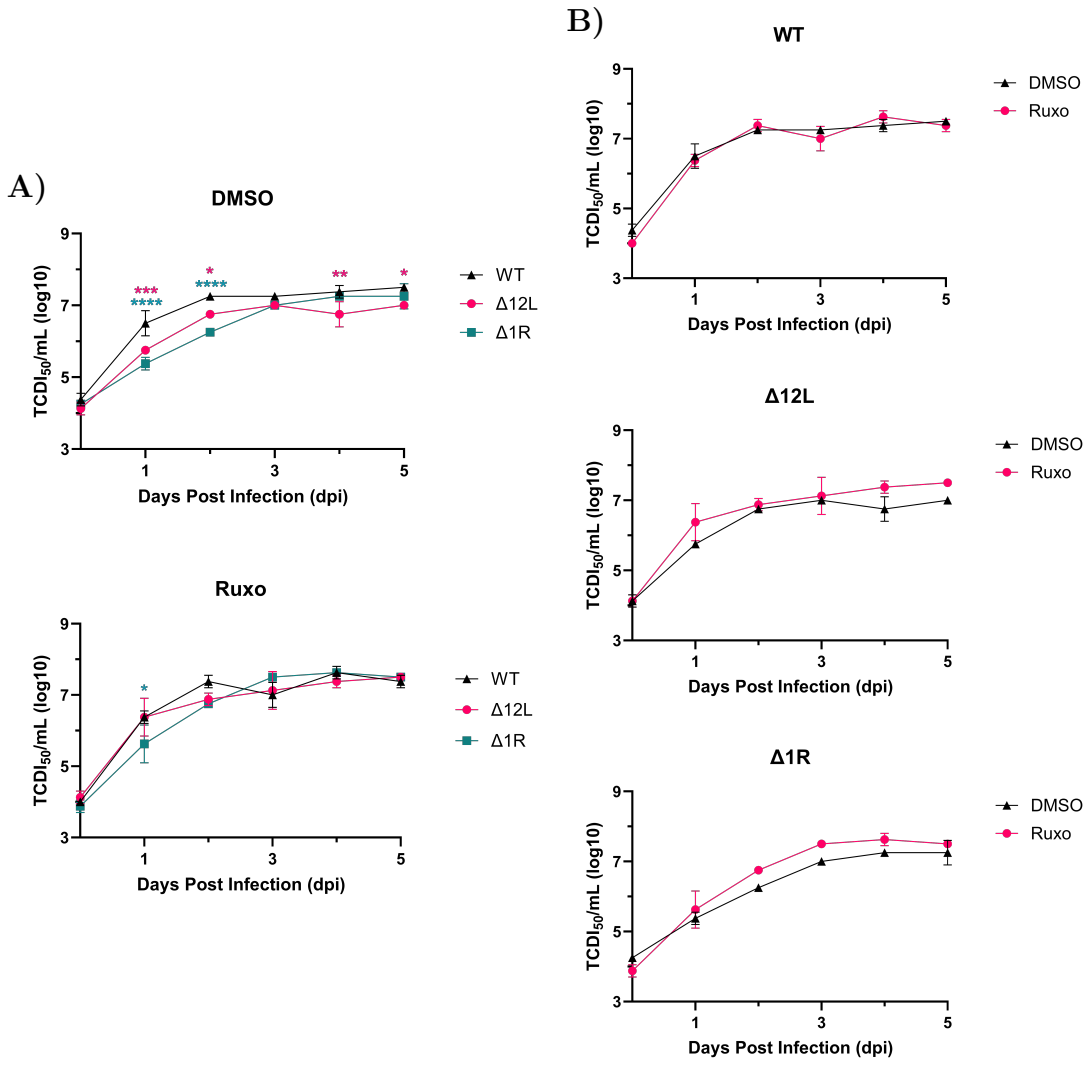

Figure 3.5: Impact of ruxolitinib on WT and recombinant virus growth *in vitro* in cells from *Swine 2*. Multistep growth curves of the mutant gene-deleted viruses were performed over 5 days in cells pre-treated overnight with Ruxo [10 μM] or DMSO VC [1 μL/mL]. Grouped by **A)** treatment or **B)** by viral inoculant. Experimental parameters and statistical analyses as in analogous experiments.

In each biological replicate, Ruxo pre-treatment slightly reduced the significance of the titre differences between Δ12L and wt at 5 dpi, from ** to * in figure 3.4A and from * to non-significant (ns) in figure 3.5A. However, the decreased significance in the titre difference of Δ12L in figure 3.4A likely results from the Ruxo treatment somehow impairing the growth of wt in PBMs from Swine 1. In the cells from Swine 2, Δ12L grew notably better, and the growth defect was much less evident (Fig. 3.5A). These observations may be attributable to biological variability between

the porcine macrophages used in each experiment[227], highlighting the importance of considering inter-individual differences when interpreting these results. Besides the expected variability between primary macrophages, the treatment did not significantly increase the titres of either deletion mutant when tested across both biological duplicates (Figs. 3.4B and 3.5B). This suggests that JAK/STAT inhibition alone is insufficient to fully revert the growth defect observed with the Δ12L mutant.

The inability of Ruxo to significantly enhance the growth of Δ12L suggests that the deleterious impact of the 12L deletion on viral replication is not solely due to the early induction of ISGs. These findings indicate that 12L likely has additional functions impacting virus growth.

3.2.5 Ultracentrifugation of Δ12L Decreased Excess IFN and Reverted Early ISG Induction

Previous findings have shown that infection with the Δ12L mutant results in the induction of various ISGs as early as 2hpi (Fig. 3.2). The immediate induction of ISGs, coupled with its reversal upon JAK/STAT inhibition (Fig. 3.3), suggests that these effects may be linked to the carry-over of type I IFN in the Δ12L stock. This carry-over might include PAMPs or cytokines produced during the growth of virus stock. Given the replication deficiency of Δ12L, larger volumes of inoculant were used to achieve the same MOI as the wt. This study aims to determine whether the observed early induction of ISGs is directly attributable to the deletion of 12L or a consequence of carry-over type I IFN.

To investigate this, two new sets of viral stocks were prepared for the Δ12L and GeorgiaΔK145RΔMGF505-1R (Δ1R) deletion mutants, as well as the wt, in parallel. One set of viruses was harvested using ultracentrifugation, allowing the resuspension of the viral pellets in fresh medium, hence reducing the levels of IFN or other cytokines carried over in the virus preparation.

The amount of IFN-α in the virus stocks harvested by both standard methods and ultracentrifugation was measured using ELISA (Fig. 3.6A). Results were adjusted by titres to reflect the amount of IFN-α added to a well at an MOI of

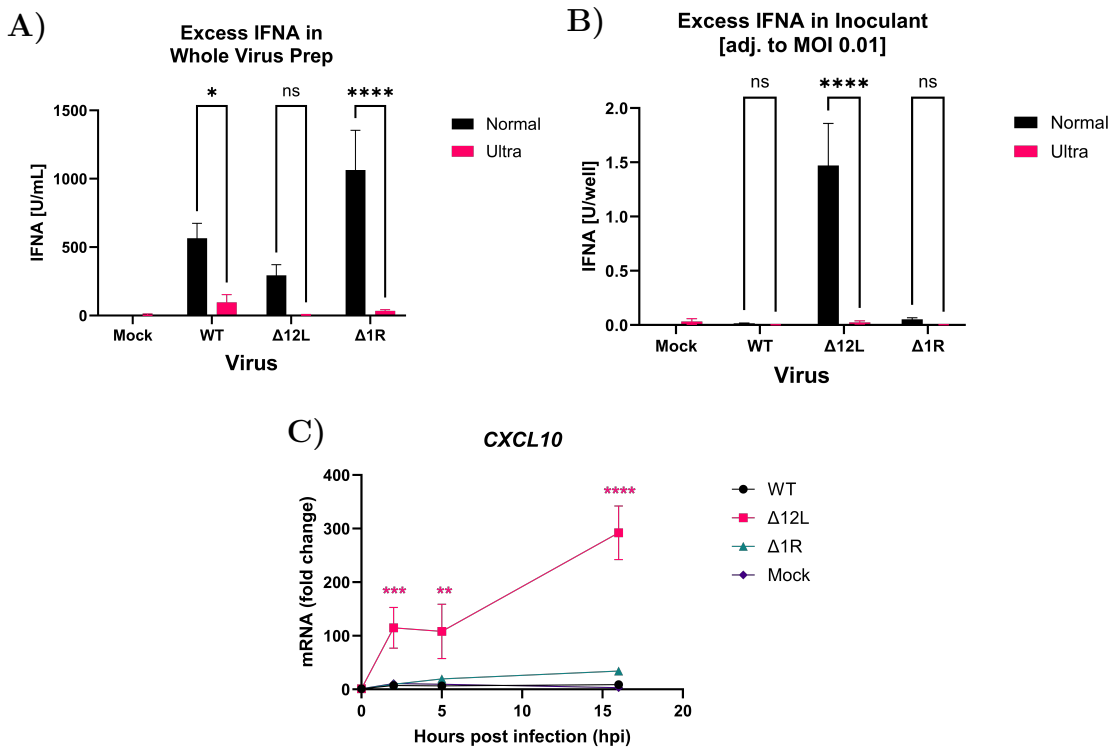

Figure 3.6: Effects of ultracentrifugation of viral preparation: A) Excess IFN-α detected in the whole virus preparations used for inoculation. **C)** Excess adjusted IFN-α detected by ELISA and adjusted to virus titre, represented with the lowest MOI used in any experiment (proportional to other MOIs). **C)** Fold change in mRNA levels of *CXCL10* in PBMs infected with ultracentrifuged virus, at an MOI of 0.5, relative to *GAPDH*, by RT-qPCR.

0.01 (Fig. 3.6B), the lowest used in any experiment. This adjustment to titres revealed that the inoculum from Δ12L harvested by standard methods contained 60 times more IFN-α than by ultracentrifugation, significantly decreasing IFN-α levels (Fig. 3.6A, ****: $p<0.0001$). Furthermore, infection with ultracentrifuged Δ12L altered the temporal expression profile of *CXCL10*, making it more similar to the expression pattern elicited by mutants without the 12L deletion (Fig. 3.2B). Specifically, higher induction was observed at 16 hpi rather than at 2hpi, although overall *CXCL10* expression remained higher compared to wt or Δ1R (Fig. 3.6C).

The strong induction of ISGs previously observed at 2hpi with Δ12L was likely due to excess IFN produced during virus growth and carried over in the inoculum before infection. Ultracentrifugation effectively reduces the impact of IFN and other cytokines, which may be produced in excess during the growth of

mutant viruses with deletions involving innate immune evasion and should hence be used when studying these viruses.

3.2.6 Ultracentrifugation Does Not Revert *In Vitro* Δ12L Growth Defect

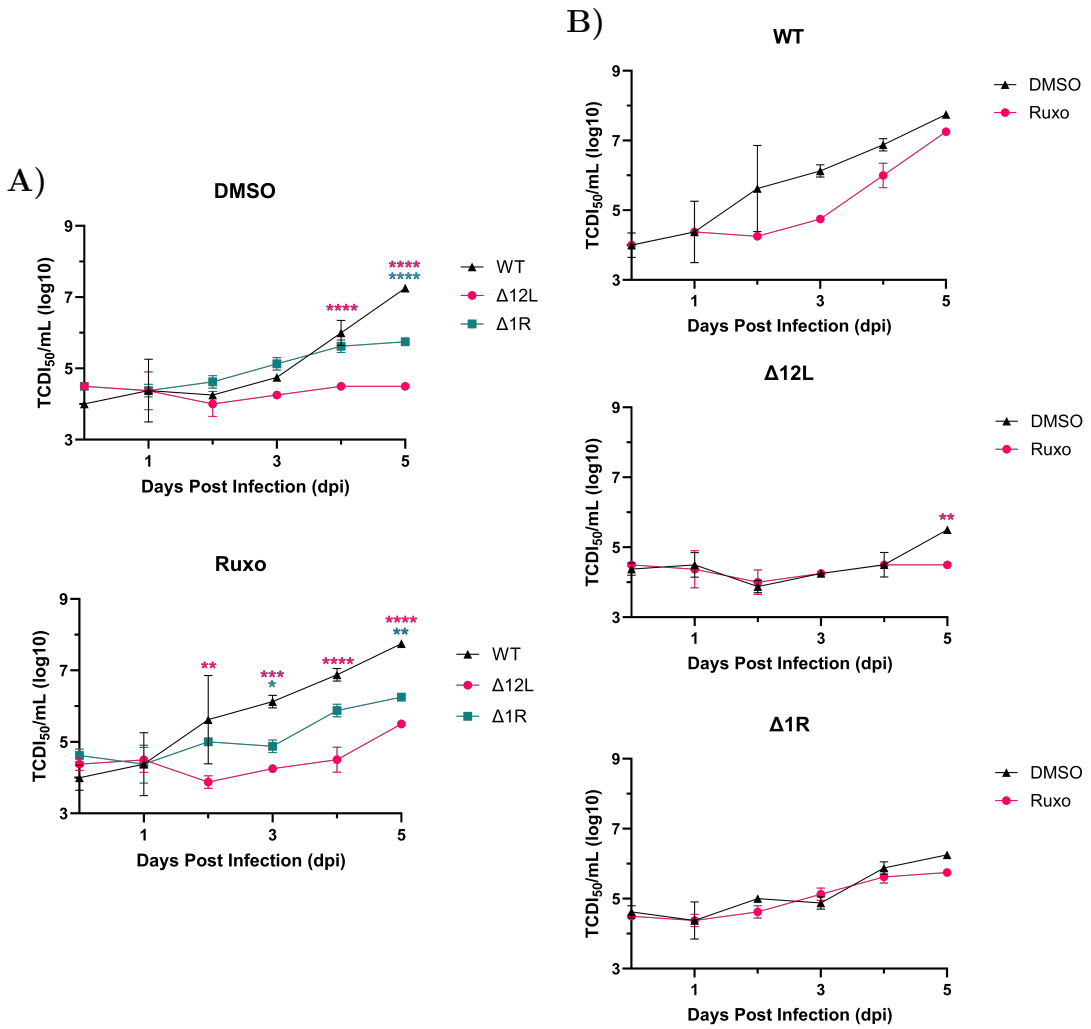

Figure 3.7: Impact of ruxolitinib on the growth of ultracentrifuged WT and recombinant viruses *in vitro*, in cells from *Swine 1*. Multistep growth curves of the mutant gene-deleted viruses were performed over 5 days in cells pre-treated overnight with Ruxo [10 μM] or DMSO VC [1 μL/mL]. Grouped by **A)** treatment or **B)** by viral inoculant. Experimental parameters and statistical analyses as in analogous experiments.

To minimize the impact of type I IFN detected in the inoculant of Δ12L (Fig. 3.6A) on our results, and since JAK/STAT inhibition alone was not sufficient to revert the *in vitro* growth defect of Δ12L (Section 3.2.4), we sought to assess the impact

of IFN response inhibition via JAK/STAT on the growth of ultracentrifuged viruses.

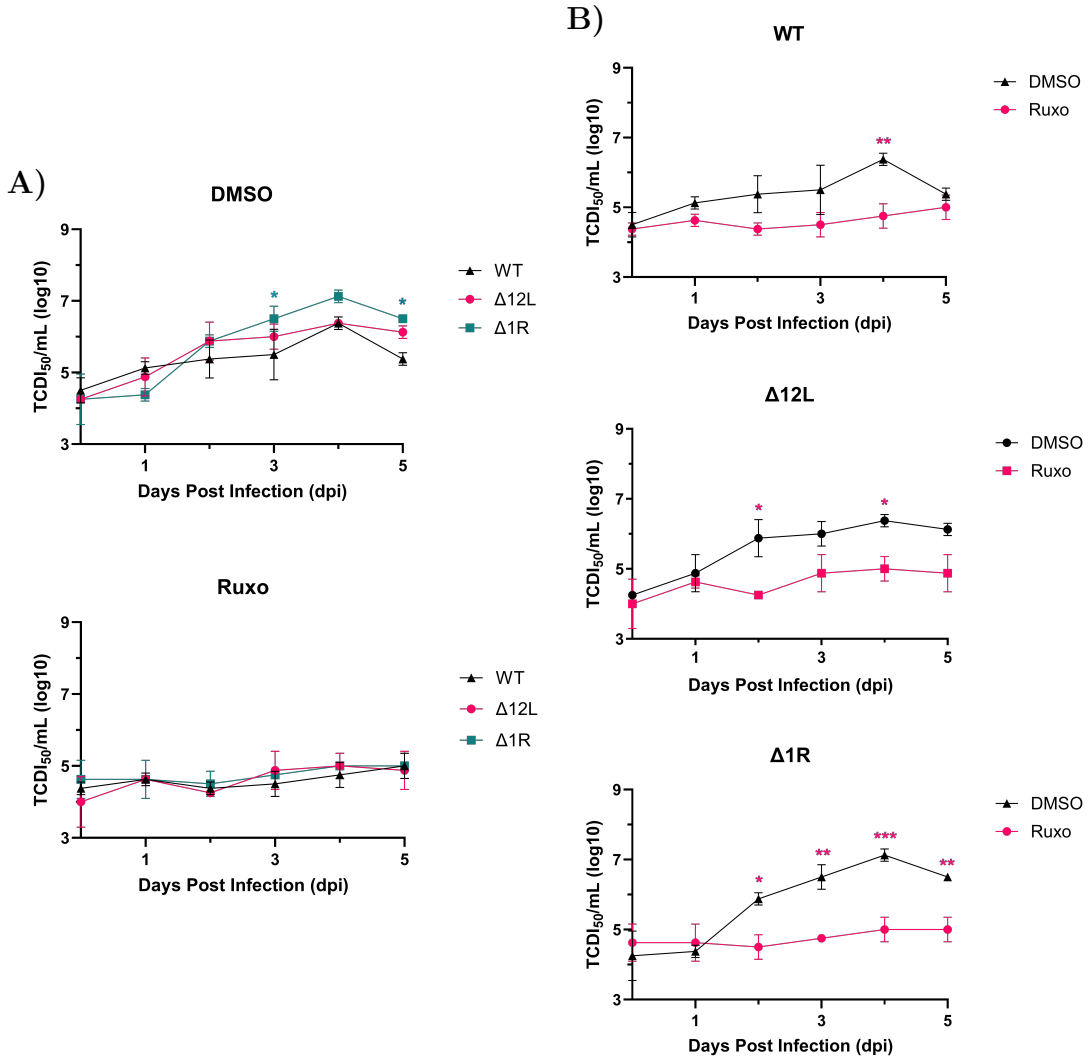

Figure 3.8: Impact of ruxolitinib on the growth of ultracentrifuged WT and recombinant viruses *in vitro*, in cells from *Swine 2*. Multistep growth curves of the mutant gene-deleted viruses were performed over 5 days in cells pre-treated overnight with Ruxo [10 μM] or DMSO VC [1 μL/mL]. Grouped by **A)** treatment or **B)** by viral inoculant. Experimental parameters and statistical analyses as in analogous experiments.

We repeated the experiment described in 3.2.4, but this time using ultracentrifuged virus stocks as the inoculant to reduce the potential influence of carry-over IFN or other cytokines.

The results showed that the significance of the difference in titres between Δ12L and the wt did not change in either biological replicate upon treatment (Figs. 3.7A and 3.8A). It is worth noting that in swine 2, the titres for all viruses tested were

generally lower when treated, compared to the VC (Fig. 3.8B). Furthermore, the titres of Δ12L after treatment did not significantly increase by day five compared to the DMSO VC. In fact, in swine 1, the titres were actually lower following Ruxo treatment at 5 dpi (**: p = 0.0015)(Fig. 3.7B), and there was no variation in swine 2 (Fig. 3.8B).

These findings indicate that JAK/STAT inhibition is not sufficient to recover the replication deficiency of Δ12L, even after minimizing potential artefacts caused by carryover IFN or other cytokines. This suggests that the observed *in vitro* replication deficiency of Δ12L does not appear to be linked to its impact upon the IFN response.

3.2.7 Cell Viability of PBMs Treated with Ruxo

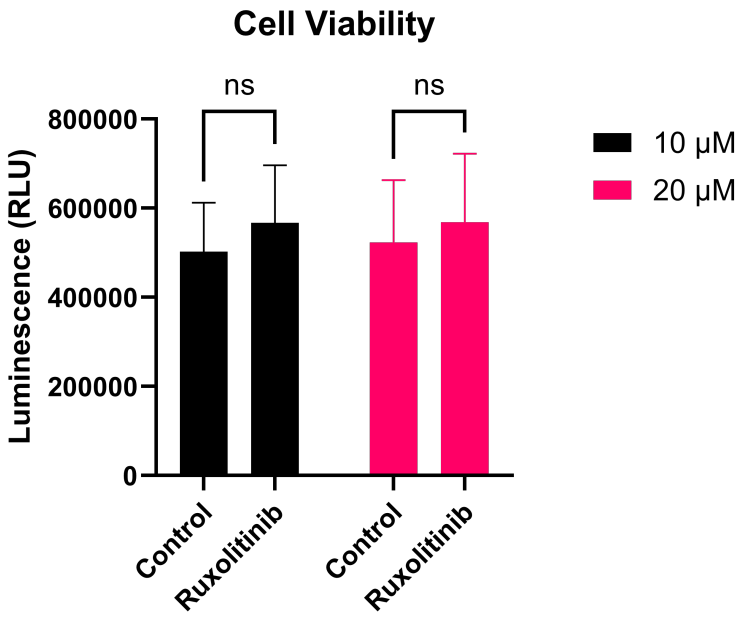

Figure 3.9: Cell viability of PBMs treated with ruxolitinib. PBMs were treated with Ruxo $[10\mu M]/[20\mu M]$ or DMSO VC $[1\mu L/mL]/[2\mu L/mL]$ for the length of a 5 day time course (including overnight pre-treatment). Cell viability was assessed using the RealTime-Glo™ MT Cell Viability Assay 5 days and 1 night post-treatment. The luminescent signal correlates with the number of viable cells. Significance was assessed by ordinary two-way ANOVA, with main effects only, and a Tukey's multiple comparisons test, with a single pooled variance, using the resulting mean and standard deviation of sixteen technical replicates.

To assess the impact of Ruxo on the viability of PBMs, we used the RealTime-Glo™ MT Cell Viability Assay (see Section 2.6 for detailed methods). Approximately

5×10^6 cells/mL were plated and pre-treated overnight with Ruxo [10 or 20 μM] or DMSO VC (1 or 2 μL/mL). Cell viability was measured at 6 days post-treatment, which corresponds to the longest treated incubation time in previous experiments.

The results (Fig. 3.9) show that the cell viability, indicated by luminescence, is similar between the Ruxo-treated group and the DMSO control group. This suggests that Ruxo does not significantly affect the viability of PBMs. Therefore, the observed effects on ISG induction and viral replication in previous experiments are not due to cytotoxic effects of Ruxo, but rather its specific inhibition of the JAK/STAT signalling pathway.

3.3 Discussion

The results presented in this chapter elucidate the intricate role of the *MGF360-12L* gene in modulating the immune response during ASFV infection and its implications for vaccine development. The deletion of MGF360-12L significantly impacts the expression of ISGs, underscoring the gene's function in immune evasion by ASFV.

The deletion of MGF360-12L from the Georgia2007/1 ASFV isolate resulted in a marked increase in *CXCL10* expression at both mRNA and protein levels, showing a greater than 70-fold increase compared to the wild-type isolate at 16 hpi. This substantial upregulation highlights *MGF360-12L*'s role in suppressing type I IFN responses, which are crucial for initiating antiviral states in host cells (Figure 3.1). This finding is consistent with previous studies that have demonstrated the importance of MGF360 and MGF505 genes in modulating the host immune response.[92, 192, 193] However, since even at a lower MOI, mutants with the 12L deletion strongly induced expression of ISGs as early as 2 hpi, we suspected that excess IFN produced by the mutants during viral replication may be carried over from harvest onto subsequent experiments, leading to confounding effects on our observations.

To address this complication, we pre-treated PBMs with Ruxo, a JAK/STAT pathway inhibitor. This reduced the early induction of ISGs in the Δ12L mutant at 2 hpi to levels comparable with the wt isolate (Fig. 3.3), but was not sufficient

to revert its reported *in vitro* growth defect (Figs. 3.4 and 3.5). This suggests that while the JAK/STAT pathway is significant in the antiviral response induced by the deletion of *MGF360-12L*, other host pathways are also likely to be involved in controlling viral replication (See 3.2.4).[228]

Indeed, Golding et al. [92] demonstrated that only the Pr4Δ35 mutant, which lacks multiple MGF genes (MGF360-9L through 14L, MGF505-1R and -MGF505-2R (2R)), showed significantly reduced replication in porcine alveolar macrophages (PAMs) treated with recombinant IFN-α. Importantly, a mutant lacking just 12L along with MGF360-13L (13L) and 14L (Pr4Δ3-C2) was not inhibited by IFN-α, suggesting that the deletion of 12L alone or in combination with a small number of MGF genes is not sufficient to sensitize the virus to IFN. This finding appears to contrast with more recent work by Fan et al. [229], who reported that ASFV replication *in vitro* and viral load *in vivo* could be reduced with recombinant porcine IFNs pre-treatment. However, this apparent discrepancy may be explained by several factors: Fan et al. [229] used a different viral strain (SY18 versus Pr4), different combinations of type I and II IFNs, and different experimental conditions including timing of IFN treatment. Additionally, while Golding et al. [92] focused specifically on studying IFN sensitivity in the context of MGF deletions, Fan et al. [229] examined the potential of IFN treatment as an antiviral strategy more broadly. These differences highlight the complexity of viral-host interactions and emphasise the importance of considering experimental context when interpreting results across different studies. This competitive redundancy in viral immune evasion strategies parallels mechanisms observed in other large DNA viruses like poxviruses, which also encode multiple interferon antagonists at their genomic terminal ends to ensure robust suppression of host antiviral responses.[12]

Our findings build upon these observations by demonstrating that while deletion of 12L alone is sufficient to significantly impact viral replication and ISG induction, the relationship between IFN sensitivity and viral attenuation is complex and likely involves multiple cellular pathways and competitive interactions between MGF proteins. The robust ISG induction we observed in Δ12L-infected cells,

even after removing excess IFN through ultracentrifugation (Fig. 3.6), highlights that effective attenuation strategies may need to consider the combined deletion of multiple immune evasion genes while maintaining sufficient viral fitness to elicit immunogenicity.

The similarity of ISG expression levels in Δ12L-infected cells treated with Ruxo to those in cells inoculated with the wild-type isolate (Fig. 3.3) indicate that infection with the Δ12L deletion mutant has a strong impact on the host innate immune response upstream of the JAK/STAT pathway. This complex interaction with host signalling pathways is characteristic of ASFV's multimodal approach to immune evasion.[70, 205]

Ultracentrifugation of the Δ12L virus stock decreased excess IFN levels and shifted the temporal expression profile of *CXCL10* to closer resemble that of other mutants without the *12L* deletion with a higher expression peak at 16 hpi, whilst maintaining a reduced, yet significantly higher expression at 2 hpi (Fig. 3.6). However, ultracentrifugation did not revert the *in vitro* growth defect of the Δ12L mutant, confirming that factors beyond IFN levels and ISG induction timing contribute to the observed growth defect (See 3.2.6). Additionally, Ruxo treatment did not significantly affect the viability of PBM cells, confirming that the observed effects on ISG induction and viral replication are due to specific inhibition of the JAK/STAT pathway and not cytotoxic effects (Fig. 3.9).

Our findings extend previous work by showing that the deletion of 12L alone is sufficient to induce early ISG expression, suggesting a specific role for this gene in countering the establishment of an antiviral state in target cells via IFN signalling. This early ISG induction in the Δ12L mutant marks 12L as a prime candidate for deletion to achieve attenuation, since in other viral systems, such as influenza A virus, early ISG induction contributes to viral clearance.[230]

These findings have significant implications for future ASFV LAV development. While the strong induction of ISGs and growth defect observed with the Δ12L mutant initially suggest its potential as a vaccine candidate, caution must be exercised when targeting IFN inhibitory genes. Rathakrishnan et al. [205] demonstrated that

deletion of 12L together with 1R and K145R (Δ1R12L) resulted in attenuation but only protected 2 out of 6 pigs against challenge. Higher protection levels (66.7%) were achieved when additional MGF360 genes were deleted alongside 12L and 1R. The relevance of carefully selecting gene deletions for vaccine development is further highlighted by findings from Reis et al. [231], where deletion of the type I IFN inhibitor I329L (Table 1.3) from the attenuated OURT88/3 isolate unexpectedly reduced protection against challenge, associated with impaired antibody and cellular immune responses. This counter-intuitive outcome emphasizes that while type I IFN is crucial for controlling early viral replication and stimulating adaptive immunity, excessive or prolonged IFN exposure can actually lead to immunosuppression. This phenomenon has been well-documented in studies of chronic viral infections, where sustained type I IFN signalling can dysregulate immune responses to enable infection.[232, 233] Thus, effective LAV development requires achieving a delicate balance - the deletions must sufficiently attenuate the virus while maintaining enough immune evasion capacity to prevent detrimental IFN responses. Our detailed characterisation of how individual MGF proteins like 12L disrupt cellular signalling pathways provides crucial insights for the rational design of balanced attenuation strategies.

Collectively, these studies suggest that an effective and safe vaccine will likely require the selective deletion of MGFs and other ASFV genes that suppress type I IFN signalling to achieve an optimal balance between attenuation and immunogenicity. This approach could lead to the development of LAVs that stimulate a robust immune response by maintaining a sufficient level of viral replication for effective immunisation.

While this study provides significant insights, several limitations must be addressed in future research. The use of *in vitro* systems may not fully replicate the complexities of an actual infection in pigs. Primary macrophages exhibit variability between different pigs and even amongst macrophage subpopulations, which can affect reproducibility and viral susceptibility.[61, 214] The development of immortalized porcine macrophage cell lines could help standardise results and

improve experimental reproducibility.[234] Future *in vitro* studies should use ultracentrifuged virus stocks, or use an analogous method, before using deletion mutants with deletions of IFN inhibiting genes. Beneficial future work with these mutants would include: investigating the impact of infection on endogenous protein levels of different transcription factors (i.e. IRFs) in PBMs to complement *in vitro* data, or characterising their growth dynamics in other immune cells likely relevant to ASFV *in vivo* infection (such as: specialist IFN-α-producing pDC) or in differently stimulated monocyte-derived macrophages. Moreover, *in vivo* studies in pigs are essential to validate these findings and examine the levels of IFN in sera following vaccination and/or infection. Golding et al. [92] and Rathakrishnan et al. [205] showed that pigs infected with virulent ASFV produced high levels of type I IFN in serum, which correlated with disease progression rather than protection. In contrast, pigs vaccinated with attenuated strains showed lower IFN levels but were protected against challenge. This highlights the complex relationship between IFN levels and protection, and how ASFV research requires both *in vitro* and *in vivo* studies to inform vaccine development strategies.

In conclusion, our findings contribute to the understanding of ASFV immune evasion mechanisms and provide valuable insights for the development of LAVs. By elucidating the role of MGF360-12L in modulating the host immune response, we have characterised a potential target for vaccine development.

4
Host Interactions of MGFs

Contents

4.1 Introduction 79
4.2 IRF7 81
4.2.1 Impact of MGFs on *IFNA6* promoter activity 81
4.2.2 12L Does Not Co-Immunoprecipitate With IRF7 85
4.2.3 Impact of 12L on IRF7 Protein Levels 86
4.2.4 12L Inhibits IRF7 Nuclear Translocation 88
4.3 IFN Response Pathway 93
4.3.1 MGFs Inhibit Warthog ISG Promoter Activity 93
4.3.2 MGFs Do Not Promote Degradation of STATs 94
4.4 Discussion 96

4.1 Introduction

The MGFs of ASFV represent approximately 30% of its genome and account for most of the genetic variation observed between viral isolates.[8] These gene families, clustered at the terminal ends of the viral genome, are expressed very early during infection and play crucial roles in immune evasion.[7, 14] The immediate-early expression and genomic location of these genes parallel similar immune evasion strategies found in related large DNA viruses, particularly poxviruses, which also encode immediate-early interferon-inhibiting genes at their terminal

ends.[12] Given the relevance of multigene family members in ASFV immune evasion, these have become the subject of exhaustive research in this field (see section 1.4 and tables 1.2 & 1.4).

Of particular interest for our study are the MGF360 and 505 families, of which some members have also been shown to contain ANK repeats - protein-protein interaction motifs that are widespread throughout eukaryotic signalling proteins but rarely found in viruses.[124] The presence of these domains in both ASFV and poxviruses highlights their importance in host immune modulation for these large DNA viruses, and the evolutionary advantage they represent.[194] Previous work also identified putative VHL and SOCS-box motifs in 12L and 1R respectively, suggesting these proteins might recruit CRL machinery to modulate host protein levels; their interaction with CRL components was also later demonstrated (see 1.4.3).[124] Indeed, mutations in the SOCS-box of 1R were shown to alleviate its inhibition of IRF3/NF-κB-dependent transcription and IRF3 nuclear translocation, although, similar mutations in the VHL-box of 12L had no effect.[124]

While the role of these genes in suppressing IFN-β induction has been well characterized, their impact on IFN-α regulation remains largely unexplored. This is particularly relevant as IFN-α expression is primarily regulated by IRF7, which plays a crucial role in amplifying the type-I interferon response through a positive feedback loop (see Fig. 1.9).[108, 109] Although most cells maintain low basal levels of IRF7, certain cells including pDCs, B and other mononuclear myeloid cells constitutively express it, enabling rapid and robust IFN responses.[108, 110]

The difference in IFN responses observed between *in vitro* and *in vivo* ASFV infections suggest complex mechanisms of immune modulation, likely involving multiple cell types. Virulent ASFV isolates maintain remarkably low IFN levels in infected macrophages *in vitro*, even when cells are externally stimulated, while triggering cytokine storms and elevated IFN levels *in vivo*.[79, 92] Counter to this, attenuated strains produce high levels of IFN-α *in vitro* but much less *in vivo*, suggesting that effective IFN suppression in m-MΦs is linked to virulence.[92] This ability to modulate IFN responses in macrophages is particularly crucial as these cells

are central to orchestrating immune responses through antigen presentation, cytokine production, and recruitment of other immune cells.[74, 78, 81] Indeed, virulent strains are more effective at controlling downstream ISG expression through mechanisms that appear independent of IRF3 modulation, suggesting involvement of additional pathways.[79, 235]

Notably, our collaborators in the ASFV-Int consortium recently identified UBA3 as a binding partner of 12L (Dr. Grégory Caignard and Dr. Juliette Dupré, Unpublished) (See 1.4.3). This interaction is particularly intriguing as UBA3, the catalytic subunit of the only known NAE complex, mediates neddylation: a crucial post-translational modification known to regulate both CRL function and IRF7 activity. UBA3-mediated neddylation is essential for IRF7 stability, nuclear translocation, and transcriptional activity,[117–119] suggesting a potential mechanism by which ASFV could interfere with IFN signalling through 12L.

To further investigate the impact of MGF on IFN induction and signalling beyond IRF3-dependent IFN-β, we performed a series of *in vitro* studies using codon-optimized MGF expression constructs and their corresponding mutants. We examined their effects on IRF7-dependent IFN-α transcription, IRF7 protein levels and cellular localization, and assessed the role of proteasomal degradation in these processes. Additionally, we investigated their impact on endogenous STAT1/2 levels to understand how these viral proteins might modulate downstream IFN signalling pathways.

4.2 Results: IRF7

4.2.1 Impact of MGFs on IRF7-dependent *IFNα6* promoter activity

To investigate the role of ASFV MGF genes in modulating IFN-α induction, we employed a dual luciferase assay with a firefly luciferase reporter gene under the control of the interferon alpha-6 (IFNα6) promoter. This assay was designed to assess the direct impact of various MGF genes on the induction of IRF7-dependent IFN-α.

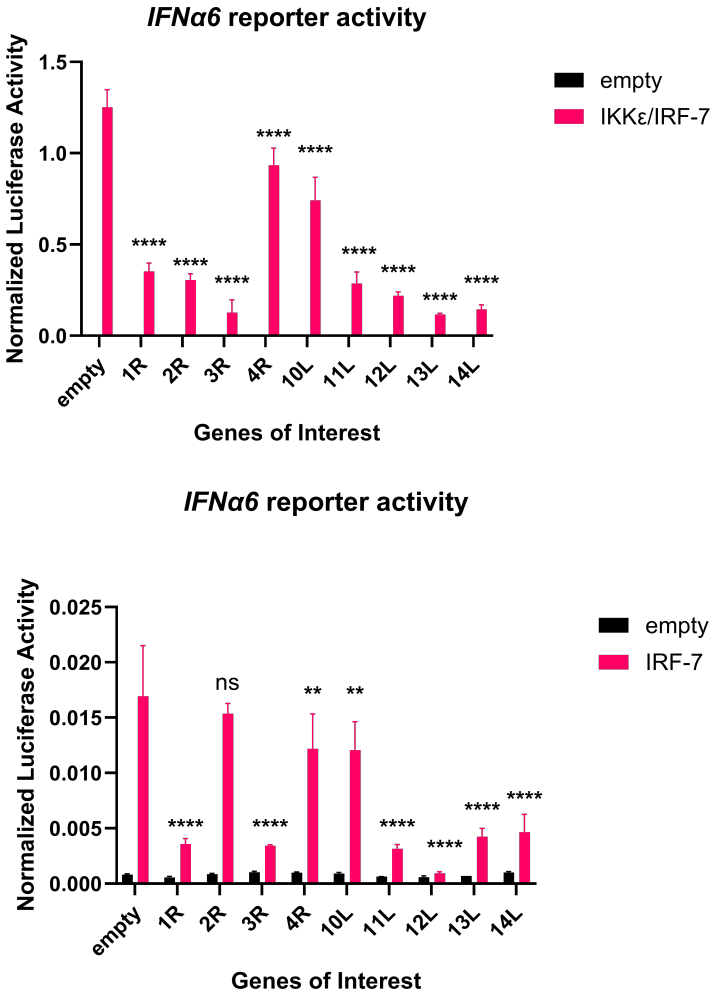

Figure 4.1: MGF505 and 360s inhibit *IFNα6* promoter activity. Activity of the Firefly Luciferase reporter under the control of the IRF7-dependent *IFNα6* promoter was normalised to Renilla luciferase in a Dual-Luciferase®-Reporter assay. Plasmids encoding ASFV MGF genes were co-transfected with IRF7 alone (bottom) or with IRF7 and IKKε (top). Sample transfections were performed in triplicates, and each experiment was replicated four times, this is a representative result. Ordinary two-way ANOVA and Dunnett's MCT, with a single pooled variance. Displayed significance corresponds to comparisons against positive empty control.

As shown in Figure 4.1, both 12L and 1R significantly reduced IFNα6 reporter activity under two distinct conditions: overexpression of both IRF7 and IKKε, or IRF7 alone. This inhibitory effect was highly significant ($p < 0.0001$) and consistent across four experimental repeats.

Interestingly, all tested MGF genes significantly inhibited IFNα6 reporter activity ($p < 0.0001$) compared to the empty control when both IKKε and IRF7 were co-transfected. However, when only IRF7 was co-transfected, the impact of MGF overexpression on reporter activity varied. While most MGF genes maintained a highly significant inhibitory effect ($p < 0.0001$), 2R showed no significant difference, and MGF505-4R (4R) and 10L exhibited a less pronounced, but still significant inhibition (**: $p \leq 0.002$).

These results suggest that multiple MGF genes play crucial roles in suppressing IRF7-mediated activation of the IFNα6 promoter, with some genes showing consistent inhibition across different stimulation conditions, while others display context-dependent effects. Given the homology of MGF members, as they arise from duplication events, it is understandable that they may share analogous functionality. However, assays such as this allow us to differentiate the impact that different MGF members have upon a specific pathway. Some of these genes may act at the level of the kinase or above, not inhibiting transcription in cells overexpressing IRF7 alone (i.e. 2R), whilst others may impact both IKKε and IRF7 or the transcription factor alone. This finding provides insight into the mechanisms by which ASFV may modulate host innate immune responses, specifically the induction of type I IFN.

We sought to further investigate the impact of 12L and 1R, as their overexpression consistently inhibited the IFNα6 reporter across four experimental replicates (Fig. 4.1). To elucidate the role of putative VHL and SOCS-Boxes previously identified in these genes, we co-transfected cells under the same conditions using constructs with mutations designed to inactivate either each box (mVHL/mSOCS) or only their respective BC or Cullin2/5 box (mBC and mCUL). By comparing the behavior of these mutated constructs to their wt counterparts, we aimed to

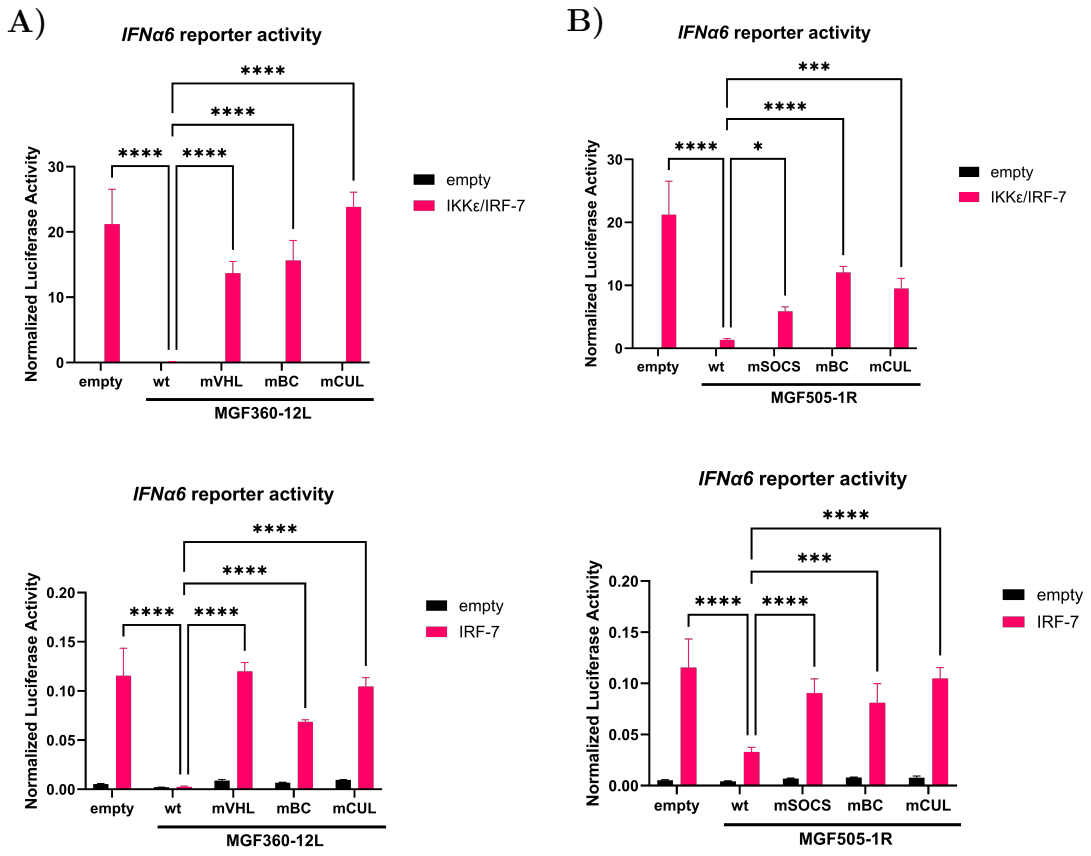

Figure 4.2: Impact of MGF360-12L, MGF505-1R and Mutants on *IFNα6* Promoter Activity. Activity of the Firefly Luciferase reporter under the control of the IRF7-dependent *IFNα6* promoter was normalised to Renilla Luciferase in a Dual-Luciferase®-Reporter assay. Plasmids encoding ASFV MGF genes were co-transfected with IRF7 alone (bottom) or with IRF7 and IKKε (top). Sample transfections were performed in triplicates, and each experiment was replicated four times, this is a representative result. Ordinary two-way ANOVA and Tukey's MCT, with a single pooled variance. **A)** 12L and mutants; **B)** 1R and mutants.

identify whether these putative domains play a significant role in the function of our ASFV genes of interest.

For 12L, we successfully replicated the inhibition of *IFNα6* reporter activity observed with the wt construct. This signal suppression was significantly reversed by all mutants when transfected in its place, both downstream of IRF7/IKKε and IRF7 alone (****: $p < 0.0001$) (Fig. 4.2A).

Interestingly, the significance of improved *IFNα6* reporter activity in samples transfected with mutant constructs versus their corresponding wt differed notably between 12L and 1R downstream of IRF7 and IKKε. For 12L, the difference

in activity for all its mutants compared to the wt was highly significant (****: $p < 0.0001$). However, when compared to the empty control, the observed differences were remarkably less significant (not displayed) (mVHL/mBC/mCUL, **/*/ns: $p = 0.003/0.0339/0.5737$) (Fig. 4.2A). Conversely, for 1R and its mutants, the difference with their wt (mSOCS/mBC/mCUL, */****/***: $p = 0.0447/ < 0.0001/ = 0.0002$) had a lower significance than against the negative empty control (not displayed) (****: $p < 0.0001$) (Fig. 4.2B).

Collectively, these data suggest that 12L inhibits the induction of IRF7-dependent type-I interferon and this appears to depend on structural motifs located in the protein's putative VHL-box domain.

4.2.2 MGF360-12L Does Not Co-Immunoprecipitate With IRF7

To further elucidate the mechanism by which 12L inhibits IRF7-dependent transcription, we investigated whether these proteins directly interact. We hypothesized that if 12L binds to IRF7 to inhibit its activity, we should be able to co-immunoprecipitate the two proteins.

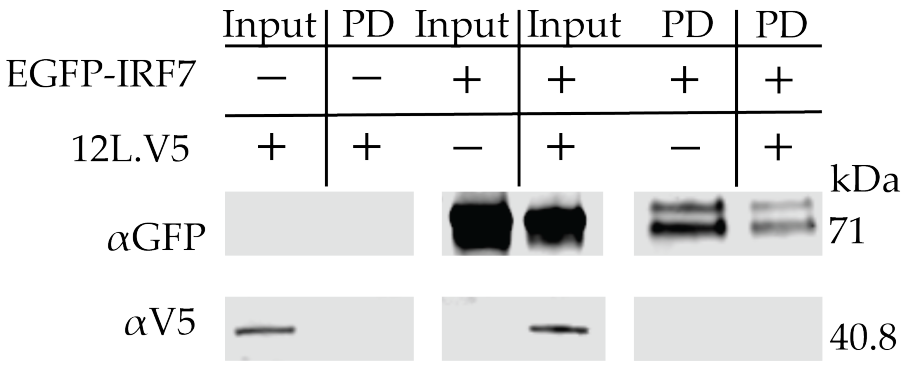

Figure 4.3: MGF360-12L Does Not Immunoprecipitate With IRF7. Cells were transfected with plasmids expressing V5-tagged 12L and/or EGFP-tagged IRF7 as indicated (+/-) above each lane. Cell lysates (Input) were subjected to IP using GFP-trap magnetic beads (see methods section 2.8.2). Both input and pull-down (PD) samples were analysed by Western blot using antibodies against: GFP (αGFP) to detect EGFP-IRF7, or V5 (αV5) to detect 12L.V5.

We developed and optimized a pull-down assay using GFP-trap magnetic beads to isolate EGFP-tagged IRF7. HEK293T cells were transfected with EGFP-IRF7,

12L, or both constructs. As shown in Figure 4.3, we successfully detected EGFP-IRF7 in the immunoprecipitates from GFP-trap beads (Fig. 4.3, last two lanes). However, 12L was not co-immunoprecipitated with IRF7, indicating that they do not interact under the tested conditions.

4.2.3 Impact of MGF360-12L on IRF7 Protein Levels

Given the observed impact of MGFs on IRF7-dependent *IFNα6* promoter activity, we sought to determine whether this inhibitory function translated to a modulation of exogenous IRF7 at the protein levels.

This will provide insight into a potential mechanism of viral immune evasion employed by ASFV, where certain MGF proteins, particularly those from the MGF360 family, may target IRF7 for degradation. To further investigate this hypothesis, we focused on 12L and its mutants, examining their effects on IRF7 protein levels in more detail. We focused on 12L because of its strong inhibitory effect upon IRF7-dependent transcription downstream of both IRF7 and IKKε, and because overexpression of 12L constructs with mutations in its putative VHL-box were able to strongly revert this phenotype.

We sought to ascertain whether the observed effect on IFNα6-promoter transcription translated to a dose-dependent phenotype upon exogenous IRF7 protein levels, and if our mutant constructs would revert this hypothesised effect. To do this, we transfected HEK293T cells with IRF7 and increasing amounts of pcDNA3.1 expressing 12L or its mutants against an empty control (Fig. 4.4). Western blot results showed that 12L decreases IRF7 protein levels in a dose-dependent manner. Interestingly, transfection with the mBC mutant construct of 12L had no impact on IRF7 signal, whereas mCUL appeared to reduce it in all conditions. 12L.mVHL (which has mutations in both putative motifs) was only as effective as the wt at the highest dose.

To investigate whether the 12L-mediated decrease in IRF7 levels involves proteasomal degradation, we conducted an experiment using the proteasome inhibitor MG132 (Fig. 4.5). HEK293T cells were co-transfected with EGFP-IRF7

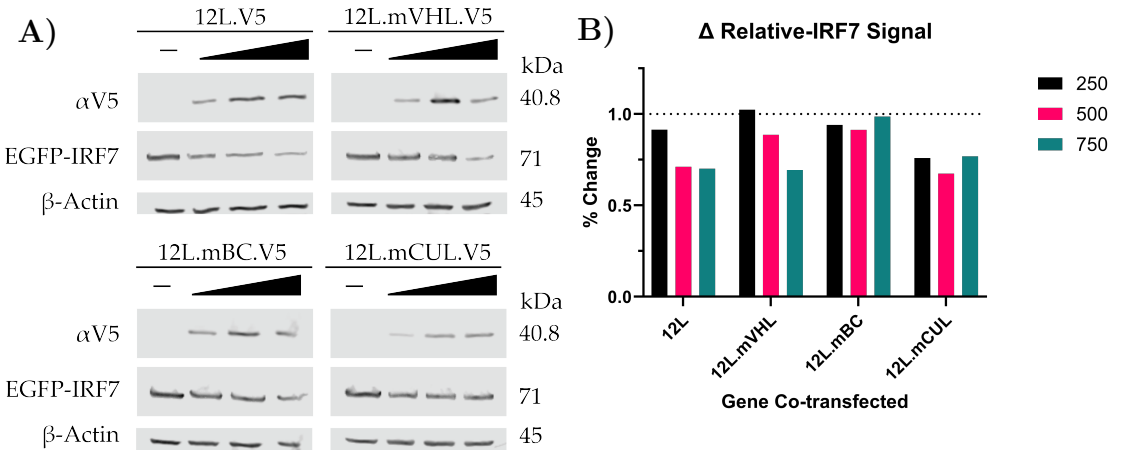

Figure 4.4: Impact of WT 12L and Mutants on IRF7. A) Western blot showing the impact of 12L wild type (wt) and mutants on exogenous IRF7 protein levels. **B)** Quantification of the change in IRF7 signal is displayed relative to each empty control and normalized to beta-actin (β-actin). Representative of three immunoblot experimental repeats.

and increasing amounts of 12L, followed by treatment with either DMSO (VC) or MG132 [20 μM] for 5 hours prior to cell lysis and immunoblotting. Western blot analysis (Fig. 4.5A) and quantification of the normalized IRF7 signal (Fig. 4.5B) confirmed our previous observations of 12L-induced reduction in IRF7 levels in the VC group. Importantly, treatment with MG132 for just 5 hours was sufficient to largely abolish this effect. In the presence of MG132, IRF7 levels remained relatively stable across increasing 12L concentrations, with only a slight, albeit significant (*: p=0.0232), decrease observed at the highest 12L concentration. These results provide strong evidence that 12L promotes the proteasomal degradation of IRF7, offering insight into the mechanism by which this viral protein may suppress host interferon responses.

Furthermore, the differential effects observed with the 12L mutants highlight the importance of specific protein domains, particularly the VHL box-like motif, in this degradation process. Together, these results provide evidence for a novel mechanism of ASFV immune evasion, where 12L promotes IRF7 proteasomal degradation, suppressing the infected host cells' ability to quickly establish an antiviral molecular state in response to type I IFNs, downstream of IRF7.

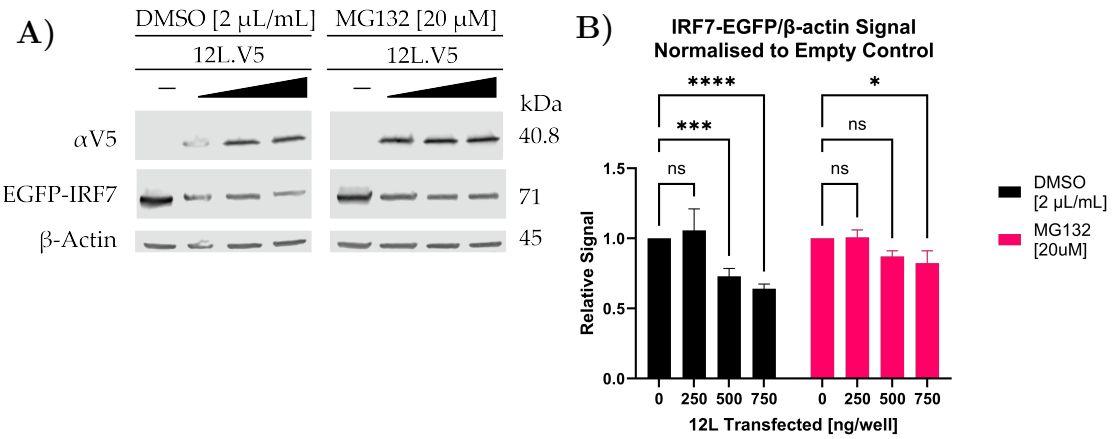

Figure 4.5: MG132 inhibits MGF360-12L dose-dependent IRF7 degradation. HEK293T cells were transfected with EGFP-IRF7 and increasing amounts of pcDNA3.1 expressing 12L. Twenty-four hours post-transfection, cells were treated with either DMSO or MG132 protease inhibitor for 5 hours before processing for immunoblotting. **A)** Western blot showing the impact of MG132 treatment on IRF7 protein levels in the presence of MGF360-12L. **B)** Quantification of the change in IRF7 signal is displayed relative to each empty control and normalized to β-actin. This data is representative of three immunoblot replicates. Statistical analysis was carried out by two-way ANOVA and Šidák's MCTs, with a single pooled variance. (***: p=0.0008; ****: p<0.0001; ns: p≥ 0.1167).

4.2.4 12L Inhibits IRF7 Nuclear Translocation

Given our previous findings that 12L overexpression strongly inhibits IRF7-dependent type I IFN transcription and decreases IRF7 protein levels in a dose-dependent manner through proteasomal degradation, we sought to investigate whether 12L also restricts IRF7 nuclear translocation. We also aimed to determine if the 12L mutants, which failed to replicate these effects in earlier experiments, would exhibit different patterns of IRF7 localization.

For these immunofluorescence experiments, we utilized Vero cells due to their relatively large cytoplasm, which makes it easier to ascertain differences in protein localisation. Cells were transfected on coverslips with the appropriate constructs, mirroring the conditions used in Section 4.2.1, and processed for immunofluorescence 48-72 hours post-transfection as described in Section 2.9.

Initially, we performed a control experiment by transfecting cells with empty pcDNA and V5-tagged 12L or its mutants, with or without IKKε (Fig. 4.6). This allowed us to observe the localization of 12L and its mutants within cells in the

absence of IRF7. We found that both 12L wt and its mutants localized in both the nucleus and cytoplasm of cells, and this distribution was not notably affected by the presence or absence of IKKε.

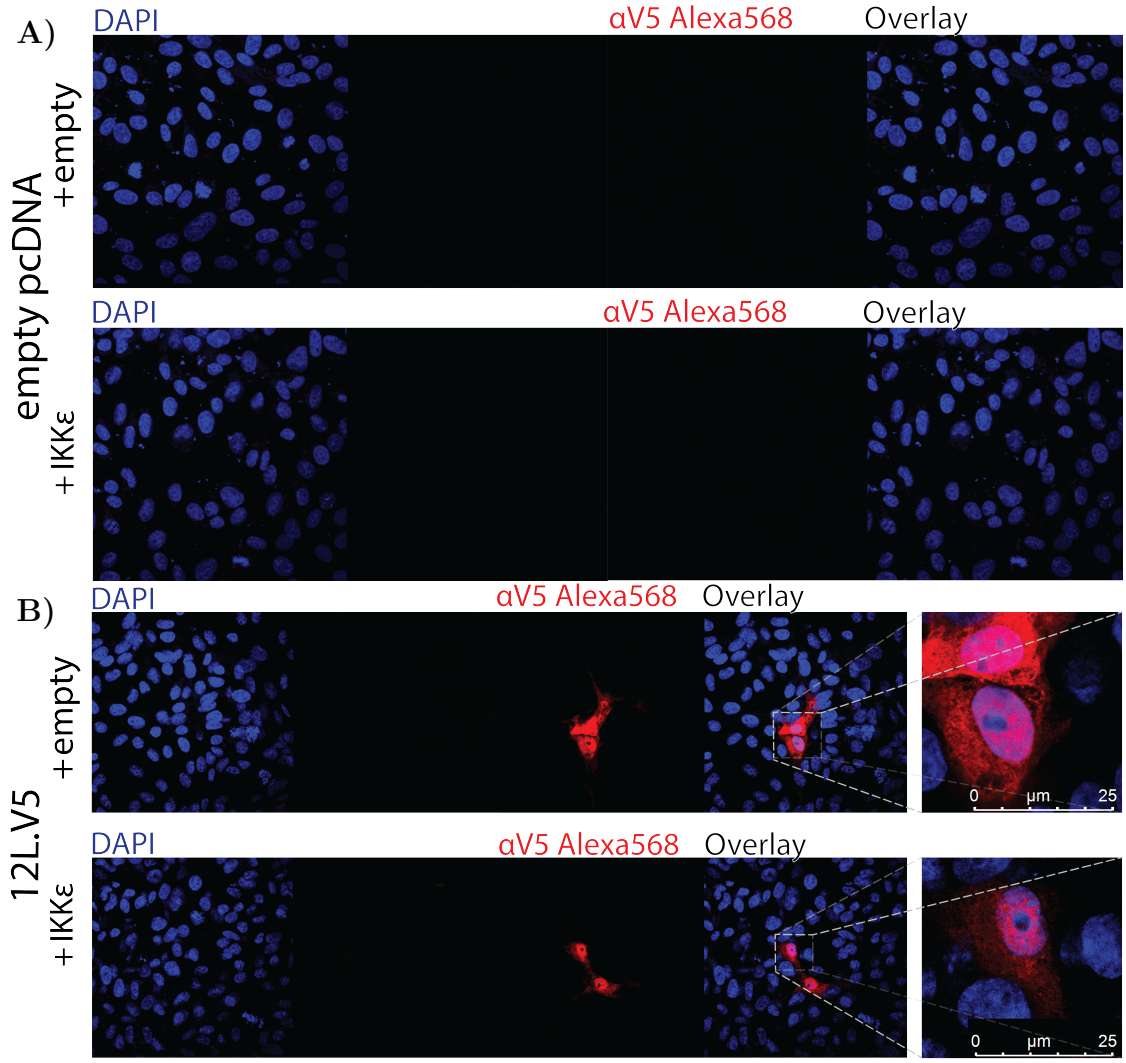

Continued on next page...

Subsequently, we co-transfected cells with EGFP-IRF7 under the same conditions (Fig. 4.7). In the empty control, IRF7 was predominantly localized in the cytoplasm of transfected cells, with minimal nuclear presence. However, when co-transfected with IKKε, IRF7 was observed mainly within the nuclei of cells, as expected (Fig. 4.7A). Notably, in the presence of V5-tagged wt 12L, IRF7 remained extranuclear under both conditions, in cells displaying both high and low levels of anti-V5 (αV5) staining (Fig. 4.7B). In contrast, samples overexpressing the 12L mutants exhibited

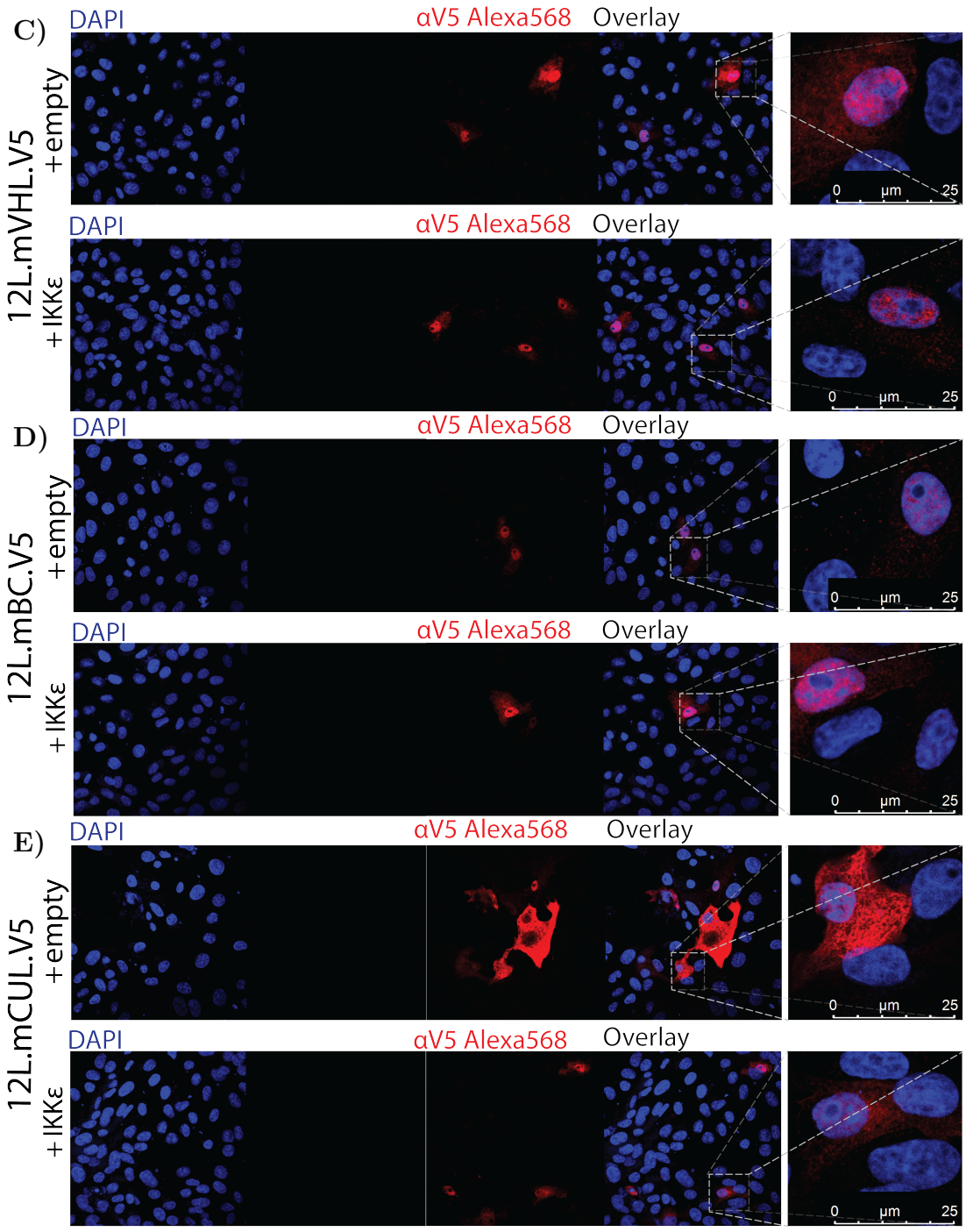

Figure 4.6: Immunofluorescence Imaging of MGF360-12L and Mutants. Vero cells were co-transfected with empty plasmid or pIKKε, with **A)** empty, or V5-tagged 12L **B)** WT, **C)** mVHL, **D)** mBC and **E)** mCUL. Coverslips with adhered cells were processed for visualisation as described in 2.9.

both intra- and extra-nuclear IRF7 in the presence of IKKε, indicating that the VHL motif might not be required for the inhibition of IRF7 translocation (Fig.

4.7C-E). It is worth noting that visual examination of the samples revealed that cells co-transfected with the 12L mutants appeared to exhibit a higher green-fluorescent intensity than the wt. This observation corroborated the findings exposed in section 4.2.3, warranting future quantitative analysis.

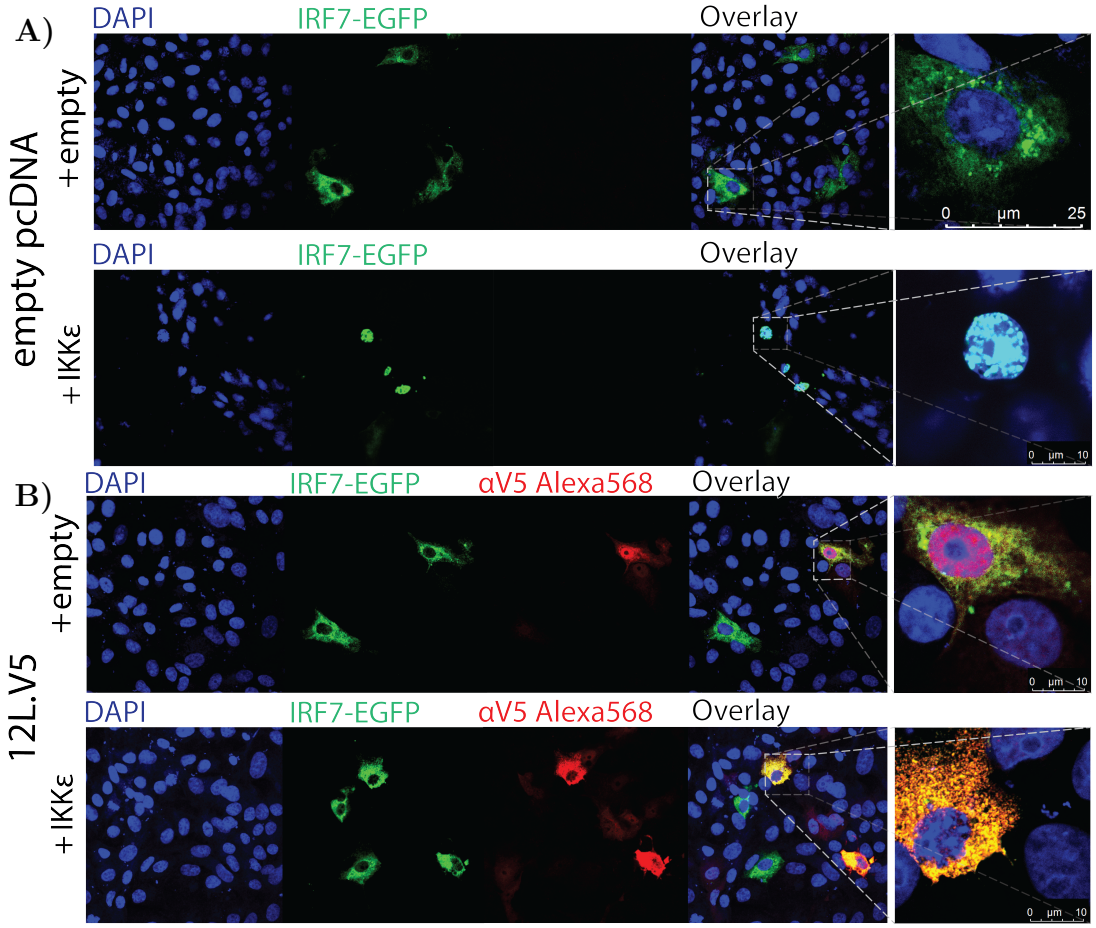

Continued on next page...

These results provide visual evidence that 12L inhibits the nuclear translocation of IRF7. This finding aligns with and extends our previous observations regarding the inhibitory effects of 12L on IRF7-dependent transcription and protein levels.

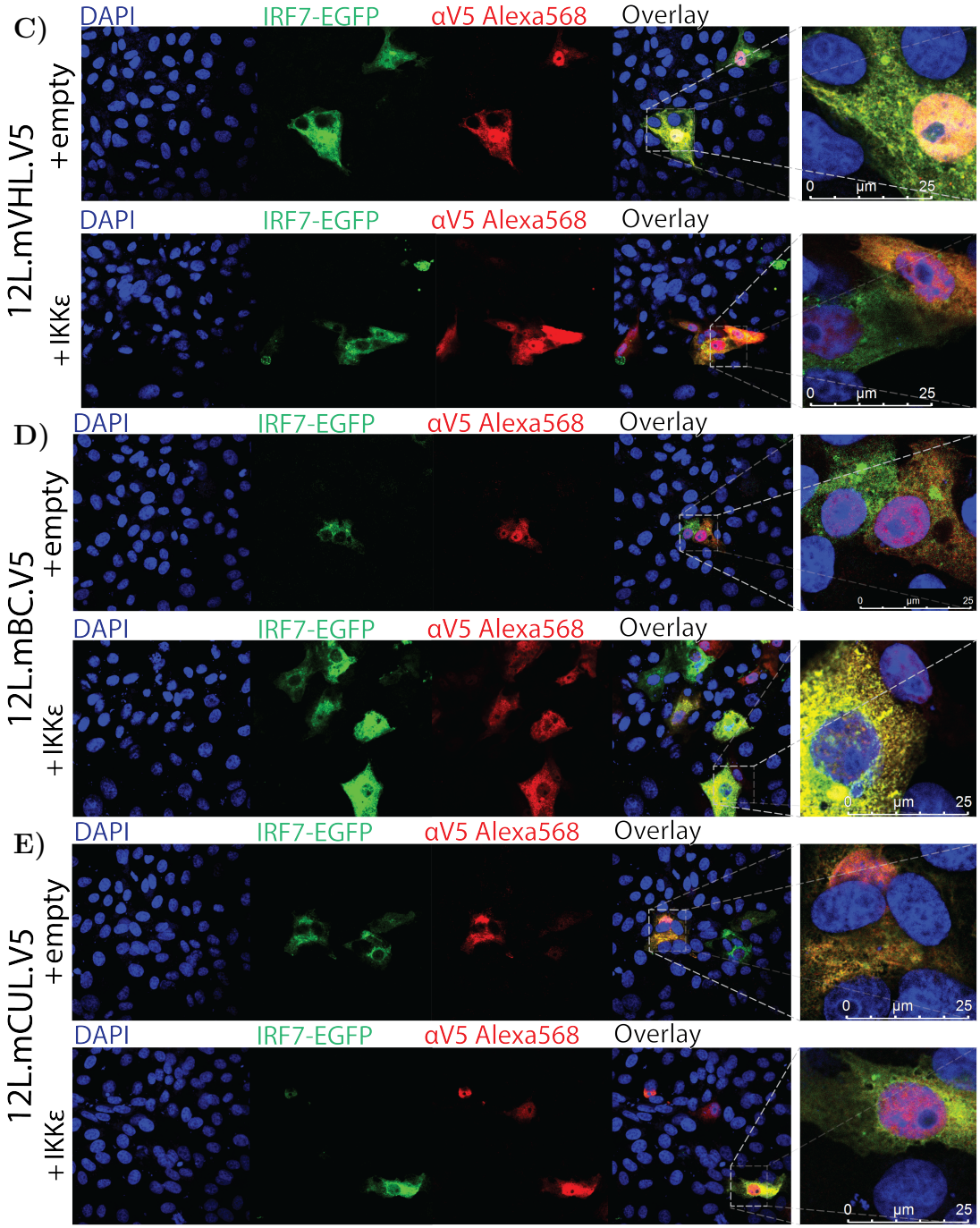

Figure 4.7: Immunofluorescence Imaging of IRF7-EGFP with MGF360-12L, WT and Mutants. Vero cells were co-transfected with pIRF7-EGFP and either empty plasmid or pIKKε, with **A)** empty, or V5-tagged 12L **B)** WT, **C)** mVHL, **D)** mBC and **E)** mCUL. Coverslips with adhered cells were processed for visualisation as described in 2.9.

4.3 Results: IFN Response Pathway

Following our research into the impact of exogenous expression of MGFs on IRF7 and IRF7-dependent IFN induction, we extended our studies to examine their effects on the broader type I IFN response pathway. We aimed to determine whether these viral proteins could influence not only the expression of IFNs but also the response of cells to IFN. Using a combination of cell-based assays, we assessed the effects of overexpressing our MGF genes of interest on the activation of porcine ISG promoters in response to type I IFN stimulation. Additionally, we investigated the impact of MGFs on endogenous STAT2 levels and examined the dose-dependent effects of 12L on both STAT1 and STAT2 levels. This comprehensive *in vitro* approach allowed us to explore multiple potential mechanisms by which ASFV might interfere with host immune responses, encompassing both the induction of IFNs and the modulation of the IFN response pathway.

4.3.1 MGF505 and 360 Genes Inhibit Warthog *MX2* Promoter Activity *In Vitro*

We utilized a DLR™ assay to assess the impact of MGF overexpression on ISG expression. Initially, we optimized assay conditions by testing the sensitivity of a panel of reporters encoding suid-derived ISG promoters to varying degrees of type I IFN stimulation (data not shown).

Using the optimized conditions, we transfected HEK293T cells with a warthog *MX2* promoter reporter and either empty vector pcDNA3.1 or one of the constructs from our panel of codon-optimized MGFs.

As shown in Figure 4.8A, all MGFs tested were able to significantly (****: $p < 0.0001$) repress warthog *MX2* promoter activity to varying degrees across four experimental repeats, with the exception of 2R, which showed non-significant inhibition in at least one repeat.

We further investigated the effects of 12L and 1R, along with their respective mutants (Fig. 4.8B). Both 12L and 1R consistently, and significantly (****: $p < 0.0001$), inhibited the reporter's activity. Interestingly, transfection with their

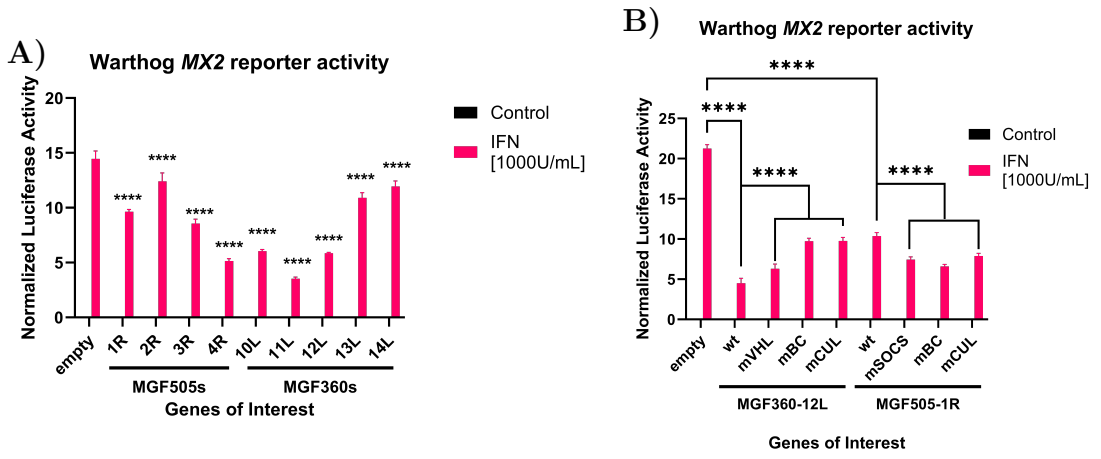

Figure 4.8: MGF360 and 505 genes inhibit the activity of warthog ISG *MX2* reporter in a dual luciferase *in vitro* assay. HEK293T cells were transfected with vectors expressing: a Firefly Luciferase reporter downstream of a warthog *MX2* promoter, an constitutive Renilla Luciferase reporter, and empty pcDNA or our genes of interest. 24-48 hours post-transfection, cells were treated with Universal IFN overnight or left untreated (control), and processed for DLR™ analysis. Normalised Luciferase activity of cells co-transfected with vectors expressing **A)** MGF505s and 360s, or only **B)** MGF360-12L, MGF505-1R and their VHL/SOCS-box mutants. This data represents mean and SD from triplicate samples, experiment representative of four repeats. Statistical analysis based on ordinary two-way ANOVA and **A)** Dunnett's or **B)** Tukey's MCT, with a single pooled variance.(****: $p < 0.0001$)

respective mutants yielded opposite effects. The 12L mutants partially reversed the reporter inhibition under IFN stimulation when compared to the wt construct. In contrast, the 1R mutants significantly increased inhibition under the same conditions (****: $p < 0.0001$). These results demonstrate that MGFs from both the 360 and 505 families can modulate the expression of ISGs, as represented by the warthog *MX2* promoter. The differential effects observed with 12L and 1R mutants suggest distinct mechanisms of action for these two genes in regulating ISG expression.

4.3.2 MGFs Do Not Promote Degradation of STATs

Given the reported impact of MGFs on type I IFN immunomodulation, we investigated their potential effect on endogenous STAT levels, which are critical factors in the molecular response to IFN. We transfected HEK293T cells with our panel of MGF genes and probed for STAT2 by immunoblotting.

As shown in Figure 4.9, we did not observe any appreciable effect on endogenous STAT2 levels by MGFs from either the 360 or 505 family clusters under these experimental conditions.

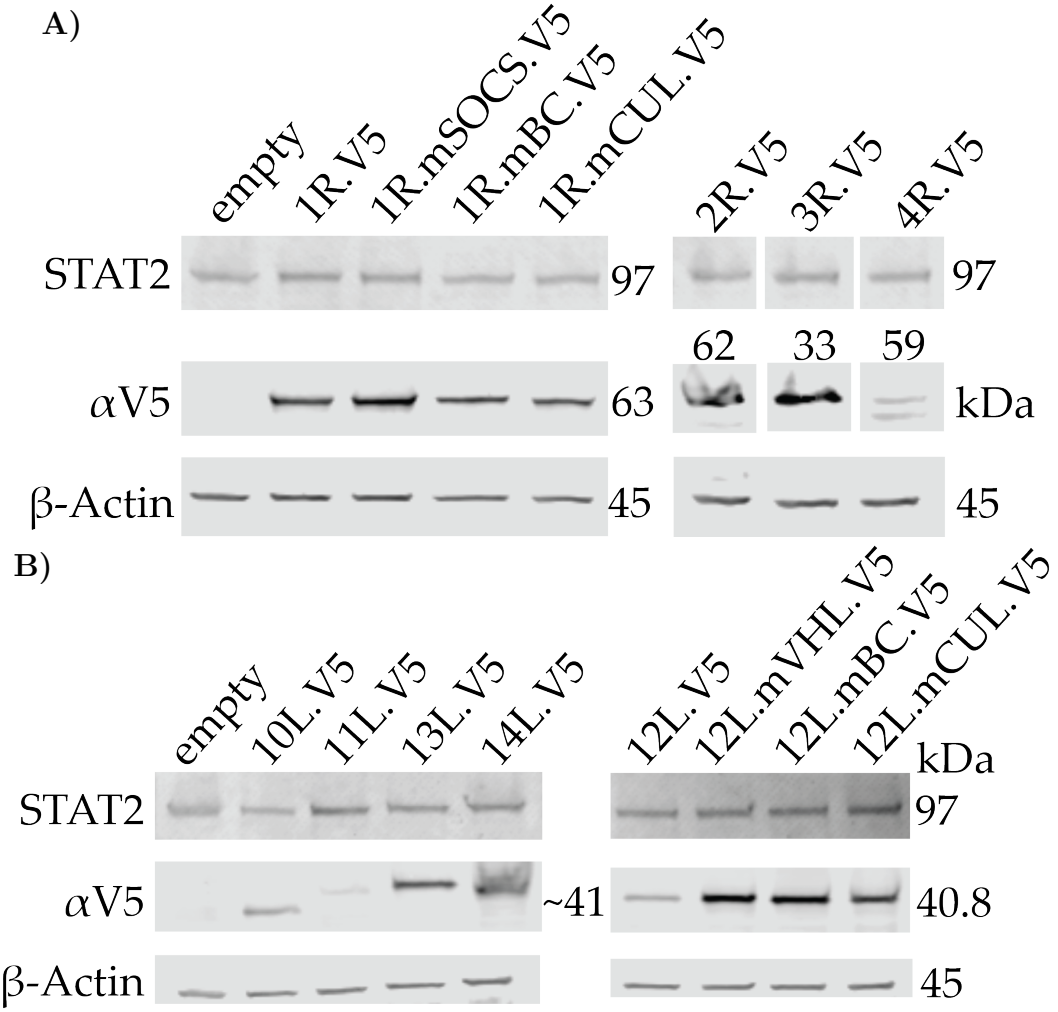

Figure 4.9: MGFs Do Not Impact Endogenous STAT2 Levels. HEK293T cells were transfected with pcDNA vectors expressing empty vector and either **A)** MGF505 or **B)** MGF360 ASFV gene constructs. After 24 hours, cells were lysed and processed for immunoblotting. Western blots were then probed for endogenous STAT2, β-actin, and exogenous V5-tagged ASFV MGF proteins.

To ensure we were not overlooking a possible dose-dependent effect, we performed a follow-up experiment focusing on 12L. We transfected HEK293T cells with increasing doses of MGF360-12L.V5, compensating with empty plasmid to maintain a consistent total amount of transfected DNA. In this instance, we probed against both endogenous STAT1 and STAT2 proteins (Figure 4.10).

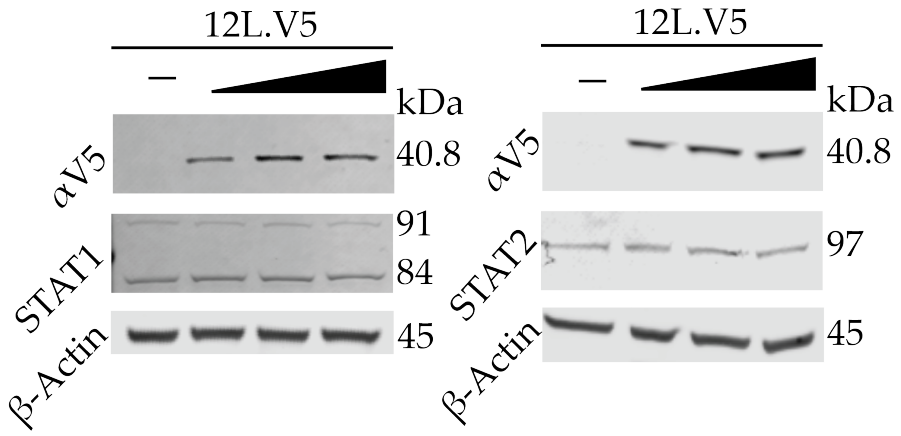

Figure 4.10: Increasing levels of 12L do not impact endogenous STAT1 or STAT2 protein levels. HEK293T cells were transfected with increasing amounts of 12L.V5, with total DNA amount kept constant using empty vector. Whole cell lysates were analysed by Western blot for V5-tag (αV5), β-actin (loading control), and either STAT1 or STAT2, 48 hours post-transfection. Representative blot from three independent experiments is shown.

These results confirmed that 12L does not significantly impact the levels of endogenous STAT1/2 proteins *in vitro*, even at increasing concentrations. Collectively, these findings suggest that the immunomodulatory effects of MGFs, particularly 12L, on type I IFN response signalling are likely not mediated through direct degradation or downregulation of STAT1 or STAT2 proteins.

4.4 Discussion

The observed variations in IFN-α transcription inhibitory potency among different MGF genes suggest a complex and potentially redundant strategy employed by ASFV to counteract the host's innate immune response. This functional overlap is likely explained by the homology found amongst MGFs, as these genes have evolved through duplication events.[8, 69] Such evolutionary strategy may confer robustness to the virus's immune evasion mechanisms, preventing the establishment of an antiviral molecular state in the host. This is particularly relevant, given ASFV's preferential tropism for m-MΦs, since the quick depletion of antigen presenting cells prevents domestic pigs from establishing effective adaptive cellular immunity.

Overexpression of all tested MGFs was able to suppress IRF7-dependent IFNα6-promoter activity downstream of both IRF7 and IKKε. However, in the presence of exogenous IRF7 alone, fewer MGFs were able to repress promoter activity, suggesting differential targeting of the signalling pathway. For instance, 2R showed no significant inhibition without IKKε co-expression, indicating it may act at the level of the kinase, while other MGFs maintained significant inhibition regardless of IKKε presence, indicating a direct effect on IRF7 or the downstream transcriptional machinery (Fig. 4.1). We sought to investigate the role of 1R and, particularly, 12L due to the strong inhibition these family members exhibited under both conditions. To assess the functional relevance of their putative CRL recruitment motifs, we repeated our DLR™ assay using constructs with mutations in either the full VHL/SOCS-box or their constituent BC and Cullin-box motifs. This revealed that mutations in the putative VHL-box of 12L significantly reversed the suppression of IFNα6-promoter activity under all tested conditions (Fig.4.2A). In contrast, mutations in the SOCS-box of 1R yielded a less significant phenotype reversal downstream of both IKKε/IRF7, suggesting distinct, albeit complementary, mechanisms of action between these two viral proteins (Fig.4.2B).

To investigate whether 12L directly interacts with IRF7, we performed IP experiments using GFP-trap magnetic beads to isolate EGFP-tagged IRF7. Despite successful pull-down of IRF7, we did not detect co-immunoprecipitation with V5-tagged 12L (Fig. 4.3). This result suggests that the 12L-mediated inhibition of IRF7-dependent transcriptional activity is likely not due to a direct, stable interaction between the two proteins. The absence of co-IP does not definitively rule out all potential interactions between 12L and IRF7. Functionally relevant weak or transient interactions may still occur but be disrupted during the pull-down process. Additionally, 12L could be indirectly influencing IRF7 stability through interactions with other cellular factors, such as those involving the host protein degradation machinery, with which a direct interaction has been previously confirmed (See Tab. 1.5). Furthermore, these results are consistent with findings from the ASFV-Int consortium project, seeking to map a host-virus interactome,

which similarly failed to detect direct interaction between 12L and IRF7, further supporting the likelihood of an indirect mechanism of action.

The absence of a direct interaction led us to investigate whether 12L's inhibitory effect on IRF7-dependent transcription could be explained through modulation of IRF7 protein levels. Western blot analysis revealed that wt 12L decreased exogenous IRF7 protein levels in a dose-dependent manner (Fig. 4.4). This effect was dependent on the BC-box component of the putative VHL-box motif, as mutation of this domain abolished the ability of 12L to reduce IRF7 levels. To determine whether this reduction occurred through the promotion of proteasomal degradation, we treated cells with the proteasome inhibitor MG132. Treatment with MG132 strongly disrupted the 12L-mediated dose-dependent decrease in IRF7 levels (Fig. 4.5), providing strong evidence that 12L promotes proteasomal degradation of IRF7. Together, these results suggest that 12L mediates its inhibitory effects on IRF7-dependent IFN transcription by promoting the proteasomal degradation of this key transcription factor through a mechanism likely involving its putative VHL-box motif, particularly the BC-box component.

The targeting of IRF7 by 12L appears to involve multiple complementary mechanisms. Beyond promoting proteasomal degradation, the interaction between 12L and UBA3 (Dr. Grégory Caignard and Dr. Juliette Dupré, Unpublished) suggests an additional layer of immune modulation. UBA3, as the catalytic subunit of the NAE complex, mediates two crucial regulatory functions: activating CRL complexes through cullin neddylation,[122] and promoting IRF7 nuclear translocation and stability via neddylation of the transcription factor.[118, 119] By interfering with UBA3, 12L could potentially enhance CRL-mediated protein degradation while simultaneously preventing proper IRF7 post-translational modification. This dual mechanism would efficiently suppress IFN induction by both destabilizing IRF7 protein levels and preventing its nuclear translocation. This hypothesis is supported by the presence of a putative VHL-box in 12L, our experiment inhibiting proteasomal degradation (Fig. 4.5), and subsequent immunofluorescence analysis (see Sec. 4.2.4).

Previous work demonstrated that 12L prevents IRF3 nuclear translocation,[124] and recent studies have also identified direct interactions between 12L (from the SY-18 isolate) and importin-α family proteins.[139] This suggests that 12L may directly interfere with the nuclear import machinery in addition to its effects on protein stability and post-translational modifications. We examined the effect of 12L on IRF7 localisation through immunofluorescence staining and confocal laser scanning microscopy. Control experiments first established that both wt 12L construct and its mutants showed similar nuclear and cytoplasmic distribution patterns, independent of IKKε co-expression (Fig.4.6). In cells transfected with IRF7 alone, the protein remained predominantly cytoplasmic, while co-expression with IKKε triggered its expected activation and nuclear translocation (Fig.4.7A). However, when co-expressed with wild-type 12L, IRF7 remained mainly extra-nuclear even in the presence of IKKε, indicating that 12L prevents IRF7 nuclear translocation (Fig. 4.7B). Notably, this inhibition was not as categorical when 12L mutants were co-transfected instead, where IRF7 was observed throughout the cells. The higher overall green signal intensity observed in cells expressing mutant 12L constructs compared to the wt further supported our previous findings regarding 12L-mediated protein degradation, though further quantitative analysis would be needed to confirm this qualitative visual observation. The parallel inhibition of both IRF3 and IRF7 nuclear translocation highlights the evolutionary advantage of targeting common mechanisms in the interferon induction pathway.

Having characterised the effects of MGFs on IRF7 and IFN induction, we next investigated their potential impact on the cellular response to IFN. Using a warthog *MX2* promoter reporter, we found that all tested MGFs significantly suppressed ISG expression following IFN stimulation, with only 2R showing inconsistent effects across replicates (Fig.4.8A). Further analysis of 12L and 1R mutants revealed contrasting behaviours - while mutations in 12L's VHL-box partially reversed its inhibitory effect, mutations in 1R's SOCS-box unexpectedly enhanced suppression (Fig.4.8B). Given these effects on ISG expression, we examined whether MGFs might target components of the JAK/STAT pathway. However, neither individual MGF

expression nor increasing doses of 12L affected endogenous STAT1/2 protein levels (Figs. 4.9 and 4.10), suggesting their inhibition of ISG expression occurs through other mechanisms. Also, further work investigating the impact of MGFs upon the phosphorylated form of STATs, and their nuclear translocation into the nucleus, is warranted, given that these modifications change the structural conformation of these signalling mediators onto their active form.

Our findings have significant implications for ASFV vaccine development, particularly in the context of LAV design through targeted gene deletion. Recent advances in this field have demonstrated that deletion of ASFV IFN inhibitory proteins, particularly combinations of MGF360 and MGF505 genes, can generate promising vaccine candidates.[193, 204] Our detailed characterisation of how 12L promotes IRF7 degradation and prevents its nuclear translocation provides crucial mechanistic insight into why deletion of this gene contributes to viral attenuation. Understanding specific mechanisms of immune evasion allows for more informed decisions in vaccine design, beyond empirical approaches that have historically relied on trial and error.[43] Furthermore, the contrasting mechanisms we observed between 12L and 1R, despite their similar effects on IFN induction and signalling, highlights the complexity of viral immune evasion and suggests why certain combinations of gene deletions may be more effective than others for vaccine development. This is particularly relevant given recent field implementation of MGF-deletion based vaccines,[196] and ongoing challenges with emerging viral variants.[34] By elucidating these molecular mechanisms, our work provides a foundation for rational design of attenuated vaccines, supporting efforts to achieve an optimal balance between attenuation and immunogenicity through targeted deletion of viral immune evasion genes.

5

Exploring the Potential of PLTA58 Cells as a Replacement for Primary Macrophages

Contents

5.1 Introduction 101
5.2 Results 104
5.2.1 ISG profile in response to infection 104
5.2.2 ASFV Growth in PLTA58s 106
5.2.3 Cell Viability 111
5.3 Discussion 112

5.1 Introduction

The scientific work required to generally study ASFV or, in particular, to generate therapeutics for ASF, be they prophylactic or otherwise, herein so far continues to depend on the use of animals. This research necessitates the sacrifice of pigs for *in vivo* experiments and to harvest primary cells for the growth, isolation and further characterisation of ASFV *in vitro*. The use of animals has, to this point, been and still remains necessary for the advancement of research into ASFV. This dependency on animals for research, pigs in the case of ASFV, in addition to ethical concerns, makes this process very costly in terms of animal life, time, experimental

reproducibility and funding resources.

The report "Responsibility in the use of animals in bioscience research: Expectations of the major research councils and charitable funding bodies", published by the National Centre for the Replacement, Refinement and Reduction of Animals in Research (NC3Rs) in collaboration with the BBSRC and other major UK research funding institutions, outlines the responsibilities for animal welfare, harm reduction, and best practices in bioscience research involving animals.[236] Researchers receiving funding from major UK Research Councils are expected to not only adhere to the provisions of the Animals (Scientific Procedures) Act 1986[237] and other relevant legislation, but also to strive to minimize animal use and fully implement the 3Rs principles. The 3Rs - Replacement, Reduction, and Refinement - represent a framework for conducting more humane animal research. Replacement involves "using alternative methods to avoid or replace animal use where possible". Reduction aims to "minimize the number of animals used per experiment". Refinement focuses on "improving experimental procedures to minimize potential pain, suffering, or distress". These principles are to be applied "for ethical reasons and to obtain the best possible scientific results".[236]

Efforts are underway to reduce the use of pigs in ASFV research by replacing primary macrophages with immortalised cell lines. The development and validation of these cell lines represent a significant step towards the Replacement principle of the 3Rs, potentially reducing the need for animal-derived primary cells. This approach not only addresses ethical concerns but also offers practical advantages such as improved reproducibility, reduced variability, and increased experimental throughput. So far, researchers in Japan have been able to grow different field isolates of ASFV in immortalized porcine kidney macrophage (IPKM) cells[218] and use these cells for diagnostic isolation without attenuated isolates reverting to virulence.[219]

Meanwhile, ASFV groups at The Pirbright Institute, in collaboration with researchers at the University of Plymouth, have been working on validating the use of another immortalised macrophage porcine cell line for its different applications for ASFV and PRRSV research, henceforth referred to as porcine large tumour antigen

58 (PLTA58) cells. These cells were immortalised by delivering the simian virus 40 (SV40) large tumour antigen (LTA) oncogene in lentiviral vectors very similarly to how the IPKMs developed in Japan.[218, 219] In particular, PLTA58 cells have a mutated form of the LTA (LTA58) that is temperature sensitive[238–240] conditionally expressed at 33 degrees. The transformed cells grow at the permissive temperature but when shifted to higher temperatures, between 37 and 39 degrees for 4 days, there is a marked reduction in LTA58 expression (manuscript in preparation) and cell growth is arrested. The LTA58 expression in PLTA58 cells has a high impact in the gene expression profile as observed in proteomics studies (manuscript in preparation), and hence its suppression at higher temperatures is a useful feature, allowing the cells to return to a more primary phenotype.

In line with BBSRC guidelines[236] and ongoing efforts to assess the potential of PLTA58s for ASFV and PRRSV in vitro research and diagnostics, we aimed to contribute to this validation process within the scope of our project. PLTA58s, like primary macrophages, are susceptible to ASFV infection but offer the advantages of immortalized cell lines, including experimental consistency and reduced reliance on animal-derived cells. By replicating key experiments from our previous work with primary macrophages using PLTA58s, we sought to compare results and evaluate the most suitable uses of PLTA58s for ASFV immune evasion research. Specifically, we focused on assessing ISG levels, viral growth kinetics, and the impact of Ruxo treatment on viral replication in PLTA58s infected with wt ASFV and deletion mutants. These experiments aim to determine whether PLTA58s can replicate the immune responses and viral behaviours observed *in vitro* in primary macrophages (see 3.2), potentially offering a reliable alternative for future ASFV studies. The following results section presents our findings from these comparative experiments, providing insights into the potential of PLTA58s as a tool for ASFV research.

5.2 Results

5.2.1 PLTA58s have a CXCL10 ISG response to infection similar to macrophages

We began assessing the ISG response dynamics in PLTA58s over time following infection with ASFV deletion mutants.

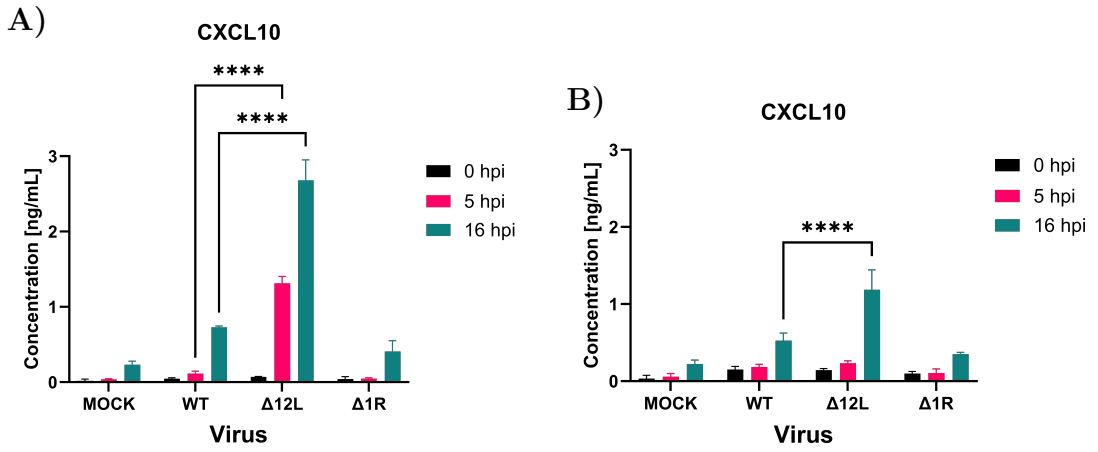

Figure 5.1: CXCL10 protein levels detected by ELISA in PLTA58 cells following infection with ASFV wt and mutants. Levels of secreted CXCL10 in the supernatants of PLTA58 cells at the above indicated time-points were measured by ELISA (See 2.5) using an MOI of 0.5, with Δ12L, Δ1R, wt ASFV or mock virus, as a negative control. Cells were infected with viruses harvested by either **A)** standard methodology or by **B)** ultracentrifugation. Two experimental replicates measured in technical replicates. Significance was assessed by ordinary two-way ANOVA and Šidák's multiple comparisons test, with a single pooled variance.

The CXCL10 protein levels detected in PLTA58s at 16 hpi showed a response to infection with Georgia2007/1 ASFV wt and deletion mutants very similar to that described in PBMs (Fig. 3.1B). The density at which PBMs are seeded is roughly 5 times that of PLTA58s (5×10^6 versus 1×10^6 [cells/mL]), however the CXCL10 protein levels detected in Δ12L infected PLTA58s at 16 hpi were <5 times lower than in PBMs (2–3 versus 8–10 [ng/mL]). Despite this overall reduction, the relative pattern of CXCL10 expression between wild-type ASFV and the deletion mutants observed in PBMs was maintained in PLTA58s. Also there are different cell types in purified PBMs and through the course of infection their phenotype may vary more widely. Infection with the Δ12L mutant resulted in significantly higher CXCL10

levels compared to wild-type (****:p<0.0001), while the Δ1R mutant showed no significant difference (ns) from the wt (Fig. 5.1A), which bear the same significance and pattern as the results in two biological replicates in PBMs (Fig. 3.1B).

Ultracentrifugation of the virus prior to infection led to a general decrease in CXCL10 detection levels across all virus types (Fig. 5.1B). However, the significant difference between Δ12L and wild-type ASFV was maintained at 16 hpi (****:p<0.0001), indicating that the enhanced CXCL10 response to Δ12L infection is a robust phenomenon observable in both standard and ultracentrifuged virus preparations.

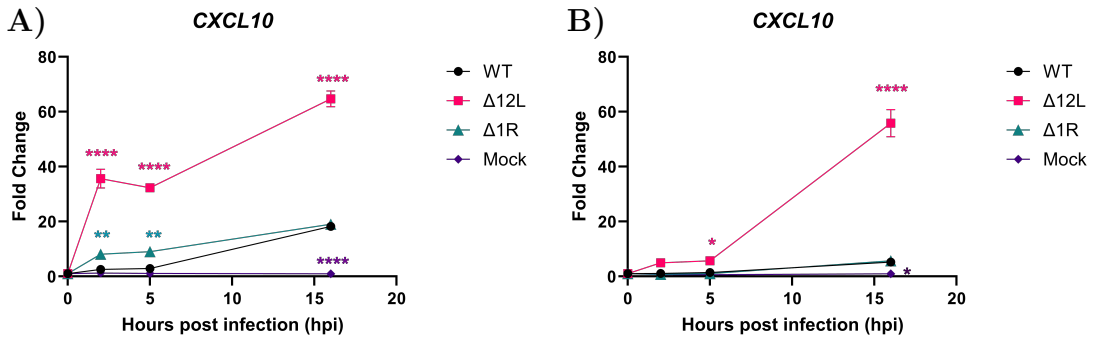

Figure 5.2: *CXCL10* mRNA levels relative to *GAPDH* measured by RT-qPCR. **A)** PLTA58 cells infected with normally harvested ASFV. **B)** PLTA58 cells infected with ultracentrifuged ASFV with 0.5 MOI. Data for each virus was corrected to t=0h time point. Statistical analysis with RM two-way ANOVA, with matched values stacked into subcolumns. Šidák's multiple comparisons test, with a single pooled variance. Two biological replicates with two further technical replicates each.

The expression profile of *CXCL10* mRNA following infection in PLTA58s shows more pronounced differences compared to macrophages than observed at the protein level. In PBMs, infection with Δ12L induced a remarkable 600-fold increase in *CXCL10* expression at 2 hpi (Fig 3.2A), approximately 15 times higher than in PLTA58s (Fig 5.2A).

Despite this overall lower magnitude of response in PLTA58s, the temporal pattern of *CXCL10* expression following Δ12L infection showed some similarities to that observed in PBMs. In PLTA58s infected with normally harvested Δ12L, *CXCL10* expression at 2 hpi remained marginally higher than at the 5-hour time point (Fig.5.2A), reminiscent of the early peak observed in PBMs (Fig.3.2).

Interestingly, the expression profiles for Δ1R (Fig. 5.2) and the ultracentrifuged Δ12L in PLTA58s (Fig.5.2B) more closely resembled that of the wild-type virus. Unlike with Δ1R, infection of PLTA58s with ultracentrifuged Δ12L stimulated the expression of *CXCL10* significantly more than the wt isolate already after 5hpi (*: p=0.0496), and with much greater confidence after 16 hours (****: p<0.0001) (Fig. 5.2B). Only the non-ultracentrifuged Δ1R stimulated *CXCL10* expression in PLTA58s significantly more than the wt very early upon infection (at 2 and 5 hpi; **: p= 0.0041 and 0.0015); however, this difference in relative mRNA expression became negligible at 16 hpi (Fig. 5.2A).

The use of ultracentrifuged viruses appeared to attenuate the early *CXCL10* response in PLTA58s for all virus types (Fig. 5.2B), further highlighting the importance of virus preparation methods in studying host cell responses to infection.

5.2.2 Use of PLTA58s for Virus Growth Experiments

Our growth curve experiments in PLTA58s revealed unexpected results compared to those previously observed in primary macrophages. Notably, the deletion mutants across all growth curves grew very similarly to the wt in PLTA58s (Figs. 5.3, 5.4, 5.5).

Contrary to our findings in primary macrophages, PLTA58s failed to replicate the reported *in vitro* growth defect of Δ12L, even in the untreated, non-centrifuged samples, where Δ12L grew slightly better than the wt (Fig. 5.3A).

Infection with virus stocks purified by ultracentrifugation also did not replicate in PLTA58s the growth defect reported in PBMs (Figs. 5.4 and 5.5, these figures represent replicates of the same experiment at different times). In the first experimental replicate, Δ12L outgrew the wt isolate under treatment after the 3rddpi (4 and 5 dpi; */**: p= 0.0119/0.0012) (Fig. 5.4A), although in this instance the wt titrated slightly less at 5 than 4 dpi. In the second experiment with ultracentrifuged virus, in the VC, Δ12L actually grew better overall than the wt, albeit only significantly so at the 2 and 3 dpi time-points (*: p= 0.0132) (Fig. 5.5A).

Interestingly, all viral yields in PLTA58s were consistently higher than those observed in PBMs. This observation suggests that PLTA58s may be particularly

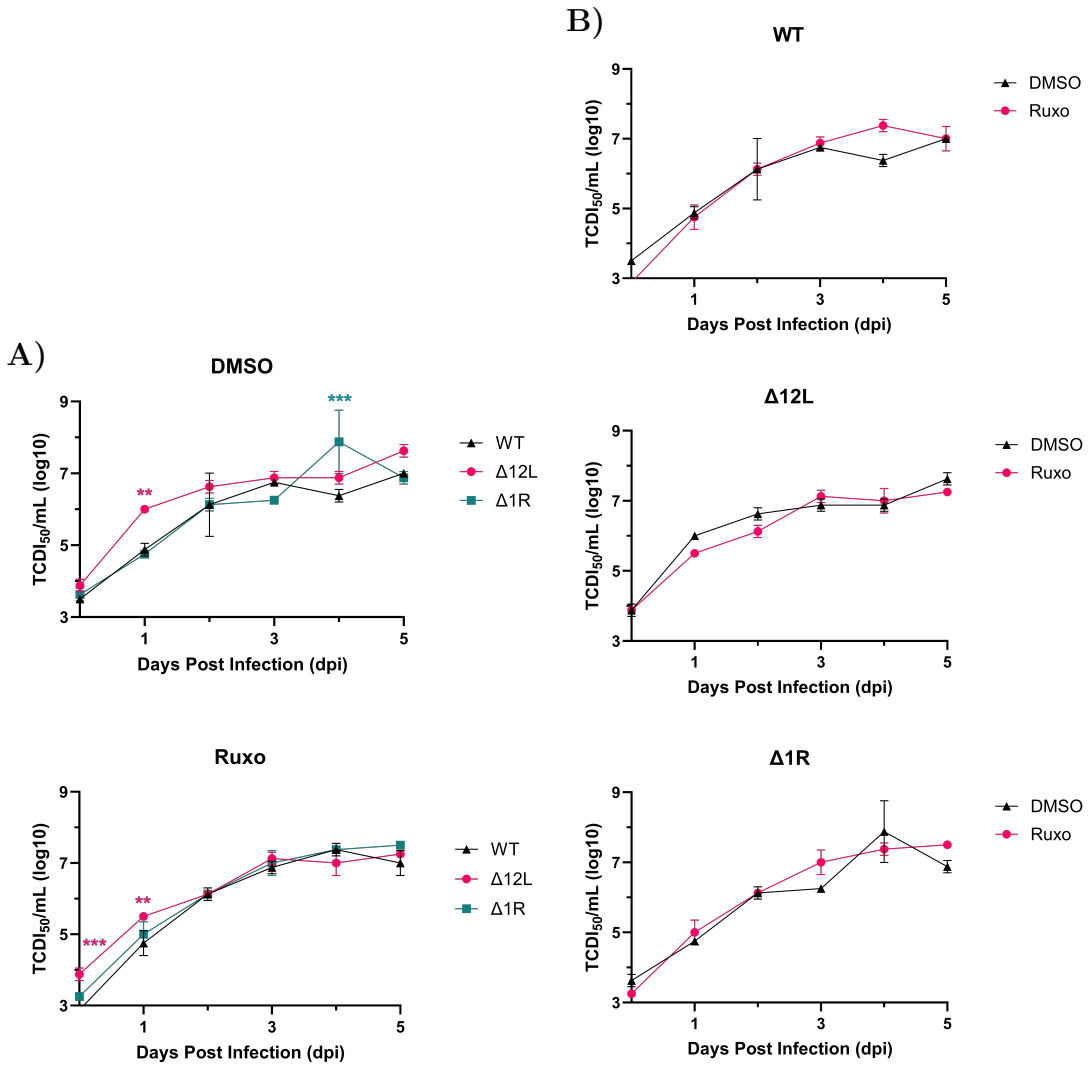

Figure 5.3: Impact of ruxolitinib on WT and recombinant virus growth *in vitro* in PLTA58s. Multistep growth curves of the mutant gene-deleted viruses were performed over 5 days in cells pre-treated overnight with Ruxo [10 μM] or DMSO VC [1 μL/mL]. Grouped by **A)** treatment or **B)** by viral inoculant. Experimental parameters and statistical analyses as in analogous experiments.

useful for virus isolation and propagation. However, the lack of differential growth between mutants indicates that these cells may not accurately reflect the molecular host barriers to viral entry and replication that are present in primary macrophages.

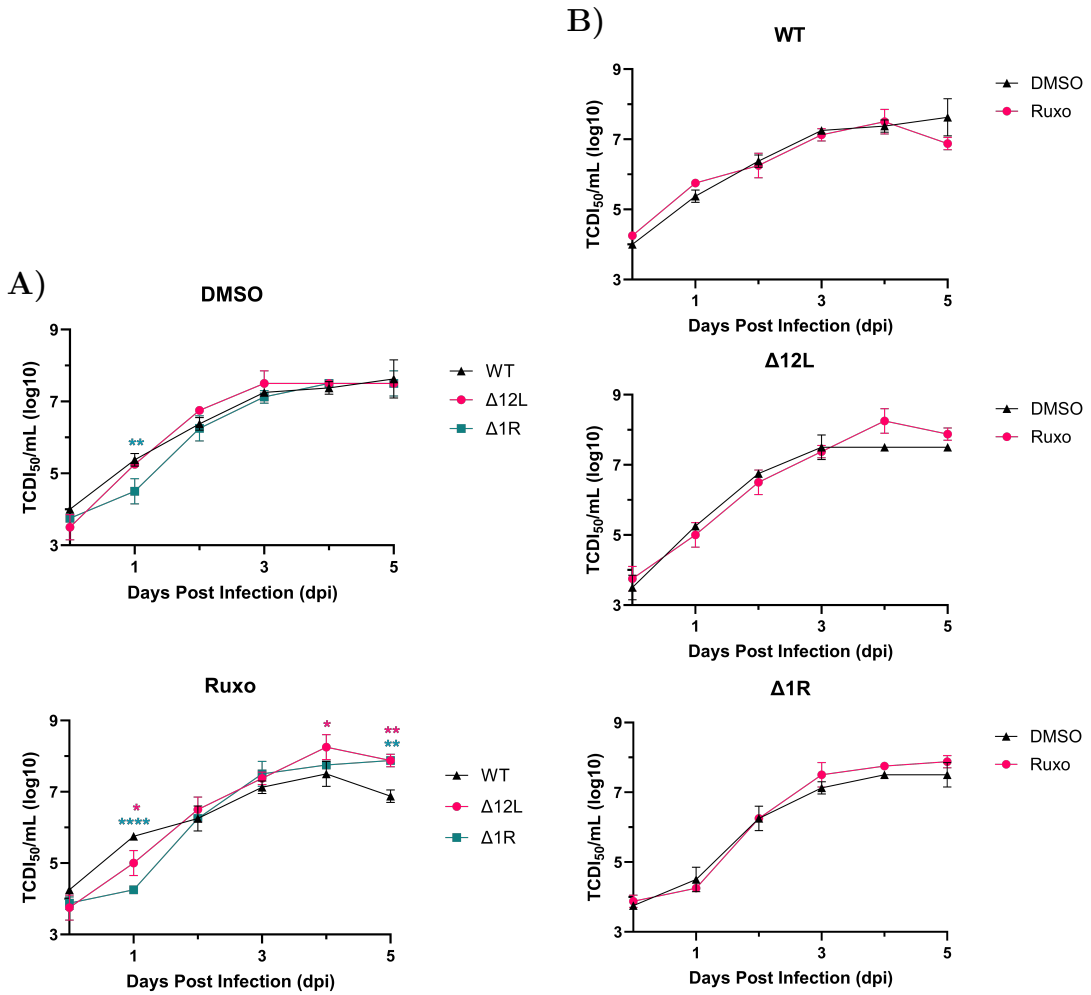

Figure 5.4: Impact of ruxolitinib on the growth of ultracentrifuged WT and recombinant viruses *in vitro* in PLTA58s. Multistep growth curves of the mutant gene-deleted viruses were performed over 5 days in cells pre-treated overnight with Ruxo [10 μM] or DMSO VC [1 μL/mL]. Grouped by **A)** treatment or **B)** by viral inoculant. Experimental parameters and statistical analyses as in analogous experiments.

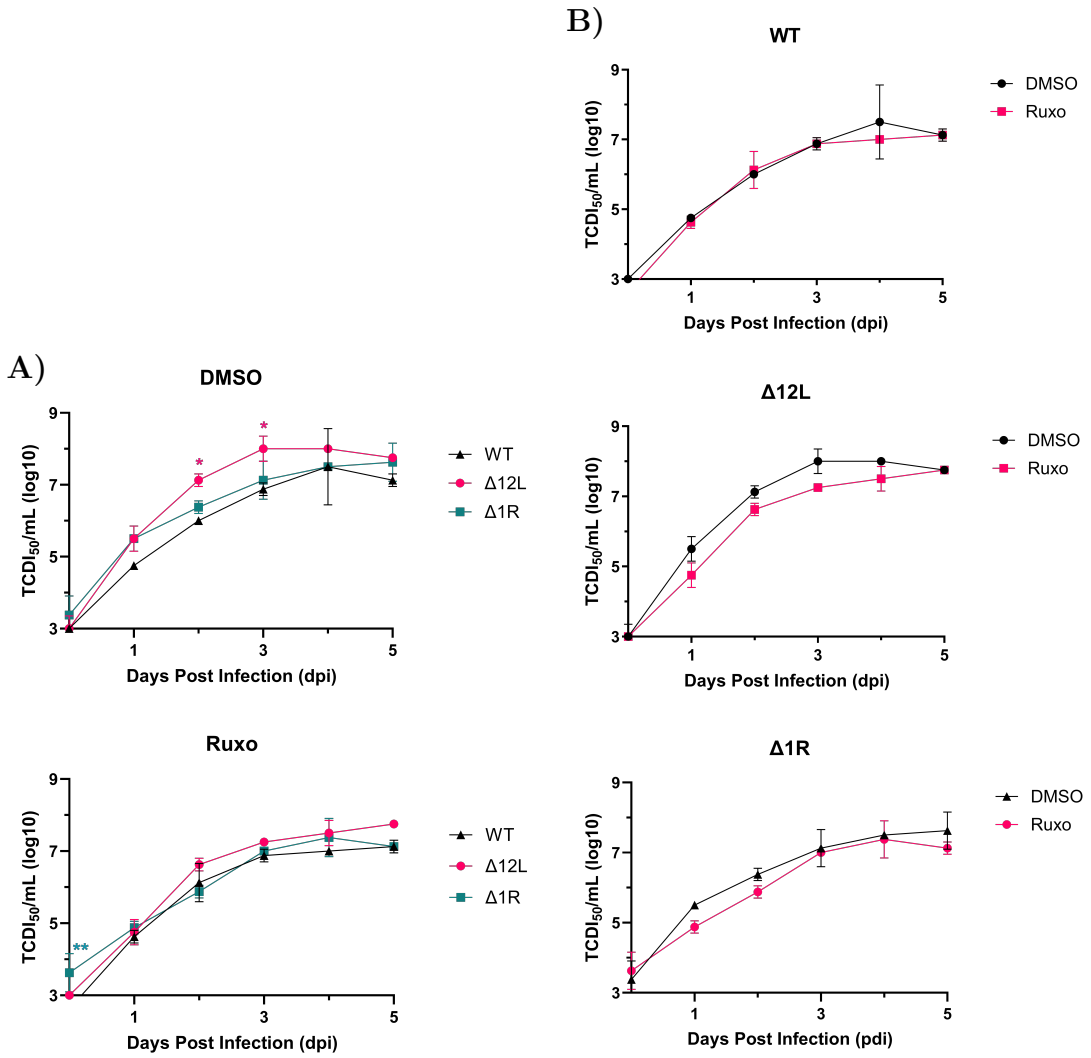

Figure 5.5: Impact of ruxolitinib on the growth of ultracentrifuged WT and recombinant viruses *in vitro* in PLTA58s. Multistep growth curves of the mutant gene-deleted viruses were performed over 5 days in cells pre-treated overnight with Ruxo [10 μM] or DMSO VC [1 μL/mL]. Grouped by **A)** treatment or **B)** by viral inoculant. Experimental parameters and statistical analyses as in analogous experiments.

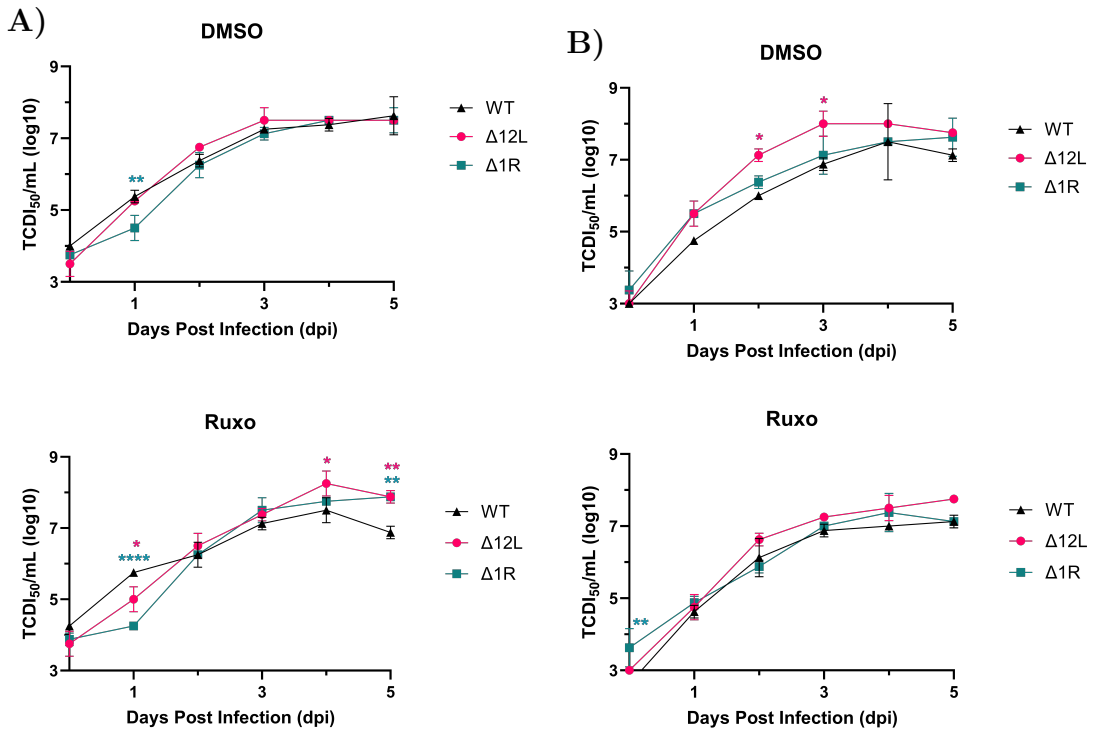

Figure 5.6: Reproducibility of data in PLTA58s. Growth curve experiments from figures **A)** 5.4 and **B)** 5.5, displayed side-by-side to demonstrate the reproducibility of experiments in PLTA58s.

5.2.3 Viability of PLTA58s in the Presence of Inhibitors

Our assessment of PLTA58 viability in the presence of inhibitors yielded unexpected results. Contrary to our observations in primary macrophages, Ruxo significantly impacted cell viability negatively (****: $p<0.0001$) at both 10 and 20 µM concentrations compared to the DMSO vehicle control (Fig. 5.7). This finding suggests that PLTA58s may be more sensitive to JAK/STAT pathway inhibition than primary macrophages.

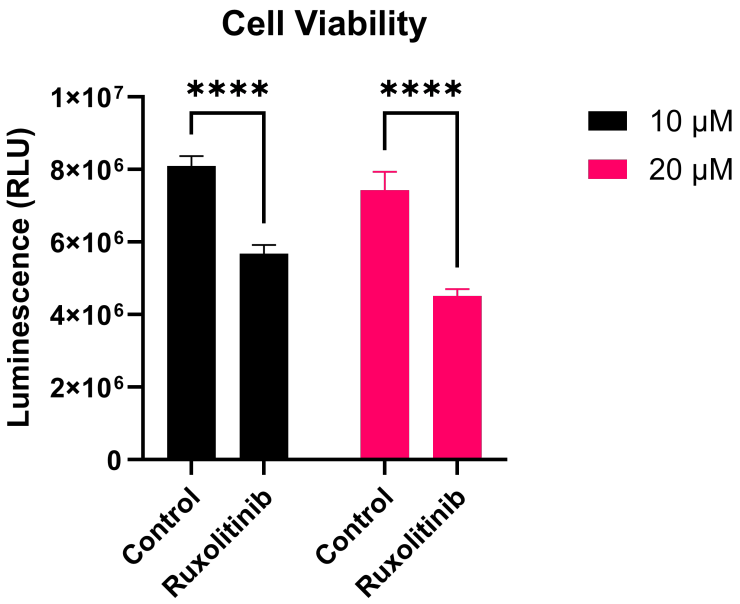

Figure 5.7: Cell viability of PLTA58s treated with Ruxolitinib. After 4 days at 37°C, were treated with Ruxo $[10\mu M]/[20\mu M]$ or DMSO VC $[1\mu L/mL]/[2\mu L/mL]$ over 6 nights (equivalent to overnight treatment and 5-day growth-curve time course). Cell viability was assessed using the RealTime-Glo™ MT Cell Viability Assay at 5 days post-treatment. The luminescent signal correlates with the number of viable cells. Both treatments were compared to the control group. Significance was assessed by ordinary two-way ANOVA, with main effects only, and a Tukey's multiple comparisons test, with a single pooled variance, using the resulting mean and standard deviation of twelve technical replicates.

5.3 Discussion

The use of PLTA58s as a potential alternative to primary porcine macrophages for ASFV research has revealed both promising aspects and significant limitations. Our experiments demonstrated that while PLTA58s can support ASFV replication and exhibit some similarities in innate immune responses, there are crucial differences that must be considered when interpreting results and evaluating their utility as a model system for studying innate immune responses to infection.

One significant observation was the lower overall magnitude of CXCL10 response in PLTA58s compared to primary macrophages. This reduced response was evident at both the protein and mRNA levels. Interestingly, despite attempts to measure IFN-α, it was below the detection threshold of our in-house ELISA. These observations could be attributed to the lower density at which PLTA58s are seeded (1×10^6 versus 5×10^6 cells/mL for PBMs), coupled with the fact that Georgia2007/1 isolate is known to produce minimal amounts of type I IFN *in vitro*[92] even though the Δ12L mutant does produce higher levels. However, the RT-qPCR results in section 5.2 are comparable to experiments in PBMs, since they are normalised in each instance to *GAPDH* mRNA.

One of the most striking observations was the lack of growth defect in the Δ12L mutant when grown in PLTA58s, which contrasts sharply with its behaviour in primary macrophages. This discrepancy suggests that the cellular environment in PLTA58s may not fully recapitulate the intrinsic barriers that typically restrict the growth of this mutant in PBMs. The higher viral yields observed across all viruses in PLTA58s further supports this notion and indicates that these cells may be more permissive to ASFV replication in general.

The differences observed between PLTA58s and PBMs highlight the complexity of ASFV's interaction with host cells. ASFV exhibits a sophisticated tropism - while the virus can infect different macrophage populations, its *in vitro* replication efficiency varies significantly depending on both their activation state and pathogen virulence.[71] This varying susceptibility mirrors the phenotypic and functional diversity of macrophages, from pro-inflammatory M1 to anti-inflammatory M2

subtypes, with attenuated ASFV isolates containing MGF deletions, including 12L, showing enhanced replication in M2 m-MΦs compared to classically activated (M1) m-MΦs.[71, 74] Unpublished work (Raquel Portugal et al.), further characterising PLTA58 cells, showed they produce higher levels of the anti-inflammatory cytokine IL-10 compared to primary PAMs when infected with Georgia 2007/1 at low MOI, suggesting they may possess M2-like characteristics, or that primary cells retain more plasticity than the cell line or simply had a higher population of M1-like cells. This could explain the Δ12L growth defect in primary macrophages, highlighting how cellular activation states can significantly impact experimental outcomes.[92]

The negative impact of Ruxo on PLTA58 viability suggests a potential dependence on JAK/STAT signalling for survival, which is not typically observed in primary macrophages. This dependence could be a consequence of the immortalisation process or the expression of the SV40 LTA, which is known to interact with various cellular pathways, including IFN signalling and overall transcription machinery.[241–243] However, ongoing work to characterise PLTA58s has shown that, after four days at 37°C, only residual expression of LTA58 was detected in PLTA58s (Portugal et al., unpublished). Hence, the observed decrease in cell viability may simply be on account of other effects of Ruxo on these cells.

These findings underscore the importance of careful validation when using immortalized cell lines for virus research. While PLTA58s offer advantages in terms of consistency and ease of use, they may not fully recapitulate the cellular environment and innate immune responses of primary macrophages. This limitation is particularly crucial when studying viruses like ASFV, which have evolved sophisticated mechanisms to modulate host cell responses.

Future work should focus on further characterizing the differences between PLTA58s and primary macrophages at the molecular level. Transcriptomic and proteomic profiling could provide valuable insights into the altered signalling pathways and innate immune components in these cells. Additionally, investigating the possible lingering effects of SV40 LTA on cellular pathways relevant to ASFV

replication and immune responses, even after expression has been depleted, could help explain some of the observed differences.

In conclusion, while PLTA58s show potential as a tool for ASFV research, particularly for virus isolation and propagation, their use as a model system for studying host-pathogen interactions and testing antiviral strategies may be limited. Researchers should carefully consider these limitations when designing experiments and interpreting results. The development of more sophisticated in vitro models, possibly combining PLTA58s with other cell types or using organoid systems, may be necessary to more accurately recapitulate the complexity of ASFV infection in vivo. Despite these limitations, the use of PLTA58s represents a step towards reducing the reliance on animal-derived cells in ASFV research, aligning with the principles of the 3Rs of animal research. Further refinement of these cell models may contribute to more ethical and efficient ASFV research in the future.

6 Discussion

Contents

6.1 Research Aims 115
6.2 Key Findings 116
6.2.1 PBMs Infected with Deletion Mutants 116
6.2.2 Host Interactions 116
6.2.3 Validation of PLTA58 Cells for ASFV Research 119
6.3 Future Work 120
6.4 Conclusion 121

6.1 Aims of Our Research

African swine fever virus employs sophisticated mechanisms to modulate host innate immunity, particularly type-I interferon signalling, whose suppression is crucial for successful viral replication.[70] As reviewed in Chapter 1, the virus's ability to modulate antiviral signalling is crucial for establishing infection in myeloid cells, which differentiate into specialist immune cells.[81] The MGFs, located at the terminal ends of the ASFV genome, represent a key family of virulence factors that have evolved through gene duplication events to inhibit various aspects of type I IFN signalling.[8, 69] These genes comprise approximately 30% of the viral genome and some members of the MGF360 and 505 families are enriched in ANK

repeat motifs,[124] which are protein-protein interaction domains commonly found in eukaryotic regulatory proteins but rare in viruses outside of the *Poxviridae* family.[124, 194] Recent studies have revealed that MGFs target multiple components of both IFN induction and response pathways.[147] Our research aimed to further characterise MGFs mechanisms of action, with particular focus on MGF360-12L and MGF505-1R, which strongly impact viral virulence and contain putative motifs linked to protein degradation.[124]

6.2 Key Findings

6.2.1 Macrophage Responses to ASFV Deletion Mutants

Our investigation of primary macrophage responses to ASFV deletion mutants revealed several key findings regarding the role of MGFs in immune modulation. The deletion of 12L resulted in significantly elevated expression of ISGs, particularly CXCL10, as early as 2 hpi. This early induction was partially attributable to excess IFN carried over in virus preparations, as demonstrated through ultracentrifugation experiments. These findings align with previous studies showing the importance of MGF proteins in suppressing early innate immune responses.[92]

Notably, while JAK/STAT pathway inhibition with Ruxo reversed the early ISG induction in Δ12L-infected cells, it did not rescue the mutant's growth defect. This suggests that 12L's impact on viral replication extends beyond its role in suppressing IFN responses, possibly involving additional mechanisms of immune evasion or viral replication.[228]

6.2.2 Host Interactions of MGF Proteins

Analysis of MGF protein interactions with host factors revealed novel mechanisms of immune evasion. Both 12L and 1R significantly inhibited IRF7-dependent IFNα6 promoter activity when co-expressed with IRF7 alone or in combination with IKKε. This inhibitory effect was dependent on their respective CRL recruitment motifs, as mutations in these domains significantly reduced their ability to suppress promoter activity. Additionally, both proteins demonstrated capacity to inhibit the warthog

Mx2 ISG promoter in response to IFN stimulation, suggesting roles in both the induction and response to type I IFN. This functional diversity among MGF proteins reflects their evolution through gene duplication events,[7, 8] potentially providing redundancy in immune evasion strategies. Interestingly, previous work with deletion mutants showed that the individual deletion of 12L had a greater impact than the double deletion mutant (Δ1R12L), in the production of IFN-α *in vitro*,[205] suggesting complex interactions between these genes in regulating immune responses.

Through Yeast-2-Hybrid screening and GST-tagged pull-down validation, our colleagues and collaborators in the ASFV-Int consortium identified UBA3 as a binding partner of 12L (Dr. Grégory Caignard and Dr. Juliette Dupré, Unpublished). This interaction is particularly significant as UBA3 is the catalytic subunit of the NAE complex, which mediates IRF7 neddylation, a crucial post-translational modification required for IRF7's nuclear translocation and transcriptional activity.[117–119] By potentially interfering with UBA3 function, 12L could impair IRF7 neddylation, thereby affecting IRF7 stability, preventing its nuclear translocation and subsequent activation of type I IFN genes. This mechanism would be particularly effective in myeloid cells, which maintain higher basal levels of IRF7 and rely on proper post-translational modification for rapid IFN responses.[110] Whilst we did not detect direct interaction between 12L and IRF7 through co-IP, we found that 12L overexpression decreased exogenous IRF7 levels in a dose-dependent manner and appeared to inhibit the nuclear translocation of exogenously expressed IRF7 when co-expressed with IKKε. This observation parallels previous findings showing 12L-mediated inhibition of IRF3 nuclear translocation.[124] While recent studies have suggested 12L may interact with importin-α family proteins,[139] the effects we observed on nuclear translocation could be explained either through this reported direct interference with the nuclear import machinery, or indirectly through 12L's effects on post-translational modifications of host proteins, such as neddylation or ubiquitination pathways.

12L was found to promote proteasomal degradation of IRF7 in a manner dependent on its VHL-box motif, representing a previously uncharacterised mech-

anism of IFN suppression. The targeting of IRF7 is particularly significant as this transcription factor plays a central role in amplifying the type I IFN response through a positive feedback loop (Fig. 1.9),[108] highlighting the importance of 12L for the virus to establish secondary infection in cells that may already be IFN activated. This mechanism is particularly important for viral pathogenesis, as m-MΦs serve as both the primary target for ASFV infection and as crucial antigen presenting cells. By preventing these cells from establishing an effective antiviral state through IRF7 degradation, ASFV ensures its efficient replication and also impairs the development of adaptive immunity, as infected macrophages are depleted before they can effectively present antigens to T cells. Furthermore, once systemic infection is established, the virus can infect other cell types further hindering the appropriate production of IFN. However, when the virus infects cells such as pDCs, which specialise in IFN-α production and constitutively express high levels of IRF7,[77, 244] the inhibitory effect of MGFs may not be enough to overcome their specialised function, potentially contributing to the high levels of IFN-α and cytokine storms observed *in vivo* with virulent isolates as early as 3 days post infection.[90, 92] The phenotypic differences between myeloid derived cells and how they behave when ASFV infects them, likely plays a crucial role within pathogenesis; this is further supported by recent work which demonstrated that pig-derived pDCs were more susceptible to infection with the attenuated OURT88/3 ASFV isolate (lacking several MGF360/505 genes, including 12L)[6] than with its parental, highly virulent, OURT88/1 isolate.[245] Our findings extend the understanding of how ASFV modulates host protein degradation pathways, whilst tangentially supporting the efforts to reveal the means of ASFV pathogenesis.

Our investigation of STAT protein regulation revealed that, contrary to expectations based on recent literature,[181] neither 12L nor other tested MGFs significantly impacted STAT1/2 protein levels. This finding highlights the complexity and potential redundancy of ASFV immune evasion strategies, suggesting that individual MGFs may have specialized rather than overlapping functions in modulating different aspects of innate immunity.

6.2.3 Validation of PLTA58 Cells for ASFV Research

Our evaluation of PLTA58s as an alternative to primary macrophages revealed both opportunities and limitations for ASFV research. While these cells supported higher viral replication than primary macrophages, they failed to recapitulate key phenotypes such as the Δ12L growth defect. These findings parallel challenges observed with other immortalized cell lines for ASFV research.[215]

The ISG response patterns in PLTA58s showed similarities to primary cells but with reduced magnitude, suggesting altered innate immune regulation in these immortalized cells. Interestingly, the absence of growth defects in MGF deletion mutants and their enhanced replication in PLTA58s suggests these cells may exhibit characteristics more closely aligned with alternatively activated (M2) macrophages. This observation is particularly relevant given previous findings that attenuated ASFV isolates containing MGF deletions, including 12L, showed enhanced replication in M2 macrophages compared to classically activated (M1) cells.[71] Indeed, while attenuated strains showed initial restricted growth in M1 macrophages, they replicated efficiently in M2 cells, displaying higher viral titres in these alternatively activated macrophages.[71, 72] This differential susceptibility may help explain our observations with PLTA58s, which have been shown to produce higher levels of the anti-inflammatory cytokine IL-10 compared to primary alveolar macrophages when infected with Georgia 2007/1 at low MOI (Portugal et al., unpublished). Thus, the reported growth defect of Δ12L in primary macrophages and its absence in PLTA58s could reflect differences in cellular activation states or the reduced plasticity of the immortalised cells. Moreover, even though we used purified PBMs for our experiments in Chapter 3, these are likely not exclusively m-MΦs and their phenotypes may vary more widely through the course of infection than it would in an immortalised cell line such as PLTA58s.

The unexpected sensitivity of PLTA58s to JAK/STAT inhibition highlights fundamental differences in cellular signalling pathways compared to primary macrophages.[242] These alterations in cellular physiology likely result from the immortalisation process,[243] suggesting that while PLTA58s may be valuable for growing attenuated

virus and other aspects of ASFV research, they cannot fully recapitulate the complex immune interactions observed in PBMs.[213] Understanding these limitations and the potential M2-like characteristics of PLTA58s is crucial for their appropriate application in ASFV research and for interpreting results obtained using these cells.

6.3 Future Work

Our findings open several promising avenues for future research into ASFV immune evasion mechanisms and their implications for vaccine development. The mechanism by which 12L promotes IRF7 degradation, while clearly dependent on its VHL-box motif, requires further molecular characterization. Detailed biochemical analysis of protein complexes and interaction dynamics could reveal additional host factors involved in this process.[123] Particularly intriguing is the potential interaction between 12L and UBA3, which suggests previously uncharacterised viral interference with cellular neddylation pathways. Investigation of this mechanism using selective neddylation inhibitors and proteomic approaches could uncover novel aspects of ASFV immune modulation.[120] Importantly, we showed that Δ12L carries an excess of IFN-α onto subsequent experiments, which is exacerbated by its growth defect in relation to the wt, and that this can be minimised by ultracentrifugation of viral stocks. This finding begs for the replication of previous findings and published work with Δ12L and other mutants with similar growth defects and impact upon interferon signalling, in order to avoid misinterpretation of data.

The complex interplay between different MGFs in regulating host immunity warrants systematic investigation through combinatorial deletion studies and comprehensive pathway analysis. Such work could reveal functional redundancies, synergies and potential competition among these viral proteins, informing more effective strategies for viral attenuation in vaccine development. Additionally, our experience with PLTA58s highlights the ongoing need for improved cell culture systems that better recapitulate primary macrophage responses while reducing dependence on animal-derived cells.[217] Development of such systems, possibly incorporating advanced organoid technologies or genetic modifications to enhance

immune competence, could significantly advance both basic research and vaccine development efforts while supporting the principles of the 3Rs.

6.4 Concluding Remarks

Our findings significantly advance understanding of ASFV immune evasion mechanisms, particularly regarding the role of MGFs in modulating type-I interferon responses. The identification of novel molecular mechanisms, such as 12L-mediated IRF7 degradation, provides new insights into viral strategies for subverting host immunity. These discoveries have important implications for vaccine development, suggesting that targeted deletion of specific MGF genes might be utilized to create rationally attenuated vaccine strains.[43]

The validation of PLTA58s as a potential alternative to primary macrophages, while revealing certain limitations, represents progress toward reducing animal use in ASFV research, aligning with the NC3Rs principles.[236]

Our work supports the BBSRC's strategic priority of promoting sustainable agriculture and food security through improved animal health and welfare, by funding basic research in biological sciences.

References

[1] Penrith ML, Thomson GR & Bastos ADS. "African swine fever". *Infectious diseases of livestock*. Ed. by Coetzer JAW & Tustin RC. 2nd ed. Vol. 2. Oxford University Press, 2004, pp. 1087–1119. ISBN: 0195761707.

[2] Malogolovkin A, Sereda A & Kolbasov D. "African Swine Fever Virus". *Emerging and Transboundary Animal Viruses*. Ed. by Malik YS, Singh RK & Yadav MP. Singapore: Springer Nature, Feb. 23, 2020, pp. 27–53. ISBN: 978-981-15-0402-0. DOI: 10.1007/978-981-15-0402-0_2.

[3] OIE. *Terrestrial manual. African swine fever (infection with african swine fever virus)*. World Organisation for Animal Health (WOAH). 2019. Chap. 3.8.1.

[4] *African Swine Fever*. OIE Technical Disease Card. World Organization for Animal Health (WOAH), Feb. 2022.

[5] Alonso C, Borca M, Dixon L, Revilla Y, Rodriguez F & Escribano JM. ICTV Virus Taxonomy Profile: Asfarviridae. *J. Gen. Virol.* **99**.(5) (May 2018), pp. 613–614. ISSN: 0022-1317. DOI: 10.1099/jgv.0.001049.

[6] Chapman DAG, Tcherepanov V, Upton C & Dixon LK. Comparison of the genome sequences of non-pathogenic and pathogenic African swine fever virus isolates. *J. Gen. Virol.* **89**.(2) (Feb. 2008), pp. 397–408. ISSN: 0022-1317. DOI: 10.1099/vir.0.83343-0.

[7] Cackett G, Portugal R, Matelska D, Dixon L & Werner F. African Swine Fever Virus and Host Response: Transcriptome Profiling of the Georgia 2007/1 Strain and Porcine Macrophages. *J. Virol.* **96**.(5) (Mar. 2022). ISSN: 0022-538X. DOI: 10.1128/JVI.01939-21.

[8] Dixon LK, Chapman DA, Netherton CL & Upton C. African swine fever virus replication and genomics. *Virus Res.* **173**.(1) (2013), pp. 3–14. ISSN: 0168-1702. DOI: 10.1016/j.virusres.2012.10.020.

[9] Chapman DAG, Darby AC, Silva MD, Upton C, Radford AD & Dixon LK. Genomic analysis of highly virulent georgia 2007/1 isolate of african swine fever virus. *Emerg. infectious diseases* **17**.(4) (Apr. 2011), pp. 599–605. ISSN: 1080-6059. DOI: 10.3201/eid1704.101283.

[10] Matsuyama T, Kiryu I, Mekata T, Takano T, Umeda K & Matsuura Y. Pathogenicity, genomic analysis and structure of abalone asfa-like virus: evidence for classification in the family Asfarviridae. *J. Gen. Virol.* **104**.(8) (Aug. 2023), p. 001875. ISSN: 0022-1317. DOI: 10.1099/jgv.0.001875.

[11] Reteno DG, Benamar S, Khalil JB, Andreani J, Armstrong N, Klose T, Rossmann M, Colson P, Raoult D & Scola BL. Faustovirus, an asfarvirus-related new lineage of giant viruses infecting amoebae. *J. virology* **89**.(13) (July 2015). Ed. by McFadden G, pp. 6585–94. ISSN: 1098-5514. DOI: 10.1128/jvi.00115-15.

[12] Rubins KH, Hensley LE, Bell GW, Wang C, Lefkowitz EJ, Brown PO & Relman DA. Comparative Analysis of Viral Gene Expression Programs during Poxvirus Infection: A Transcriptional Map of the Vaccinia and Monkeypox Genomes. *PLoS ONE* **3**.(7) (July 2008), e2628. ISSN: 1932-6203. DOI: 10.1371/journal.pone.0002628.

[13] Royo S, Sainz JB, Hernández-Jiménez E, Reyburn H, López-Collazo E & Guerra S. Differential Induction of Apoptosis, Interferon Signaling, and Phagocytosis in Macrophages Infected with a Panel of Attenuated and Nonattenuated Poxviruses. *J. Virol.* **88**.(10) (May 2014), p. 5511. ISSN: 0022-538X. DOI: 10.1128/JVI.00468-14.

[14] Cackett G, Matelska D, Sýkora M, Portugal R, Malecki M, Bähler J, Dixon L & Werner F. The African Swine Fever Virus Transcriptome. *J. Virol.* (2020). ISSN: 0022-538X. DOI: 10.1128/jvi.00119-20.

[15] Colson P, Lamballerie X de, Fournous G & Raoult D. Reclassification of Giant Viruses Composing a Fourth Domain of Life in the New Order Megavirales. *Intervirology* **55**.(5) (2012), pp. 321–332. ISSN: 0300-5526. DOI: 10.1159/000336562.

[16] Dixon LK, Stahl K, Jori F, Vial L & Pfeiffer DU. African Swine Fever Epidemiology and Control. *Annu. Rev. Animal Biosci.* **8**.(1) (Feb. 2020), pp. 221–246. ISSN: 2165-8102. DOI: 10.1146/annurev-animal-021419-083741.

[17] Basto AP, Nix RJ, Boinas F, Mendes S, Silva MJ, Cartaxeiro C, Portugal RS, Leitão A, Dixon LK & Martins C. Kinetics of African swine fever virus infection in Ornithodoros erraticus ticks. *J. Gen. Virol.* **87**.(7) (July 2006), pp. 1863–1871. ISSN: 0022-1317. DOI: 10.1099/vir.0.81765-0.

[18] Boinas FS, Wilson AJ, Hutchings GH, Martins C & Dixon LJ. The persistence of african swine fever virus in field-infected ornithodoros erraticus during the asf endemic period in portugal. *PLoS ONE* **6**.(5) (May 2011), e20383. ISSN: 1932-6203. DOI: 10.1371/journal.pone.0020383.

[19] Pietschmann J, Mur L, Blome S, Beer M, Pérez-Sánchez R, Oleaga A & Sánchez-Vizcaíno JM. African swine fever virus transmission cycles in Central Europe: Evaluation of wild boar-soft tick contacts through detection of antibodies against *Ornithodoros erraticus* saliva antigen. *BMC Vet. Res.* **12**.(1) (Dec. 2016), p. 1. ISSN: 1746-6148. DOI: 10.1186/s12917-015-0629-9.

[20] Piloto-Sardiñas E, Cano-Argüelles AL, Maitre A, Wu-Chuang A, Mateos-Hernández L, Corduneanu A, Obregón D, Oleaga A, Pérez-Sánchez R & Cabezas-Cruz A. Comparison of salivary gland and midgut microbiome in the soft ticks *Ornithodoros erraticus* and *Ornithodoros moubata*. *Front. Microbiol.* **14** (May 2023). ISSN: 1664-302X. DOI: 10.3389/fmicb.2023.1173609.

[21] Chenais E, Ståhl K, Guberti V & Depner K. Identification of Wild Boar–Habitat Epidemiologic Cycle in African Swine Fever Epizootic. *Emerg. Infect. Dis.* **24**.(4) (Apr. 2018), pp. 810–812. ISSN: 1080-6040. DOI: 10.3201/eid2404.172127.

[22] Juszkiewicz M, Walczak M, Woźniakowski G & Podgórska K. African Swine Fever: Transmission, Spread, and Control through Biosecurity and Disinfection, Including Polish Trends. *Viruses* **15**.(11) (Nov. 2023), p. 2275. ISSN: 1999-4915. DOI: 10.3390/V15112275.

[23] Busch F, Haumont C, Penrith ML, Laddomada A, Dietze K, Globig A, Guberti V, Zani L & Depner K. Evidence-Based African Swine Fever Policies: Do We Address Virus and Host Adequately?: *Front. Vet. Sci.* **8** (Mar. 2021), p. 637487. ISSN: 2297-1769. DOI: 10.3389/fvets.2021.637487.

[24] Gavier-Widén D, Ståhl K, Neimanis AS, Segerstad CH av, Gortázar C, Rossi S & Kuiken T. African swine fever in wild boar in europe: a notable challenge. *Vet. Rec.* **176**.(8) (Feb. 2015), pp. 199–200. ISSN: 0042-4900. DOI: 10.1136/vr.h699.

[25] Podgórski T & Śmietanka K. Do wild boar movements drive the spread of African Swine Fever. *Tansbound. emerging diseases* **65**.(6) (Dec. 2018), pp. 1588–1596. ISSN: 1865-1682. DOI: 10.1111/TBED.12910.

[26] Sauter-Louis C, Conraths FJ, Probst C, Blohm U, Schulz K, Sehl J, Fischer M, Forth JH, Zani L, Depner K, et al. African Swine Fever in Wild Boar in Europe—A Review. *Viruses* **13**.(9) (Aug. 2021), p. 1717. ISSN: 1999-4915. DOI: 10.3390/v13091717.

[27] Brown VR, Miller RS, Pepin KM, Carlisle KM, Cook MA, Vanicek CF, Holmstrom LK, Rochette LT & Smyser TJ. African swine fever at the wildlife-livestock interface: challenges for management and outbreak response within invasive wild pigs in the United States. *Front. veterinary science* **11** (Jan. 2024), p. 1348123. ISSN: 2297-1769. DOI: 10.3389/fvets.2024.1348123.

[28] Bastos AD, Penrith ML, Crucière C, Edrich JL, Hutchings G, Roger F, Couacy-Hymann E & Thomson GR. Genotyping field strains of African swine fever virus by partial p72 gene characterisation. *Arch. Virol.* **148**.(4) (Apr. 2003), pp. 693–706. ISSN: 0304-8608. DOI: 10.1007/S00705-002-0946-8.

[29] Rajko-Nenow P & Batten C. "Genotyping of African Swine Fever Virus". *African Swine Fever Virus: Methods and Protocols*. Ed. by Netherton CL. Vol. 2503. Methods in Molecular Biology. Humana, May 2022, pp. 119–132. ISBN: 978-1-0716-2333-6. DOI: 10.1007/978-1-0716-2333-6_8.

[30] Njau EP, Machuka EM, Cleaveland S, Shirima GM, Kusiluka LJ, Okoth EA & Pelle R. African swine fever virus (ASFV): Biology, genomics and genotypes circulating in Sub-Saharan Africa. *Viruses* **13**.(11) (Nov. 2021). ISSN: 1999-4915. DOI: 10.3390/V13112285.

[31] King K, Chapman D, Argilaguet JM, Fishbourne E, Hutet E, Cariolet R, Hutchings G, Oura CA, Netherton CL, Moffat K, et al. Protection of european domestic pigs from virulent african isolates of african swine fever virus by experimental immunisation. *Vaccine* **29**.(28) (2011), pp. 4593–4600. ISSN: 1873-2518. DOI: 10.1016/J.VACCINE.2011.04.052.

[32] Malogolovkin A, Burmakina G, Titov I, Sereda A, Gogin A, Baryshnikova E & Kolbasov D. Comparative analysis of african swine fever virus genotypes and serogroups. *Emerg. Infect. Dis.* **21**.(2) (2015), pp. 312–315. ISSN: 1080-6059. DOI: 10.3201/eid2102.140649.

[33] Zhao D, Sun E, Huang L, Ding L, Zhu Y, Zhang J, Shen D, Zhang X, Zhang Z, Ren T, et al. Highly lethal genotype I and II recombinant African swine fever viruses detected in pigs. *Nat. Commun.* **14**.(1) (May 2023), p. 3096. ISSN: 2041-1723. DOI: 10.1038/s41467-023-38868-w.

[34] Diep NV, Duc NV, Ngoc NT, Dang VX, Tiep TN, Nguyen VD, Than TT, Maydaniuk D, Goonewardene K, Ambagala A, et al. Genotype II Live-Attenuated ASFV Vaccine Strains Unable to Completely Protect Pigs against the Emerging Recombinant ASFV Genotype I/II Strain in Vietnam. *Vaccines* **12**.(10) (Sept. 2024), p. 1114. ISSN: 2076-393X. DOI: 10.3390/vaccines12101114.

[35] Minoungou GL, Diop M, Dakouo M, Ouattara AK, Settypalli TBK, Lo MM, Sidibe S, Kanyala E, Kone YS, Diallo MS, et al. Molecular characterization of african swine fever viruses in burkina faso, mali, and senegal 1989-2016: genetic diversity of asfv in west africa. *Tansbound. emerging diseases* **68**.(5) (Sept. 2021), pp. 2842–2852. ISSN: 1865-1682. DOI: 10.1111/TBED.14240.

[36] Montgomery RE. On A Form of Swine Fever Occurring in British East Africa (Kenya Colony). *J. Comp. Pathol. Ther.* **34** (Jan. 1921), pp. 159–191. ISSN: 0368-1742. DOI: 10.1016/S0368-1742(21)80031-4.

[37] Mulumba-Mfumu LK, Saegerman C, Dixon LK, Madimba KC, Kazadi E, Mukalakata NT, Oura CAL, Chenais E, Masembe C, Ståhl K, et al. African swine fever: Update on Eastern, Central and Southern Africa. *Tansbound. Emerg. Dis.* (Apr. 2019), tbed.13187. ISSN: 1865-1674. DOI: 10.1111/tbed.13187.

[38] Pavone S, Iscaro C, Dettori A & Feliziani F. African Swine Fever: The State of the Art in Italy. *Animals* **13**.(19) (Sept. 2023), p. 2998. ISSN: 2076-2615. DOI: 10.3390/ani13192998.

[39] Plowright W, Parker J & Peirce MA. African swine fever virus in ticks (ornithodoros moubata, murray) collected from animal burrows in tanzania. *Nature* **221**.(5185) (Mar. 1969), pp. 1071–1073. ISSN: 0028-0836. DOI: 10.1038/2211071a0.

[40] Rowlands RJ, Michaud V, Heath L, Hutchings G, Oura C, Vosloo W, Dwarka R, Onashvili T, Albina E & Dixon LK. African Swine Fever Virus Isolate, Georgia, 2007. *Emerg. Infect. Dis.* **14**.(12) (Dec. 2008), pp. 1870–1874. ISSN: 1080-6040. DOI: 10.3201/eid1412.080591.

[41] Ge S, Li J, Fan X, Liu F, Li L, Wang Q, Ren W, Bao J, Liu C, Wang H, et al. Molecular Characterization of African Swine Fever Virus, China, 2018. *Emerg. Infect. Dis.* **24**.(11) (Nov. 2018), pp. 2131–2133. ISSN: 1080-6040. DOI: 10.3201/eid2411.181274.

[42] *WAHIS: World Animal Health Information System*. Global animal health reference database. World Organisation for Animal Health (WOAH). Sept. 2024. URL: https://wahis.woah.org/#/home.

[43] Gavier-Widén D, Ståhl K & Dixon LK. No hasty solutions for african swine fever. *Science* **367**.(6478) (Feb. 2020), pp. 622–624. ISSN: 1095-9203. DOI: 10.1126/science.aaz8590.

[44] Luskin MS, Meijaard E, Surya S, Sheherazade, Walzer C & Linkie M. African Swine Fever threatens Southeast Asia's 11 endemic wild pig species. *Conserv. Lett.* **14**.(3) (May 2021). ISSN: 1755-263X. DOI: 10.1111/conl.12784.

[45] Gale F, Kee J & Huang J. *How China's African Swine Fever Outbreaks Affected Global Pork Markets*. Report No. ERR-326. U.S. Department of Agriculture, Economic Research Service, Nov. 2023.

[46] OECD-FAO. *Agricultural outlook 2021–2030. Meat.* OECD/FAO. 2021. Chap. 6.

[47] Penrith M.-L, Bastos AD, Etter EMC & Beltrán-Alcrudo D. Epidemiology of African swine fever in Africa today: Sylvatic cycle versus socio-economic imperatives. *Tansbound. Emerg. Dis.* **66**.(2) (Mar. 2019), pp. 672–686. ISSN: 1865-1674. DOI: 10.1111/tbed.13117.

[48] Andrés G, Alejo A, Salas J & Salas ML. African Swine Fever Virus Polyproteins pp220 and pp62 Assemble into the Core Shell. *J. Virol.* **76**.(24) (Dec. 2002), pp. 12473–12482. ISSN: 0022-538X. DOI: 10.1128/JVI.76.24.12473-12482.2002.

[49] Salas ML & Andrés G. African swine fever virus morphogenesis. *Virus Res.* **173**.(1) (2013), pp. 29–41. ISSN: 0168-1702. DOI: 10.1016/j.virusres.2012.09.016.

[50] Alejo A, Matamoros T, Guerra M & Andrés G. A Proteomic Atlas of the African Swine Fever Virus Particle. *J. virology* **92**.(23) (Dec. 2018). ISSN: 1098-5514. DOI: 10.1128/jvi.01293-18.

[51] Borca M, Kutish G, Afonso C, Irusta P, Carrillo C, Brun A, Sussman M & Rock D. An African Swine Fever Virus Gene with Similarity to the T-Lymphocyte Surface Antigen CD2 Mediates Hemadsorption. *Virology* **199**.(2) (Mar. 1994), pp. 463–468. ISSN: 0042-6822. DOI: 10.1006/viro.1994.1146.

[52] Andrés G, García-Escudero R, Viñuela E, Salas ML & Rodríguez JM. African swine fever virus structural protein pE120R is essential for virus transport from assembly sites to plasma membrane but not for infectivity. *J. virology* **75**.(15) (Aug. 2001), pp. 6758–68. ISSN: 0022-538X. DOI: 10.1128/JVI.75.15.6758-6768.2001.

[53] Hooper GL, Netherton CL & Wright E. Cell entry mechanisms of African swine fever virus. *Virology* **600** (Dec. 2024), p. 110277. ISSN: 0042-6822. DOI: 10.1016/j.virol.2024.110277.

[54] Mercer J & Helenius A. Virus entry by macropinocytosis. *Nat. Cell Biol.* **11**.(5) (May 2009), pp. 510–520. ISSN: 1465-7392. DOI: 10.1038/ncb0509-510.

[55] Sobhy H. A comparative review of viral entry and attachment during large and giant dsDNA virus infections. *Arch. Virol.* **162**.(12) (Dec. 2017), pp. 3567–3585. ISSN: 0304-8608. DOI: 10.1007/s00705-017-3497-8.

[56] Canton J, Schlam D, Breuer C, Gütschow M, Glogauer M & Grinstein S. Calcium-sensing receptors signal constitutive macropinocytosis and facilitate the uptake of NOD2 ligands in macrophages. *Nat. Commun.* **7**.(1) (Apr. 2016), p. 11284. ISSN: 2041-1723. DOI: 10.1038/ncomms11284.

[57] Chen X, Zheng J, Li T, Liu C, Bao M, Wang X, Li X, Li J, Huang L, Zhang Z, et al. Coreceptor AXL Facilitates African Swine Fever Virus Entry via Apoptotic Mimicry. *J. Virol.* **97**.(7) (July 2023). ISSN: 0022-538X. DOI: 10.1128/jvi.00616-23.

[58] Gao P, Zhou L, Wu J, Weng W, Wang H, Ye M, Qu Y, Hao Y, Zhang Y, Ge X, et al. Riding apoptotic bodies for cell–cell transmission by African swine fever virus. *Proc. Natl. Acad. Sci.* **120**.(48) (Nov. 2023). ISSN: 0027-8424. DOI: 10.1073/pnas.2309506120.

[59] Hernaez B & Alonso C. Dynamin- and clathrin-dependent endocytosis in african swine fever virus entry. *J. Virol.* **84**.(4) (Feb. 2010), pp. 2100–2109. ISSN: 0022-538X. DOI: 10.1128/JVI.01557-09.

[60] Chen X, Zheng J, Liu C, Li T, Wang X, Li X, Bao M, Li J, Huang L, Zhang Z, et al. CD1d facilitates african swine fever virus entry into the host cells via clathrin-mediated endocytosis. *Emerg. Microbes & Infect.* **12**.(2) (Dec. 2023). ISSN: 2222-1751. DOI: 10.1080/22221751.2023.2220575.

[61] Sánchez-Torres C, Gómez-Puertas P, Gómez-Del-Moral M, Alonso F, Escribano JM, Ezquerra A & Domínguez J. Expression of porcine cd163 on monocytes/macrophages correlates with permissiveness to african swine fever infection. *Arch. virology* **148**.(12) (Dec. 2003), pp. 2307–2323. ISSN: 0304-8608. DOI: 10.1007/S00705-003-0188-4.

[62] Hernáez B, Tarragó T, Giralt E, Escribano JM & Alonso C. Small Peptide Inhibitors Disrupt a High-Affinity Interaction between Cytoplasmic Dynein and a Viral Cargo Protein. *J. Virol.* **84**.(20) (Oct. 2010), pp. 10792–10801. ISSN: 0022-538X. DOI: 10.1128/JVI.01168-10.

[63] Aicher S.-M, Monaghan P, Netherton CL & Hawes PC. Unpicking the Secrets of African Swine Fever Viral Replication Sites. *Viruses* **13**.(1) (Jan. 2021). ISSN: 1999-4915. DOI: 10.3390/v13010077.

[64] Alejo A, Andrés G & Salas ML. African swine fever virus proteinase is essential for core maturation and infectivity. *J. virology* **77**.(10) (May 2003), pp. 5571–5577. ISSN: 0022-538X. DOI: 10.1128/jvi.77.10.5571-5577.2003.

[65] Andrés G, García-Escudero R, Simón-Mateo C & Viñuela E. African Swine Fever Virus Is Enveloped by a Two-Membraned Collapsed Cisterna Derived from the Endoplasmic Reticulum. *J. Virol.* **72**.(11) (Nov. 1998), pp. 8988–9001. ISSN: 1098-5514. DOI: 10.1128/JVI.72.11.8988-9001.1998.

[66] Jouvenet N, Monaghan P, Way M & Wileman T. Transport of African Swine Fever Virus from Assembly Sites to the Plasma Membrane Is Dependent on Microtubules and Conventional Kinesin. *J. Virol.* **78**.(15) (Aug. 2004), pp. 7990–8001. ISSN: 0022-538X. DOI: 10.1128/JVI.78.15.7990-8001.2004.

[67] Galindo I & Alonso C. African swine fever virus: a review. *Viruses* **9**.(5) (2017). ISSN: 1999-4915. DOI: 10.3390/v9050103.

[68] Pérez-Núñez D, Madden DW, Vigara-Astillero G, Meekins DA, McDowell CD, Libanori-Artiaga B, García-Belmonte R, Bold D, Trujillo JD, Cool K, et al. Generation and Genetic Stability of a PolX and 5′ MGF-Deficient African Swine Fever Virus Mutant for Vaccine Development. *Vaccines* **12**.(10) (Sept. 2024), p. 1125. ISSN: 2076-393X. DOI: 10.3390/vaccines12101125.

[69] Zhu Z, Chen H, Liu L, Cao Y, Jiang T, Zou Y & Peng Y. Classification and characterization of multigene family proteins of african swine fever viruses. *Briefings Bioinform.* (Dec. 2020). ISSN: 1467-5463. DOI: 10.1093/bib/bbaa380.

[70] Dixon LK, Islam M, Nash R & Reis AL. African swine fever virus evasion of host defences. *Virus Res.* **266** (2019), pp. 25–33. ISSN: 1872-7492. DOI: 10.1016/j.virusres.2019.04.002.

[71] Franzoni G, Razzuoli E, Giudici SD, Carta T, Galleri G, Zinellu S, Ledda M, Angioi P, Modesto P, Graham SP, et al. Comparison of Macrophage Responses to African Swine Fever Viruses Reveals that the NH/P68 Strain is Associated with Enhanced Sensitivity to Type I IFN and Cytokine Responses from Classically Activated Macrophages. *Pathogens* **9**.(3) (Mar. 2020). ISSN: 2076-0817. DOI: 10.3390/PATHOGENS9030209.

[72] Franzoni G, Graham SP, Giudici SD, Bonelli P, Pilo G, Anfossi AG, Pittau M, Nicolussi PS, Laddomada A & Oggiano A. Characterization of the interaction of African swine fever virus with monocytes and derived macrophage subsets. *Vet. Microbiol.* **198** (Jan. 2017), pp. 88–98. ISSN: 0378-1135. DOI: 10.1016/j.vetmic.2016.12.010.

[73] Schäfer A, Franzoni G, Netherton CL, Hartmann L, Blome S & Blohm U. Adaptive cellular immunity against african swine fever virus infections. *Pathogens* **11**.(2) (Feb. 2022), p. 274. ISSN: 2076-0817. DOI: 10.3390/pathogens11020274.

[74] Yan L, Wang J, Cai X, Liou Y.-C, Shen H.-M, Hao J, Huang C, Luo G & He W. Macrophage plasticity: signaling pathways, tissue repair, and regeneration. *MedComm* **5**.(8) (Aug. 2024), e658. ISSN: 2688-2663. DOI: 10.1002/mco2.658.

[75] Greig A & Plowright W. The excretion of two virulent strains of African swine fever virus by domestic pigs. *Epidemiol. Infect.* **68**.(4) (Dec. 1970), pp. 673–682. ISSN: 0950-2688. DOI: 10.1017/S0022172400042613.

[76] Sierra MA, Carrasco L, Gómez-Villamandos JC, Mulas JM de las, Méndez A & Jover A. Pulmonary intravascular macrophages in lungs of pigs inoculated with african swine fever virus of differing virulence. *J. comparative pathology* **102**.(3) (Apr. 1990), pp. 323–34. ISSN: 0021-9975. DOI: 10.1016/s0021-9975(08)80021-7.

[77] Gregg DA, Schlafer DH & Mebus CA. African Swine Fever Virus Infection of Skin-Derived Dendritic Cells in Vitro Causes Interference with Subsequent Foot-and-Mouth Disease Virus Infection. *J. Vet. Diagn. Investig.* **7**.(1) (Jan. 1995), pp. 44–51. ISSN: 1040-6387. DOI: 10.1177/104063879500700106.

[78] Roberts NJ, Douglas RG, Simons RM & Diamond ME. Virus-induced interferon production by human macrophages. . *J. Immunol.* **123**.(1) (July 1979), pp. 365–369. ISSN: 0022-1767. DOI: 10.4049/JIMMUNOL.123.1.365.

[79] Portugal R, Leitão A & Martins C. Modulation of type I interferon signaling by African swine fever virus (ASFV) of different virulence L60 and NHV in macrophage host cells. *Vet. Microbiol.* **216** (Mar. 2018), pp. 132–141. ISSN: 0378-1135. DOI: 10.1016/j.vetmic.2018.02.008.

[80] Zhang F, Hopwood P, Abrams CC, Downing A, Murray F, Talbot R, Archibald A, Lowden S & Dixon LK. Macrophage transcriptional responses following in vitro infection with a highly virulent african swine fever virus isolate. *J. Virol.* **80**.(21) (Nov. 2006), pp. 10514–10521. ISSN: 0022-538X. DOI: 10.1128/JVI.00485-06.

[81] Gómez-Villamandos J, Bautista M, Sánchez-Cordón P & Carrasco L. Pathology of African swine fever: The role of monocyte-macrophage. *Virus Res.* **173**.(1) (Apr. 2013), pp. 140–149. ISSN: 0168-1702. DOI: 10.1016/j.virusres.2013.01.017.

[82] Revilla Y, Pérez-Núñez D & Richt JA. "African Swine Fever Virus Biology and Vaccine Approaches". Vol. 100. 2018, pp. 41–74. ISBN: 9780128152010. DOI: 10.1016/bs.aivir.2017.10.002.

[83] Alizon S, Hurford A, Mideo N & Baalen MV. Virulence evolution and the trade-off hypothesis: history, current state of affairs and the future. *J. evolutionary biology* **22**.(2) (Feb. 2009), pp. 245–59. ISSN: 1420-9101. DOI: 10.1111/j.1420-9101.2008.01658.x.

[84] Alizon S & Magnus C. Modelling the course of an HIV infection: insights from ecology and evolution. *Viruses* **4**.(10) (Oct. 2012), pp. 1984–2013. ISSN: 1999-4915. DOI: 10.3390/v4101984.

[85] Sasaki A, Lion S & Boots M. Antigenic escape selects for the evolution of higher pathogen transmission and virulence. *Nat. Ecol. & Evol.* **6**.(1) (Dec. 2021), pp. 51–62. ISSN: 2397-334X. DOI: 10.1038/s41559-021-01603-z.

[86] Oura CA, Powell PP, Anderson E & Parkhouse RM. The pathogenesis of African swine fever in the resistant bushpig. *J. Gen. Virol.* **79**.(6) (June 1998), pp. 1439–1443. ISSN: 0022-1317. DOI: 10.1099/0022-1317-79-6-1439.

[87] Sánchez-Vizcaíno J, Mur L, Gomez-Villamandos J & Carrasco L. An Update on the Epidemiology and Pathology of African Swine Fever. *J. Comp. Pathol.* **152**.(1) (Jan. 2015), pp. 9–21. ISSN: 0021-9975. DOI: 10.1016/j.jcpa.2014.09.003.

[88] Salguero FJ. Comparative Pathology and Pathogenesis of African Swine Fever Infection in Swine. *Front. Vet. Sci.* **7** (May 2020). ISSN: 2297-1769. DOI: 10.3389/fvets.2020.00282.

[89] Carrasco L, Lara FC.-M de, Mulas JM de las, Gómez-Villamandos J, Pérez J, Wilkinson P & Sierra M. Apoptosis in lymph nodes in acute African swine fever. *J. Comp. Pathol.* **115** (4 Nov. 1996), pp. 415–428. ISSN: 0021-9975. DOI: 10.1016/S0021-9975(96)80075-2.

[90] Salguero F, Ruiz-Villamor E, Bautista M, Sánchez-Cordón P, Carrasco L & Gómez-Villamandos J. Changes in macrophages in spleen and lymph nodes during acute African swine fever: expression of cytokines. *Vet. Immunol. Immunopathol.* **90**.(1-2) (Nov. 2002), pp. 11–22. ISSN: 01652427. DOI: 10.1016/S0165-2427(02)00225-8.

[91] Salguero F, Sánchez-Cordón P, Núñez A, Marco MF de & Gómez-Villamandos J. Proinflammatory Cytokines Induce Lymphocyte Apoptosis in Acute African Swine Fever Infection. *J. Comp. Pathol.* **132**.(4) (May 2005), pp. 289–302. ISSN: 0021-9975. DOI: 10.1016/j.jcpa.2004.11.004.

[92] Golding JP, Goatley L, Goodbourn S, Dixon LK, Taylor G & Netherton CL. Sensitivity of African swine fever virus to type I interferon is linked to genes within multigene families 360 and 505. *Virology* **493** (June 2016), pp. 154–161. ISSN: 0042-6822. DOI: 10.1016/J.VIROL.2016.03.019.

[93] Salguero F, Gil S, Revilla Y, Gallardo C, Arias M & Martins C. Cytokine mRNA expression and pathological findings in pigs inoculated with African swine fever virus (E-70) deleted on A238L. *Vet. Immunol. Immunopathol.* **124**.(1-2) (July 2008), pp. 107–119. ISSN: 0165-2427. DOI: 10.1016/j.vetimm.2008.02.012.

[94] Palese P. *Modulation of Host Gene Expression and Innate Immunity by Viruses*. Ed. by Palese P. Springer Netherlands, 2005, pp. 1–304. ISBN: 978-1-4020-3241-7. DOI: 10.1007/1-4020-3242-0.

[95] Reis AL, Netherton C & Dixon LK. Unraveling the Armor of a Killer: Evasion of Host Defenses by African Swine Fever Virus. *J. Virol.* **91**.(6) (Mar. 2017). ISSN: 0022-538X. DOI: 10.1128/jvi.02338-16.

[96] Sun L, Wu J, Du F, Chen X & Chen ZJ. Cyclic gmp-amp synthase is a cytosolic dna sensor that activates the type i interferon pathway. *Science* **339**.(6121) (Feb. 2013), pp. 786–791. ISSN: 1095-9203. DOI: 10.1126/SCIENCE.1232458/SUPPL_FILE/SUN_CGAS_SUPPLEMENTARYTABLES1.XLSX.

[97] Zhang Y, Yeruva L, Marinov A, Prantner D, Wyrick PB, Lupashin V & Nagarajan UM. The DNA Sensor, Cyclic GMP–AMP Synthase, Is Essential for Induction of IFN-β during Chlamydia trachomatis Infection. . *J. Immunol.* **193**.(5) (Sept. 2014), pp. 2394–2404. ISSN: 0022-1767. DOI: 10.4049/JIMMUNOL.1302718.

[98] Chen Q, Sun L & Chen ZJ. Regulation and function of the cGAS-STING pathway of cytosolic DNA sensing. *Nat. Immunol.* **17**.(10) (Sept. 2016), pp. 1142–9. ISSN: 1529-2916. DOI: 10.1038/ni.3558.

[99] Jiang B, Li L, Wu Y, Wang X, Gao N, Xu Z, Guo C, He S, Zhang G, Chen Y, et al. Unveiling Shared Immune Responses in Porcine Alveolar Macrophages during ASFV and PRRSV Infection Using Single-Cell RNA-seq. *Microorganisms* **12**.(3) (Mar. 2024). ISSN: 2076-2607. DOI: 10.3390/microorganisms12030563.

[100] Chiu YH, MacMillan JB & Chen ZJ. RNA Polymerase III Detects Cytosolic DNA and Induces Type I Interferons through the RIG-I Pathway. *Cell* **138** (3 Aug. 2009), pp. 576–591. ISSN: 00928674. DOI: 10.1016/j.cell.2009.06.015.

[101] Kawai T & Akira S. TLR signaling. *Semin. immunology* **19**.(1) (Feb. 2007), pp. 24–32. ISSN: 1044-5323. DOI: 10.1016/j.smim.2006.12.004.

[102] McNab F, Mayer-Barber K, Sher A, Wack A & O'Garra A. Type I interferons in infectious disease. *Nat. Rev. Immunol.* **15**.(2) (Feb. 2015), pp. 87–103. ISSN: 1474-1733. DOI: 10.1038/nri3787.

[103] Kumar KP, McBride KM, Weaver BK, Dingwall C & Reich NC. Regulated nuclear-cytoplasmic localization of interferon regulatory factor 3, a subunit of double-stranded RNA-activated factor 1. *Mol. cellular biology* **20**.(11) (June 2000), pp. 4159–68. ISSN: 0270-7306. DOI: 10.1128/MCB.20.11.4159-4168.2000.

[104] Li Q & Verma IM. NF-kappaB regulation in the immune system. *Nat. Rev. Immunol.* **2**.(10) (Oct. 2002), pp. 725–734. ISSN: 1474-1733. DOI: 10.1038/nri910.

[105] Häcker H, Redecke V, Blagoev B, Kratchmarova I, Hsu L.-C, Wang GG, Kamps MP, Raz E, Wagner H, Häcker G, et al. Specificity in Toll-like receptor signalling through distinct effector functions of TRAF3 and TRAF6. *Nature* **439**.(7073) (Jan. 2006), pp. 204–7. ISSN: 1476-4687. DOI: 10.1038/nature04369.

[106] Lin M, Ji X, Lv Y, Cui D & Xie J. The Roles of TRAF3 in Immune Responses. *Dis. markers* **2023** (2023), p. 7787803. ISSN: 1875-8630. DOI: 10.1155/2023/7787803.

[107] Merika M, Williams AJ, Chen G, Collins T & Thanos D. Recruitment of CBP/p300 by the IFN beta enhanceosome is required for synergistic activation of transcription. *Mol. cell* **1**.(2) (Jan. 1998), pp. 277–87. ISSN: 1097-2765. DOI: 10.1016/s1097-2765(00)80028-3.

[108] Honda K, Yanai H, Negishi H, Asagiri M, Sato M, Mizutani T, Shimada N, Ohba Y, Takaoka A, Yoshida N, et al. IRF-7 is the master regulator of type-I interferon-dependent immune responses. *Nature* **434**.(7034) (Apr. 2005), pp. 772–7. ISSN: 1476-4687. DOI: 10.1038/nature03464.

[109] Marié I, Durbin JE & Levy DE. Differential viral induction of distinct interferon-alpha genes by positive feedback through interferon regulatory factor-7. . *EMBO journal* **17**.(22) (Nov. 1998), pp. 6660–9. ISSN: 0261-4189. DOI: 10.1093/emboj/17.22.6660.

[110] Au WC, Moore PA, LaFleur DW, Tombal B & Pitha PM. Characterization of the interferon regulatory factor-7 and its potential role in the transcription activation of interferon A genes. . *J. biological chemistry* **273**.(44) (Oct. 1998), pp. 29210–7. ISSN: 0021-9258. DOI: 10.1074/jbc.273.44.29210.

[111] Randall RE & Goodbourn S. Interferons and viruses: an interplay between induction, signalling, antiviral responses and virus countermeasures. *J. Gen. Virol.* **89**.(1) (Jan. 2008), pp. 1–47. ISSN: 0022-1317. DOI: 10.1099/vir.0.83391-0.

[112] Der SD, Zhou A, Williams BRG & Silverman RH. Identification of genes differentially regulated by interferon α, β, or γ using oligonucleotide arrays. *Proc. Natl. Acad. Sci.* **95**.(26) (Dec. 1998), pp. 15623–15628. ISSN: 0027-8424. DOI: 10.1073/pnas.95.26.15623.

[113] Katze MG, He Y & Gale M. Viruses and interferon: a fight for supremacy. *Nat. Rev. Immunol. 2002 2:9* **2**.(9) (Sept. 2002), pp. 675–687. ISSN: 1474-1741. DOI: 10.1038/nri888.

[114] Ning S, Pagano JS & Barber GN. IRF7: activation, regulation, modification and function. *Genes & Immun.* **12**.(6) (Sept. 2011), pp. 399–414. ISSN: 1466-4879. DOI: 10.1038/gene.2011.21.

[115] Honda K & Taniguchi T. IRFs: master regulators of signalling by Toll-like receptors and cytosolic pattern-recognition receptors. *Nat. Rev. Immunol.* **6**.(9) (Sept. 2006), pp. 644–658. ISSN: 1474-1741. DOI: 10.1038/nri1900.

[116] Sharma S, TenOever BR, Grandvaux N, Zhou GP, Lin R & Hiscott J. Triggering the interferon antiviral response through an IKK-related pathway. *Science* **300**.(5622) (May 2003), pp. 1148–1151. ISSN: 1095-9203. DOI: 10.1126/SCIENCE.1081315.

[117] Zhu J, Chu F, Zhang M, Sun W & Zhou F. Association Between Neddylation and Immune Response. *Front. Cell Dev. Biol.* **10** (May 2022). ISSN: 2296-634X. DOI: 10.3389/fcell.2022.890121.

[118] Honda K, Ohba Y, Yanai H, Negishi H, Mizutani T, Takaoka A, Taya C & Taniguchi T. Spatiotemporal regulation of MyD88–IRF-7 signalling for robust type-I interferon induction. *Nature* **434**.(7036) (Apr. 2005), pp. 1035–1040. ISSN: 0028-0836. DOI: 10.1038/nature03547.

[119] Zhao M, Zhang Y, Yang X, Jin J, Shen Z, Feng X, Zou T, Deng L, Cheng D, Zhang X, et al. Myeloid neddylation targets IRF7 and promotes host innate immunity against rna viruses. *PLoS Pathog.* **17**.(9) (Sept. 2021). ISSN: 1553-7374. DOI: 10.1371/journal.ppat.1009901.

[120] Wong B, Bergeron A, Maznyi G, Ng K, Jirovec A, Birdi HK, Serrano D, Spinelli M, Thomson M, Taha Z, et al. Pevonedistat, a first-in-class NEDD8-activating enzyme inhibitor, sensitizes cancer cells to VSVΔ51 oncolytic virotherapy. *Mol. Ther.* **31**.(11) (Nov. 2023), pp. 3176–3192. ISSN: 1525-0016. DOI: 10.1016/j.ymthe.2023.09.017.

[121] Li L, Wang K, Zhou Y & Liu X. Review: a silent concert in developing plants: dynamic assembly of cullin-ring ubiquitin ligases. *Plant Sci.* **330** (May 2023), p. 111662. ISSN: 1873-2259. DOI: 10.1016/j.plantsci.2023.111662.

[122] Enchev RI, Schulman BA & Peter M. Protein neddylation: beyond cullin–ring ligases. *Nat. Rev. Mol. Cell Biol. 2015 16:1* **16**.(1) (Dec. 2014), pp. 30–44. ISSN: 1471-0080. DOI: 10.1038/nrm3919.

[123] Petroski MD & Deshaies RJ. Function and regulation of cullin-RING ubiquitin ligases. *Nat. reviews. Mol. cell biology* **6** (1 Jan. 2005), pp. 9–20. ISSN: 1471-0072. DOI: 10.1038/nrm1547.

[124] Connell S. "Functional analysis of the African swine fever virus MGF360 and MGF505 proteins, and its application to vaccine development." PhD thesis. University of Oxford, 2021.

[125] Barrado-Gil L, Puerto AD, Muñoz-Moreno R, Galindo I, Cuesta-Geijo MÁ, Urquiza J, Nistal-Villán E, Motes CM de & Alonso C. African Swine Fever Virus Ubiquitin-Conjugating Enzyme Interacts With Host Translation Machinery to Regulate the Host Protein Synthesis. *Front. Microbiol.* **11** (Dec. 2020). ISSN: 1664-302X. DOI: 10.3389/fmicb.2020.622907.

[126] Gao Q, Yang Y, Luo Y, Chen X, Gong T, Wu D, Feng Y, Zheng X, Wang H, Zhang G, et al. African Swine Fever Virus Envelope Glycoprotein CD2v Interacts with Host CSF2RA to Regulate the JAK2-STAT3 Pathway and Inhibit Apoptosis to Facilitate Virus Replication. *J. Virol.* **97**.(4) (Apr. 2023). ISSN: 0022-538X. DOI: 10.1128/jvi.01889-22.

[127] Liang R, Fu Y, Li G, Shen Z, Guo F, Shi J, Guo Y, Zhang D, Wang Z, Chen C, et al. EP152R-mediated endoplasmic reticulum stress contributes to African swine fever virus infection via the PERK-eIF2α pathway. *FASEB J.* **38**.(22) (Nov. 2024), e70187. ISSN: 1530-6860. DOI: 10.1096/fj.202400931RR.

[128] Liu Y, Shen Z, Xie Z, Song Y, Li Y, Liang R, Gong L, Di D, Liu J, Liu J, et al. African swine fever virus I73R is a critical virulence-related gene: A potential target for attenuation. *Proc. Natl. Acad. Sci. United States Am.* **120**.(15) (Apr. 2023), e2210808120. ISSN: 1091-6490. DOI: 10.1073/pnas.2210808120.

[129] Liu W, Yang L, Di C, Sun J, Liu P & Liu H. Nonstructural Protein A238L of the African Swine Fever Virus (ASFV) Enhances Antiviral Immune Responses by Activating the TBK1-IRF3 Pathway. *Vet. Sci.* **11**.(6) (June 2024), p. 252. ISSN: 2306-7381. DOI: 10.3390/vetsci11060252.

[130] Ren J, Li D, Zhu G, Yang W, Ru Y, Feng T, Qin X, Hao R, Duan X, Liu X, et al. Deletion of MGF-110-9L gene from African swine fever virus weakens autophagic degradation of TBK1 as a mechanism for enhancing type I interferon production. *FASEB J.* **37**.(6) (June 2023). ISSN: 1530-6860. DOI: 10.1096/fj.202201856R.

[131] Sunwoo S.-Y, García-Belmonte R, Walczak M, Vigara-Astillero G, Kim D.-M, Szymankiewicz K, Kochanowski M, Liu L, Tark D, Podgórska K, et al. Deletion of MGF505-2R Gene Activates the cGAS-STING Pathway Leading to Attenuation and Protection against Virulent African Swine Fever Virus. *Vaccines* **12**.(4) (Apr. 2024), p. 407. ISSN: 2076-393X. DOI: 10.3390/vaccines12040407.

[132] Yao M, Cao H, Li W, Hu Z, Rong Z, Yin M, Tian L, Hu D, Li X & Qian P. African swine fever virus MGF505-6R attenuates type I interferon production by targeting STING for degradation. *Front. immunology* **15** (2024), p. 1380220. ISSN: 1664-3224. DOI: 10.3389/fimmu.2024.1380220.

[133] Li D, Yang W, Li L, Li P, Ma Z, Zhang J, Qi X, Ren J, Ru Y, Niu Q, et al. African Swine Fever Virus MGF-505-7R Negatively Regulates cGAS–STING-Mediated Signaling Pathway. . *J. Immunol.* **206**.(8) (Apr. 2021), pp. 1844–1857. ISSN: 0022-1767. DOI: 10.4049/jimmunol.2001110.

[134] Yang K, Xue Y, Niu H, Shi C, Cheng M, Wang J, Zou B, Wang J, Niu T, Bao M, et al. African swine fever virus MGF360-11L negatively regulates cGAS-STING-mediated inhibition of type I interferon production. *Vet. research* **53**.(1) (Jan. 2022), p. 7. ISSN: 1297-9716. DOI: 10.1186/s13567-022-01025-0.

[135] Cheng M, Luo J, Duan Y, Yang Y, Shi C, Sun Y, Lu Y, Wang J, Li X, Wang J, et al. African swine fever virus MGF505-3R inhibits cGAS-STING-mediated IFN-β pathway activation by degrading TBK1. *Animal Dis.* **2**.(1) (Dec. 2022), p. 13. ISSN: 2731-0442. DOI: 10.1186/s44149-022-00046-8.

[136] Wang T, Luo R, Zhang J, Lu Z, Li L.-F, Zheng Y.-H, Pan L, Lan J, Zhai H, Huang S, et al. The MGF300-2R protein of African swine fever virus is associated with viral pathogenicity by promoting the autophagic degradation of IKKα and IKKβ through the recruitment of TOLLIP. *PLOS Pathog.* **19**.(8) (Aug. 2023), e1011580. ISSN: 1553-7374. DOI: 10.1371/journal.ppat.1011580.

[137] Wang T, Luo R, Zhang J, Lan J, Lu Z, Zhai H, Li LF, Sun Y & Qiu HJ. The African swine fever virus MGF300-4L protein is associated with viral pathogenicity by promoting the autophagic degradation of IKKβ and increasing the stability of IκBα. *Emerg. Microbes & Infect.* **13**.(1) (2024), p. 2333381. ISSN: 2222-1751. DOI: 10.1080/22221751.2024.2333381.

[138] Zhuo Y, Guo Z, Ba T, Zhang C, He L, Zeng C & Dai H. African Swine Fever Virus MGF360-12L Inhibits Type I Interferon Production by Blocking the Interaction of Importin α and NF-κB Signaling Pathway. *Virol. Sinica* **36**.(2) (Apr. 2021), pp. 176–186. ISSN: 1995-820X. DOI: 10.1007/S12250-020-00304-4.

[139] Chen Q, Wang XX, Jiang SW, Gao XT, Huang SY, Liang Y, Jia H & Zhu HF. MGF360-12L of ASFV-SY18 is an immune-evasion protein that inhibits host type I IFN, NF-κB, and JAK/STAT pathways. *Pol. J. Vet. Sci.* **26**.(1) (2023), pp. 119–130. DOI: 10.24425/pjvs.2023.145013.

[140] Wang Y, Cui S, Xin T, Wang X, Yu H, Chen S, Jiang Y, Gao X, Jiang Y, Guo X, et al. African Swine Fever Virus MGF360-14L Negatively Regulates Type I Interferon Signaling by Targeting IRF3. *Front. Cell. Infect. Microbiol.* **11** (Jan. 2022), pp. 818–969. ISSN: 2235-2988. DOI: 10.3389/fcimb.2021.818969.

[141] Chaudhari J, Lai DC & Vu HL. African swine fever viral proteins that inhibit cGAS-STING pathway and type-I interferon production. *Virology* **602** (Jan. 2025), p. 110317. ISSN: 0042-6822. DOI: 10.1016/j.virol.2024.110317.

[142] Lu Z, Luo R, Lan J, Chen S, Qiu H.-J, Wang T & Sun Y. The MGF300-2R Protein of African Swine Fever Virus Promotes IKKβ Ubiquitination by Recruiting the E3 Ubiquitin Ligase TRIM21. *Viruses* **16**.(6) (June 2024), p. 949. ISSN: 1999-4915. DOI: 10.3390/v16060949.

[143] Dupré J, Dimna ML, Hutet E, Dujardin P, Fablet A, Leroy A, Fleurot I, Karadjian G, Roesch F, Caballero I, et al. Exploring type I interferon pathway: virulent vs. attenuated strain of African swine fever virus revealing a novel function carried by MGF505-4R. *Front. Immunol.* **15** (Mar. 2024). ISSN: 1664-3224. DOI: 10.3389/fimmu.2024.1358219.

[144] Yang K, Xue Y, Niu T, Li X, Cheng M, Bao M, Zou B, Shi C, Wang J, Yang W, et al. African swine fever virus MGF505-7R protein interacted with IRF7 and TBK1 to inhibit type I interferon production. *Virus Res.* **322** (Dec. 2022). ISSN: 1872-7492. DOI: 10.1016/j.virusres.2022.198931.

[145] Li J, Song J, Kang L, Huang L, Zhou S, Hu L, Zheng J, Li C, Zhang X, He X, et al. pMGF505-7R determines pathogenicity of African swine fever virus infection by inhibiting IL-1β and type I IFN production. *PLOS Pathog.* **17**.(7) (July 2021). Ed. by Dixon LK, e1009733. ISSN: 1553-7374. DOI: 10.1371/journal.ppat.1009733.

[146] Liu X, Ao D, Jiang S, Xia N, Xu Y, Shao Q, Luo J, Wang H, Zheng W, Chen N, et al. African swine fever virus a528r inhibits tlr8 mediated nf-ϰb activity by targeting p65 activation and nuclear translocation. *Viruses* **13**.(10) (Oct. 2021), p. 2046. ISSN: 1999-4915. DOI: 10.3390/v13102046.

[147] Netherton CL, Shimmon GL, Hui JYK, Connell S & Reis AL. "African swine fever virus host–pathogen interactions". *Virus infected cells*. Vol. 106. Subcellular Biochemistry. Springer International Publishing, 2023, pp. 283–331. DOI: 10.1007/978-3-031-40086-5_11.

[148] Ranathunga L, Dodantenna N, Cha J.-W, Chathuranga K, Chathuranga WAG, Weerawardhana A, Subasinghe A, Haluwana DK, Gamage N & Lee J.-S. African swine fever virus B175L inhibits the type I interferon pathway by targeting STING and 2′3′-cGAMP. *J. Virol.* **97**.(11) (Nov. 2023). ISSN: 0022-538X. DOI: 10.1128/jvi.00795-23.

[149] Liu X, Chen H, Ye G, Liu H, Feng C, Chen W, Hu L, Zhou Q, Zhang Z, Li J, et al. African swine fever virus pB318L, a trans-geranylgeranyl-diphosphate synthase, negatively regulates cGAS-STING and IFNAR-JAK-STAT signaling pathways. *PLoS pathogens* **20**.(4) (Apr. 2024), e1012136. ISSN: 1553-7374. DOI: 10.1371/journal.ppat.1012136.

[150] Cheng M, Kanyema MM, Sun Y, Zhao W, Lu Y, Wang J, Li X, Shi C, Wang J, Wang N, et al. African Swine Fever Virus L83L Negatively Regulates the cGAS-STING-Mediated IFN-I Pathway by Recruiting Tollip To Promote STING Autophagic Degradation. *J. Virol.* **97**.(2) (Feb. 2023). ISSN: 0022-538X. DOI: 10.1128/jvi.01923-22.

[151] Dodantenna N, Cha J.-W, Chathuranga K, Chathuranga WAG, Weerawardhana A, Ranathunga L, Kim Y, Jheong W & Lee J.-S. The African Swine Fever Virus Virulence Determinant DP96R Suppresses Type I IFN Production Targeting IRF3. *Int. journal molecular sciences* **25**.(4) (Feb. 2024). ISSN: 1422-0067. DOI: 10.3390/ijms25042099.

[152] Liu H, Zhu Z, Feng T, Ma Z, Xue Q, Wu P, Li P, Li S, Yang F, Cao W, et al. African Swine Fever Virus E120R Protein Inhibits Interferon Beta Production by Interacting with IRF3 To Block Its Activation. *J. Virol.* **95**.(18) (Aug. 2021). Ed. by Shisler JL, pp. 824–845. ISSN: 0022-538X. DOI: 10.1128/JVI.00824-21.

[153] Liu X, Liu H, Ye G, Xue M, Yu H, Feng C, Zhou Q, Liu X, Zhang L, Jiao S, et al. African swine fever virus pE301R negatively regulates cGAS-STING signaling pathway by inhibiting the nuclear translocation of IRF3. *Vet. Microbiol.* **274** (Nov. 2022), p. 109556. ISSN: 0378-1135. DOI: 10.1016/j.vetmic.2022.109556.

[154] Revilla Y, Callejo M, Rodríguez JM, Culebras E, Nogal ML, Salas ML, Viñuela E & Fresno M. Inhibition of Nuclear Factor κB Activation by a Virus-encoded IκB-like Protein. *J. Biol. Chem.* **273**.(9) (Feb. 1998), pp. 5405–5411. ISSN: 0021-9258. DOI: 10.1074/jbc.273.9.5405.

[155] Hong J, Chi X, Yuan X, Wen F, Rai KR, Wu L, Song Z, Wang S, Guo G & Chen JL. I226R Protein of African Swine Fever Virus Is a Suppressor of Innate Antiviral Responses. *Viruses* **14**.(3) (Mar. 2022). ISSN: 1999-4915. DOI: 10.3390/v14030575.

[156] Correia S, Moura PL, Ventura S, Leitão A & Parkhouse RME. I329L: A Dual Action Viral Antagonist of TLR Activation Encoded by the African Swine Fever Virus (ASFV). *Viruses* **15**.(2) (Feb. 2023), p. 445. ISSN: 1999-4915. DOI: 10.3390/v15020445.

[157] Ran Y, Li D, Xiong M.-G, Liu H.-N, Feng T, Shi Z.-W, Li Y.-H, Wu H.-N, Wang S.-Y, Zheng H.-X, et al. African swine fever virus I267L acts as an important virulence factor by inhibiting RNA polymerase III-RIG-I-mediated innate immunity. *PLoS pathogens* **18**.(1) (Jan. 2022), e1010270. ISSN: 1553-7374. DOI: 10.1371/journal.ppat.1010270.

[158] Sun M, Yu S, Ge H, Wang T, Li Y, Zhou P, Pan L, Han Y, Yang Y, Sun Y, et al. The A137R Protein of African Swine Fever Virus Inhibits Type I Interferon Production via the Autophagy-Mediated Lysosomal Degradation of TBK1. *J. Virol.* **96**.(9) (May 2022). Ed. by Williams BRG. ISSN: 0022-538X. DOI: 10.1128/jvi.01957-21.

[159] Li Y, Huang L, Li H, Zhu Y, Yu Z, Zheng X, Weng C & Feng W.-H. ASFV pA151R negatively regulates type I IFN production via degrading E3 ligase TRAF6. *Front. Immunol.* **15** (Feb. 2024), p. 1339510. ISSN: 1664-3224. DOI: 10.3389/fimmu.2024.1339510.

[160] Granja AG, Nogal ML, Hurtado C, Aguila C del, Carrascosa AL, Salas ML, Fresno M & Revilla Y. The Viral Protein A238L Inhibits TNF-α Expression through a CBP/p300 Transcriptional Coactivators Pathway. . *J. Immunol.* **176**.(1) (Jan. 2006), pp. 451–462. ISSN: 0022-1767. DOI: 10.4049/jimmunol.176.1.451.

[161] Granja AG, Sabina P, Salas ML, Fresno M & Revilla Y. Regulation of Inducible Nitric Oxide Synthase Expression by Viral A238L-Mediated Inhibition of p65/RelA Acetylation and p300 Transactivation. *J. Virol.* **80**.(21) (Nov. 2006), pp. 10487–10496. ISSN: 0022-538X. DOI: 10.1128/JVI.00862-06.

[162] Granja AG, Perkins ND & Revilla Y. A238L Inhibits NF-ATc2, NF-ϰB, and c-Jun Activation through a Novel Mechanism Involving Protein Kinase C-ϑ-Mediated Up-Regulation of the Amino-Terminal Transactivation Domain of p300. . *J. Immunol.* **180**.(4) (Feb. 2008), pp. 2429–2442. ISSN: 0022-1767. DOI: 10.4049/jimmunol.180.4.2429.

[163] Correia S, Ventura S & Parkhouse RM. Identification and utility of innate immune system evasion mechanisms of ASFV. *Virus Res.* **173**.(1) (Apr. 2013), pp. 87–100. ISSN: 0168-1702. DOI: 10.1016/j.virusres.2012.10.013.

[164] Zhang K, Ge H, Zhou P, Li L.-F, Dai J, Cao H, Luo Y, Sun Y, Wang Y, Li J, et al. The D129L protein of African swine fever virus interferes with the binding of transcriptional coactivator p300 and IRF3 to prevent beta interferon induction. *J. Virol.* **97**.(10) (Oct. 2023). ISSN: 0022-538X. DOI: 10.1128/jvi.00824-23.

[165] Chen H, Wang Z, Gao X, Lv J, Hu Y, Jung Y.-S, Zhu S, Wu X, Qian Y & Dai J. ASFV pD345L protein negatively regulates NF-ϰB signalling by inhibiting IKK kinase activity. *Vet. Res.* **53**.(1) (Dec. 2022), p. 32. ISSN: 1297-9716. DOI: 10.1186/s13567-022-01050-z.

[166] Zhu Z, Li S, Ma C, Yang F, Cao W, Liu H, Chen X, Feng T, Shi Z, Tian H, et al. African Swine Fever Virus E184L Protein Interacts with Innate Immune Adaptor STING to Block IFN Production for Viral Replication and Pathogenesis. . *J. Immunol.* **210**.(4) (Feb. 2023), pp. 442–458. ISSN: 0022-1767. DOI: 10.4049/jimmunol.2200357.

[167] Dodantenna N, Ranathunga L, Chathuranga WAG, Weerawardhana A, Cha J.-W, Subasinghe A, Gamage N, Haluwana DK, Kim Y, Jheong W, et al. African Swine Fever Virus EP364R and C129R Target Cyclic GMP-AMP To Inhibit the cGAS-STING Signaling Pathway. *J. Virol.* **96**.(15) (Aug. 2022). ISSN: 0022-538X. DOI: 10.1128/jvi.01022-22.

[168] Yang J, Li S, Feng T, Zhang X, Yang F, Cao W, Chen H, Liu H, Zhang K, Zhu Z, et al. African Swine Fever Virus F317L Protein Inhibits NF-κB Activation To Evade Host Immune Response and Promote Viral Replication. *mSphere* **6**.(5) (Oct. 2021). ISSN: 2379-5042. DOI: 10.1128/msphere.00658-21.

[169] Zhou P, Dai J, Zhang K, Wang T, Li L.-F, Luo Y, Sun Y, Qiu H.-J & Li S. The H240R Protein of African Swine Fever Virus Inhibits Interleukin 1β Production by Inhibiting NEMO Expression and NLRP3 Oligomerization. *J. Virol.* **96**.(22) (Nov. 2022). ISSN: 0022-538X. DOI: 10.1128/jvi.00954-22.

[170] Ye G, Liu H, Liu X, Chen W, Li J, Zhao D, Wang G, Feng C, Zhang Z, Zhou Q, et al. African Swine Fever Virus H240R Protein Inhibits the Production of Type I Interferon through Disrupting the Oligomerization of STING. *J. Virol.* **97**.(9) (Sept. 2023). ISSN: 0022-538X. DOI: 10.1128/jvi.00577-23.

[171] Huang L, Liu H, Ye G, Liu X, Chen W, Wang Z, Zhao D, Zhang Z, Feng C, Hu L, et al. Deletion of African Swine Fever Virus (ASFV) H240R Gene Attenuates the Virulence of ASFV by Enhancing NLRP3-Mediated Inflammatory Responses. *J. Virol.* **97**.(2) (Feb. 2023). ISSN: 0022-538X. DOI: 10.1128/jvi.01227-22.

[172] Chen X, Li L.-F, Yang Z.-Y, Li M, Fan S, Shi L.-F, Ren Z.-Y, Cao X.-J, Zhang Y, Han S, et al. The African swine fever virus I10L protein inhibits the NF-κB signaling pathway by targeting IKKβ. *J. Virol.* **97**.(9) (Sept. 2023). ISSN: 0022-538X. DOI: 10.1128/jvi.00569-23.

[173] Huang L, Xu W, Liu H, Xue M, Liu X, Zhang K, Hu L, Li J, Liu X, Xiang Z, et al. African Swine Fever Virus pI215L Negatively Regulates cGAS-STING Signaling Pathway through Recruiting RNF138 to Inhibit K63-Linked Ubiquitination of TBK1. . *J. Immunol.* **207**.(11) (Dec. 2021), pp. 2754–2769. ISSN: 0022-1767. DOI: 10.4049/jimmunol.2100320.

[174] Cui S, Wang Y, Gao X, Xin T, Wang X, Yu H, Chen S, Jiang Y, Chen Q, Jiang F, et al. African swine fever virus M1249L protein antagonizes type I interferon production via suppressing phosphorylation of TBK1 and degrading IRF3. *Virus Res.* **319** (Oct. 2022). ISSN: 1872-7492. DOI: 10.1016/j.virusres.2022.198872.

[175] Zheng W, Xia N, Zhang J, Cao Q, Jiang S, Luo J, Wang H, Chen N, Zhang Q, Meurens F, et al. African Swine Fever Virus Structural Protein p17 Inhibits cGAS-STING Signaling Pathway Through Interacting With STING. *Front. Immunol.* **13** (July 2022). ISSN: 1664-3224. DOI: 10.3389/fimmu.2022.941579.

[176] Wang S, Xiang Z, Gao P, Zhang Y, Zhou L, Ge X, Guo X, Han J & Yang H. African swine fever virus structural protein p17 inhibits IRF3 activation by recruiting host protein PR65A and inducing apoptotic degradation of STING. *Front. Microbiol.* **15** (June 2024). ISSN: 1664-302X. DOI: 10.3389/fmicb.2024.1428233.

[177] Hao S, Zheng X, Zhu Y, Yao Y, Li S, Xu Y & Feng W.-H. African swine fever virus qp383r dampens type i interferon production by promoting cgas palmitoylation. *Front. immunology* **14** (May 9, 2023), p. 1186916. ISSN: 1664-3224. DOI: 10.3389/fimmu.2023.1186916.

[178] Luo J, Zhang J, Ni J, Jiang S, Xia N, Guo Y, Shao Q, Cao Q, Zheng W, Chen N, et al. The african swine fever virus protease ps273r inhibits dna sensing cgas-sting pathway by targeting ikkε. *Virulence* **13**.(1) (2022), p. 740. ISSN: 2150-5608. DOI: 10.1080/21505594.2022.2065962.

[179] Li H, Zheng X, Li Y, Zhu Y, Xu Y, Yu Z & Feng WH. African swine fever virus S273R protein antagonizes type I interferon production by interfering with TBK1 and IRF3 interaction. *Virol. Sinica* **38**.(6) (Dec. 2023), pp. 911–921. ISSN: 1995-820X. DOI: 10.1016/j.virs.2023.08.009.

[180] Li D, Peng J, Wu J, Yi J, Wu P, Qi X, Ren J, Peng G, Duan X, Ru Y, et al. African swine fever virus MGF-360-10L is a novel and crucial virulence factor that mediates ubiquitination and degradation of JAK1 by recruiting the E3 ubiquitin ligase HERC5. *mBio* **14**.(4) (Aug. 2023), e0060623. ISSN: 2150-7511. DOI: 10.1128/mbio.00606-23.

[181] Zhang K, Yang B, Shen C, Zhang T, Hao Y, Zhang D, Liu H, Shi X, Li G, Yang J, et al. MGF360-9L Is a Major Virulence Factor Associated with the African Swine Fever Virus by Antagonizing the JAK/STAT Signaling Pathway. *mBio* **13**.(1) (Feb. 2022). ISSN: 2150-7511. DOI: 10.1128/mbio.02330-21.

[182] Li D, Zhang J, Yang W, Li P, Ru Y, Kang W, Li L, Ran Y & Zheng H. African swine fever virus protein MGF-505-7R promotes virulence and pathogenesis by inhibiting JAK1- and JAK2-mediated signaling. *J. Biol. Chem.* (Sept. 2021), p. 101190. ISSN: 0021-9258. DOI: 10.1016/J.JBC.2021.101190.

[183] Huang Z, Cao H, Zeng F, Lin S, Chen J, Luo Y, You J, Kong C, Mai Z, Deng J, et al. African Swine Fever Virus MGF505-7R Interacts with Interferon Regulatory Factor 9 to Evade the Type I Interferon Signaling Pathway and Promote Viral Replication. *J. Virol.* **97**.(3) (Mar. 2023). ISSN: 0022-538X. DOI: 10.1128/jvi.01977-22.

[184] Ye G, Zhang Z, Liu X, Liu H, Chen W, Feng C, Li J, Zhou Q, Zhao D, Zhang S, et al. African swine fever virus pH240R enhances viral replication via inhibition of the type I IFN signaling pathway. *J. Virol.* **98**.(3) (Mar. 2024). ISSN: 0022-538X. DOI: 10.1128/jvi.01834-23.

[185] Huang Z, Kong C, Zhang WB, You J, Gao C, Yi J, Mai Z, Chen X, Zhou P, Gong L, et al. pK205R targets the proximal element of IFN-I signaling pathway to assist African swine fever virus to escape host innate immunity at the early stage of infection. *PLoS Pathog.* **20**.(10) (Oct. 2024). ISSN: 1553-7374. DOI: 10.1371/journal.ppat.1012613.

[186] Li L, Fu J, Li J, Guo S, Chen Q, Zhang Y, Liu Z, Tan C, Chen H & Wang X. African Swine Fever Virus pI215L Inhibits Type I Interferon Signaling by Targeting Interferon Regulatory Factor 9 for Autophagic Degradation. *J. virology* **96**.(17) (Sept. 2022). ISSN: 1098-5514. DOI: 10.1128/JVI.00944-22.

[187] Li Y.-H, Peng J.-L, Xu Z.-S, Xiong M.-G, Wu H.-N, Wang S.-Y, Li D, Zhu G.-Q, Ran Y & Wang Y.-Y. African Swine Fever Virus Cysteine Protease pS273R Inhibits Type I Interferon Signaling by Mediating STAT2 Degradation. *J. virology* **97**.(3) (Mar. 2023). ISSN: 1098-5514. DOI: 10.1128/jvi.01942-22.

[188] Chen Q, Li L, Guo S, Liu Z, Liu L, Tan C, Chen H & Wang X. African swine fever virus pA104R protein acts as a suppressor of type I interferon signaling. *Front. Microbiol.* **14** (Apr. 2023). ISSN: 1664-302X. DOI: 10.3389/fmicb.2023.1169699.

[189] Huang Z, Mai Z, Kong C, You J, Lin S, Gao C, Zhang W, Chen X, Xie Q, Wang H, et al. African swine fever virus pB475L evades host antiviral innate immunity via targeting STAT2 to inhibit IFN-I signaling. *J. Biol. Chem.* **300**.(7) (July 2024), p. 107472. ISSN: 0021-9258. DOI: 10.1016/j.jbc.2024.107472.

[190] Riera E, García-Belmonte R, Madrid R, Pérez-Núñez D & Revilla Y. African swine fever virus ubiquitin-conjugating enzyme pI215L inhibits IFN-I signaling pathway through STAT2 degradation. *Front. Microbiol.* **13** (Jan. 2023). ISSN: 1664-302X. DOI: 10.3389/fmicb.2022.1081035.

[191] Chen Q, Li L, Liu L, Liu Z, Guo S, Tan C, Chen H & Wang X. African swine fever virus pf778r attenuates type i interferon response by impeding stat1 nuclear translocation. *Virus Res.* **335** (Oct. 2023), p. 199190. ISSN: 0168-1702. DOI: 10.1016/j.virusres.2023.199190.

[192] Afonso CL, Piccone ME, Zaffuto KM, Neilan J, Kutish GF, Lu Z, Balinsky CA, Gibb TR, Bean TJ, Zsak L, et al. African Swine Fever Virus Multigene Family 360 and 530 Genes Affect Host Interferon Response. *J. Virol.* **78**.(4) (Feb. 2004), pp. 1858–1864. ISSN: 0022-538X. DOI: 10.1128/jvi.78.4.1858-1864.2004.

[193] Reis AL, Abrams CC, Goatley LC, Netherton C, Chapman DG, Sanchez-Cordon P & Dixon LK. Deletion of african swine fever virus interferon inhibitors from the genome of a virulent isolate reduces virulence in domestic pigs and induces a protective response. *Vaccine* **34**.(39) (2016), pp. 4698–4705. ISSN: 1873-2518. DOI: 10.1016/j.vaccine.2016.08.011.

[194] Gupta T & Chahota R. Unique ankyrin repeat proteins in the genome of poxviruses-boon or wane, a critical review. *Gene* **927** (Nov. 2024), p. 148759. ISSN: 0378-1119. DOI: 10.1016/j.gene.2024.148759.

[195] Arias M, Torre A de la, Dixon L, Gallardo C, Jori F, Laddomada A, Martins C, Parkhouse RM, Revilla Y, Rodriguez F, et al. Approaches and perspectives for development of african swine fever virus vaccines. *Vaccines* **5**.(4) (2017), pp. 1–20. ISSN: 2076-393X. DOI: 10.3390/vaccines5040035.

[196] Vu HL & McVey DS. Recent progress on gene-deleted live-attenuated African swine fever virus vaccines. *NPJ Vaccines* **9**.(1) (Dec. 2024), p. 60. ISSN: 2059-0105. DOI: 10.1038/S41541-024-00845-9.

[197] Gaudreault NN & Richt JA. Subunit Vaccine Approaches for African Swine Fever Virus. *Vaccines* **7**.(2) (June 2019). ISSN: 2076-393X. DOI: 10.3390/vaccines7020056.

[198] Neilan J, Zsak L, Lu Z, Burrage T, Kutish G & Rock D. Neutralizing antibodies to African swine fever virus proteins p30, p54, and p72 are not sufficient for antibody-mediated protection. *Virology* **319**.(2) (Feb. 2004), pp. 337–342. ISSN: 0042-6822. DOI: 10.1016/j.virol.2003.11.011.

[199] Barderas MG, Rodríguez F, Gómez-Puertas P, Avilés M, Beitia F, Alonso C & Escribano JM. Antigenic and immunogenic properties of a chimera of two immunodominant African swine fever virus proteins. *Arch. virology* **146**.(9) (2001), pp. 1681–91. ISSN: 0304-8608. DOI: 10.1007/s007050170056.

[200] Ruiz-Gonzalvo F, Rodríguez F & Escribano JM. Functional and immunological properties of the baculovirus-expressed hemagglutinin of african swine fever virus. *Virology* **218**.(1) (Apr. 1996), pp. 285–9. ISSN: 0042-6822. DOI: 10.1006/viro.1996.0193.

[201] Goatley LC, Reis AL, Portugal R, Goldswain H, Shimmon GL, Hargreaves Z, Ho C.-S, Montoya M, Sánchez-Cordón PJ, Taylor G, et al. A Pool of Eight Virally Vectored African Swine Fever Antigens Protect Pigs against Fatal Disease. *Vaccines* **8**.(2) (May 2020), p. 234. ISSN: 2076-393X. DOI: 10.3390/vaccines8020234.

[202] Gladue DP & Borca MV. Recombinant ASF Live Attenuated Virus Strains as Experimental Vaccine Candidates. *Viruses* **14**.(5) (Apr. 2022), p. 878. ISSN: 1999-4915. DOI: 10.3390/v14050878.

[203] Petrini S, Righi C, Mészáros I, D'Errico F, Tamás V, Pela M, Olasz F, Gallardo C, Fernandez-Pinero J, Göltl E, et al. The Production of Recombinant African Swine Fever Virus Lv17/WB/Rie1 Strains and Their In Vitro and In Vivo Characterizations. *Vaccines* **11**.(12) (Dec. 2023). ISSN: 2076-393X. DOI: 10.3390/vaccines11121860.

[204] O'Donnell V, Holinka LG, Gladue DP, Sanford B, Krug PW, Lu X, Arzt J, Reese B, Carrillo C, Risatti GR, et al. African Swine Fever Virus Georgia Isolate Harboring Deletions of MGF360 and MGF505 Genes Is Attenuated in Swine and Confers Protection against Challenge with Virulent Parental Virus. *J. Virol.* **89**.(11) (June 2015), pp. 6048–6056. ISSN: 0022-538X. DOI: 10.1128/jvi.00554-15.

[205] Rathakrishnan A, Connell S, Petrovan V, Moffat K, Goatley LC, Jabbar T, Sánchez-Cordón PJ, Reis AL & Dixon LK. Differential Effect of Deleting Members of African Swine Fever Virus Multigene Families 360 and 505 from the Genotype II Georgia 2007/1 Isolate on Virus Replication, Virulence, and Induction of Protection. *J. Virol.* **96**.(6) (Mar. 2022). ISSN: 1098-5514. DOI: 10.1128/JVI.01899-21.

[206] Chandana MS, Nair SS, Chaturvedi VK, Abhishek, Pal S, Charan MSS, Balaji S, Saini S, Vasavi K & Deepa P. Recent progress and major gaps in the vaccine development for African swine fever. *Braz. J. Microbiol.* **55**.(1) (Mar. 2024), pp. 997–1010. ISSN: 1517-8382. DOI: 10.1007/s42770-024-01264-7.

[207] Borca MV, Ramirez-Medina E, Espinoza N, Rai A, Spinard E, Velazquez-Salinas L, Valladares A, Silva E, Burton L, Meyers A, et al. Deletion of the EP402R Gene from the Genome of African Swine Fever Vaccine Strain ASFV-G-ΔI177L Provides the Potential Capability of Differentiating between Infected and Vaccinated Animals. *Viruses* **16**.(3) (Mar. 2024), p. 376. ISSN: 1999-4915. DOI: 10.3390/V16030376.

[208] Deutschmann P, Forth JH, Sehl-Ewert J, Carrau T, Viaplana E, Mancera JC, Urniza A, Beer M & Blome S. Assessment of African swine fever vaccine candidate ASFV-G-ΔMGF in a reversion to virulence study. *npj Vaccines* **8**.(1) (Dec. 2023). ISSN: 2059-0105. DOI: 10.1038/s41541-023-00669-z.

[209] Rathakrishnan A, Reis AL, Goatley LC, Moffat K & Dixon LK. Deletion of the K145R and DP148R Genes from the Virulent ASFV Georgia 2007/1 Isolate Delays the Onset, but Does Not Reduce Severity, of Clinical Signs in Infected Pigs. *Viruses* **13**.(8) (July 2021), p. 1473. ISSN: 1999-4915. DOI: 10.3390/v13081473.

[210] Afonso CL, Alcaraz C, Brun A, Sussman MD, Onisk DV, Escribano JM & Rock DL. Characterization of p30, a highly antigenic membrane and secreted protein of african swine fever virus. *Virology* **189**.(1) (1992). ISSN: 1096-0341. DOI: 10.1016/0042-6822(92)90718-5.

[211] Prados FJ, Viñuela E & Alcamí A. Sequence and characterization of the major early phosphoprotein p32 of african swine fever virus. *J. virology* **67**.(5) (May 1993), pp. 2475–2485. ISSN: 0022-538X. DOI: 10.1128/JVI.67.5.2475-2485.1993.

[212] Petrovan V, Yuan F, Li Y, Shang P, Murgia MV, Misra S, Rowland RR & Fang Y. Development and characterization of monoclonal antibodies against p30 protein of African swine fever virus. *Virus Res.* **269** (Aug. 2019), p. 197632. ISSN: 0168-1702. DOI: 10.1016/J.VIRUSRES.2019.05.010.

[213] León PD, Bustos MJ & Carrascosa AL. Laboratory methods to study african swine fever virus. *Virus Res.* **173**.(1) (2013), pp. 168–179. ISSN: 0168-1702. DOI: 10.1016/j.virusres.2012.09.013.

[214] Duan X, Nauwynck HJ & Pensaert MB. Effects of origin and state of differentiation and activation of monocytes/macrophages on their susceptibility to porcine reproductive and respiratory syndrome virus (PRRSV). *Arch. Virol.* **142**.(12) (1997), pp. 2483–2497. ISSN: 0304-8608. DOI: 10.1007/S007050050256.

[215] Sánchez EG, Riera E, Nogal M, Gallardo C, Fernández P, Bello-Morales R, López-Guerrero JA, Chitko-Mckown CG, Richt JA & Revilla Y. Phenotyping and susceptibility of established porcine cells lines to African Swine Fever Virus infection and viral production. *Sci. Reports* **7**.(1) (Dec. 2017). ISSN: 20452322. DOI: 10.1038/S41598-017-09948-X.

[216] Gómez-Villamandos JC, Bautista MJ, Sánchez-Cordón PJ & Carrasco L. Pathology of African swine fever: the role of monocyte-macrophage. *Virus Res.* **173**.(1) (Apr. 2013), pp. 140–149. ISSN: 0168-1702. DOI: 10.1016/J.VIRUSRES.2013.01.017.

[217] Portugal R, Goatley LC, Husmann R, Zuckermann FA & Dixon LK. A porcine macrophage cell line that supports high levels of replication of OURT88/3, an attenuated strain of African swine fever virus. *Emerg. Microbes & Infect.* **9**.(1) (Jan. 2020), pp. 1245–1253. ISSN: 2222-1751. DOI: 10.1080/22221751.2020.1772675.

[218] Masujin K, Kitamura T, Kameyama K ichiro, Okadera K, Nishi T, Takenouchi T, Kitani H & Kokuho T. An immortalized porcine macrophage cell line competent for the isolation of African swine fever virus. *Sci. Reports* **11**.(1) (Dec. 2021), p. 4759. ISSN: 2045-2322. DOI: 10.1038/s41598-021-84237-2.

[219] Kameyama KI, Kitamura T, Okadera K, Ikezawa M, Masujin K & Kokuho T. Usability of Immortalized Porcine Kidney Macrophage Cultures for the Isolation of ASFV without Affecting Virulence. *Viruses* **14**.(8) (Aug. 2022). ISSN: 1999-4915. DOI: 10.3390/V14081794/S1.

[220] Hierholzer J & Killington R. "Virus isolation and quantitation". *Virology Methods Manual*. Ed. by Mahy BW & Kangro HO. London: Academic Press, 1996. Chap. 2, pp. 25–46. ISBN: 978-0-12-465330-6. DOI: 10.1016/B978-012465330-6/50003-8.

[221] Livak KJ & Schmittgen TD. Analysis of Relative Gene Expression Data Using Real-Time Quantitative PCR and the 2-ΔΔCT Method. *Methods* **25**.(4) (Dec. 2001), pp. 402–408. ISSN: 1046-2023. DOI: 10.1006/meth.2001.1262.

[222] Fishbourne E, Abrams CC, Takamatsu HH & Dixon LK. Modulation of chemokine and chemokine receptor expression following infection of porcine macrophages with African swine fever virus. *Vet. microbiology* **162**.(2-4) (Mar. 2013), pp. 937–943. ISSN: 1873-2542. DOI: 10.1016/J.VETMIC.2012.11.027.

[223] Loving CL, Brockmeier SL, Ma W, Richt JA & Sacco RE. Innate Cytokine Responses in Porcine Macrophage Populations: Evidence for Differential Recognition of Double-Stranded RNA. . *J. Immunol.* **177**.(12) (Dec. 2006), pp. 8432–8439. ISSN: 0022-1767. DOI: 10.4049/JIMMUNOL.177.12.8432.

[224] *RealTime-Glo™ MT Cell Viability Assay Technical Manual TM431*. Promega Corporation. 2022.

[225] Ostojic A, Vrhovac R & Verstovsek S. Ruxolitinib: a new JAK1/2 inhibitor that offers promising options for treatment of myelofibrosis. *Future Oncol.* **7**.(9) (2011), pp. 1035–1043. DOI: 10.2217/fon.11.81.

[226] Ivashkiv LB & Donlin LT. Regulation of type I interferon responses. *Nat. Rev. Immunol.* **14**.(1) (Jan. 2014), pp. 36–49. ISSN: 1474-1733. DOI: 10.1038/nri3581.

[227] Karalyan Z, Zakaryan H, Arzumanyan H, Sargsyan K, Voskanyan H, Hakobyan L, Abroyan L, Avetisyan A & Karalova E. Pathology of porcine peripheral white blood cells during infection with african swine fever virus. *BMC Vet. Res.* **8** (2012). ISSN: 1746-6148. DOI: 10.1186/1746-6148-8-18.

[228] Carrero JA. Confounding roles for type I interferons during bacterial and viral pathogenesis. *Int. Immunol.* **25**.(12) (2013). ISSN: 0953-8178. DOI: 10.1093/intimm/dxt050.

[229] Fan W, Jiao P, Zhang H, Chen T, Zhou X, Qi Y, Sun L, Shang Y, Zhu H, Hu R, et al. Inhibition of African Swine Fever Virus Replication by Porcine Type I and Type II Interferons. *Front. Microbiol.* **11** (June 2020). ISSN: 1664-302X. DOI: 10.3389/fmicb.2020.01203.

[230] Teijaro JR, Walsh KB, Rice S, Rosen H & Oldstone MBA. Mapping the innate signaling cascade essential for cytokine storm during influenza virus infection. *Proc. Natl. Acad. Sci.* **111**.(10) (Mar. 2014), pp. 3799–3804. ISSN: 0027-8424. DOI: 10.1073/pnas.1400593111.

[231] Reis AL, Goatley LC, Jabbar T, Lopez E, Rathakrishnan A & Dixon LK. Deletion of the Gene for the Type I Interferon Inhibitor I329L from the Attenuated African Swine Fever Virus OURT88/3 Strain Reduces Protection Induced in Pigs. *Vaccines* **8**.(2) (2020). ISSN: 2076-393X. DOI: 10.3390/vaccines8020262.

[232] Teijaro JR, Ng C, Lee AM, Sullivan BM, Sheehan KCF, Welch M, Schreiber RD, Torre JC de la & Oldstone MBA. Persistent lcmv infection is controlled by blockade of type i interferon signaling. *Science* **340**.(6129) (Apr. 2013), pp. 207–211. ISSN: 0036-8075. DOI: 10.1126/science.1235214.

[233] Wilson EB, Yamada DH, Elsaesser H, Herskovitz J, Deng J, Cheng G, Aronow BJ, Karp CL & Brooks DG. Blockade of chronic type i interferon signaling to control persistent lcmv infection. *Science* **340**.(6129) (Apr. 2013), pp. 202–207. ISSN: 0036-8075. DOI: 10.1126/science.1235208.

[234] Oh T, Do DT, Vo HV, Kwon H.-i, Lee S.-C, Kim MH, Nguyen DTT, Le QTV, Tran TM, Nguyen TT, et al. The Isolation and Replication of African Swine Fever Virus in Primary Renal-Derived Swine Macrophages. *Front. Vet. Sci.* **8** (2021). ISSN: 2297-1769. DOI: 10.3389/fvets.2021.645456.

[235] Razzuoli E, Franzoni G, Carta T, Zinellu S, Amadori M, Modesto P & Oggiano A. Modulation of Type I Interferon System by African Swine Fever Virus. *Pathogens* **9**.(5) (May 2020), p. 361. ISSN: 2076-0817. DOI: 10.3390/pathogens9050361.

[236] NC3Rs, BBSRC, Defra, MRC, NERC, Royal Society & Wellcome Trust. *Responsibility in the use of animals in bioscience research: expectations of the major research councils and charitable funding bodies*. Apr. 2019.

[237] *Animals (Scientific Procedures) Act 1986 (ASPA)*. Statute, c. 14, UK. 1986.

[238] Tegtmeyer P. Function of simian virus 40 gene a in transforming infection. *J. Virol.* **15**.(3) (Mar. 1975), pp. 613–618. ISSN: 0022-538X. DOI: 10.1128/jvi.15.3.613-618.1975.

[239] Martin RG & Chou JY. Simian virus 40 functions required for the establishment and maintenance of malignant transformation. *J. Virol.* **15**.(3) (Mar. 1975), pp. 599–612. ISSN: 0022-538X. DOI: 10.1128/jvi.15.3.599-612.1975.

[240] May T, Wirth D, Hauser H & Mueller PP. Transcriptionally regulated immortalization overcomes side effects of temperature-sensitive SV40 large T antigen. *Biochem. Biophys. Res. Commun.* **327**.(3) (Feb. 2005), pp. 734–741. ISSN: 0006-291X. DOI: 10.1016/J.BBRC.2004.12.065.

[241] Butel JS. SV40 large T-antigen: dual oncogene. *Cancer surveys* **5**.(2) (1986), pp. 343–65. ISSN: 0261-2429.

[242] Khalili K, Sariyer IK & Safak M. Small tumor antigen of polyomaviruses: role in viral life cycle and cell transformation. *J. Cell. Physiol.* **215**.(2) (May 2008), pp. 309–319. ISSN: 0021-9541. DOI: 10.1002/jcp.21326.

[243] Forero A, Giacobbi NS, McCormick KD, Gjoerup OV, Bakkenist CJ, Pipas JM & Sarkar SN. Simian Virus 40 Large T Antigen Induces IFN-Stimulated Genes through ATR Kinase. . *J. Immunol.* **192**.(12) (June 2014), pp. 5933–5942. ISSN: 0022-1767. DOI: 10.4049/jimmunol.1303470.

[244] Franzoni G, Graham SP, Sanna G, Angioi P, Fiori MS, Anfossi A, Amadori M, Giudici SD & Oggiano A. Interaction of porcine monocyte-derived dendritic cells with african swine fever viruses of diverse virulence. *Vet. Microbiol.* **216** (Mar. 2018), pp. 190–197. ISSN: 03781135. DOI: 10.1016/j.vetmic.2018.02.021.

[245] Nash RH. "Understanding the Interactions of African Swine Fever Virus With Dendritic Cells and the Adaptive Immune Response". PhD thesis. University of Surrey, 2021. DOI: 10.15126/thesis.900190.